

RESULTS AND DISCUSSION

Present work is a unique combination of two parts i.e. Histological and Biochemical studies. Most of the studies related with biodegradation are concentrated on biochemical aspects of dye degradation and dye decolourisation but how these fungi affects timbers at cellular level (histological) remains less explored. Majority of studies carried out at cellular level are based on the temperate species but similar information on Indian tropical species is almost nil. Present work is an attempt to understand the extent and mechanism of cell wall damage/degradation by the fungi. Effort is also done to explore the potential of these fungal strains for ligninolytic enzyme production, which is exploited for the biodegradation of xenobiotics compounds. Therefore, present work is divided into:

- I) Biochemical and Enzymatic Study and
- II) Histological Study

I. Biochemical and Enzymatic study

3.1 Collection and Isolation of the fungi:

The collection of the fungi was carried out from the different forests (*viz.* Junagarh, Saurashtra region; Pavagarh, Central Gujarat and

Waghai, Dangs forest from south Gujarat) of Gujarat State. About eighty five strains of wood rot fungi were collected from these forests. The sterilized fruiting bodies and the infected wood samples were processed for the isolation, purification and adaptation of the particular growth media. Among the different growth media tried (Table 2.1), Malt Extract Agar (MEA) was found to be best for the optimum growth of all the isolated fungal strains.

3.2 Screening of white rot fungi:

From all the eighty five strains, thirty six strains were found to be positive with Bavendamm's reaction, showing the complete browning of the malt agar medium enriched with 1% tannic acid (Bavendam, 1928). Among these strains, *Irpex lacteus* and *Phanerochaete chrysosporium* started browning of the medium after the 2nd day of inoculation. Plates become completely brown within 5 days of fungal incubation. Further incubation started bleaching of the media which ultimately led to the complete removal of brown colour of the media from the whole plate. Both *Irpex lacteus* and *Phanerochaete chrysosporium* grew much adaptively with malt agar medium compared to the other seven growth media tested. *Irpex lacteus* generated white, cotton-like-fluffy mycelia and radical pattern while growing on malt agar; on the other hand, *Phanerochaete chrysosporium* grew radially with very thin, white coloured mat showing granular surface.

3.3 Measuring fungal ligninolytic activity using dye decolourisation method:

3.3.1 Solid plate decolourisation:

Decolourisation and dye removal using a biotechnological approach remains technically attractive, for which several biological processes have been suggested (McMullan *et al.*, 2001; Stolz, 2001). To date, many of the fungi have been reported for their ability to degrade/decolourise the

synthetic dyes including various Poly Aromatic Hydrocarbons (Swamy and Ramsay, 1999; Kirby *et al.*, 2000; Wilkołazka *et al.*, 2002; Munari *et al.*, 2008; Xu *et al.*, 2010; Chacko and Subhramanyam, 2011; Karas *et al.*, 2011). In this regard, white rot fungi have been demonstrated to have a great potential for removal of synthetic dyes and decolourisation of coloured effluents but this potential has not so far been adequately exploited in bioremediation (Pointing, 2001; Stolz, 2001; Rabinovich *et al.*, 2004; Munari *et al.*, 2008; Xu *et al.*, 2010). However, the ability of white rot fungi to degrade synthetic dyes having diverse structures in agar plates varied significantly (Minussi *et al.*, 2001). Recently, there has been an increasing interest in white rot fungi for their capability to degrade various environmental pollutants including dyes (Maximo and Costa-Ferreira, 2004; Novotny *et al.*, 2004a, b; Li and Jia., 2008; Vanhulle *et al.*, 2008; Dashtban *et al.*, 2010; Karas *et al.*, 2011). Dye decolourisation by fungi during growth on solid medium has been widely employed to identify the ligninolytic potential and ability to degrade xenobiotic compounds by Basidiomycetes (Shah and Nerud, 2002; Wesenberg *et al.*, 2003; Machado *et al.*, 2006; Chacko *et al.*, 2011). The decolourisation of dyes by white rot fungi was first reported by Glenn and Gold (1983), who developed a method to measure the ligninolytic activity of *Phanerochaete chrysosporium* based upon the decolourisation of sulphonated polymeric dyes. This paved the way for a wealth of studies on the decolourisation of dyes under conditions in which white rot fungi produce lignin modifying enzymes (Swamy and Ramsay, 1999; Kirby *et al.*, 2000). The ability of white rot fungi to decolourise synthetic textile dyes has been widely studied by using *Phanerochaete chrysosporium* (Glenn and Gold, 1983; Bumpus and Brock, 1988, Pasti-Grigsby *et al.*, 1992; Chao and Lee, 1994; Knapp *et al.*, 1995; Banat *et al.*, 1996; Young and Yu, 1997; Conneely *et al.*, 1999; Chagas and Durrant, 2001; Kunz *et al.*, 2001; Martins *et al.*, 1999; Mielgo *et al.*, 2002) and *Trametes versicolor* (Field *et al.*, 1992; Borchert and Libra, 2001; Tekere *et al.*, 2001a, b; Hailei *et al.*, 2009; Levin *et al.*, 2010).

Munari
et al.

Irpex lacteus and *Phanerochaete chrysosporium* were well characterized for their capacity to decolourise diverse synthetic dyestuffs representing the main chemical dye groups under various conditions. Their growth tolerance towards the presence of the dyes in the environment was also evaluated by Novotny *et al.*, (2001a, b). Minussi *et al.*, (2001) has assessed the efficiency of *Phanerochaete chrysosporium* for visual disappearance of colour from the plates, starting from the third day of its inoculation up to the 25th day of growth. It has also been reported to decolourise several azo dyes and their simplified chemical substitutes (Glenn and Gold, 1983; Paszczynski *et al.*, 1992; Pasti-Grigsby *et al.*, 1992; Spadaro *et al.*, 1992). The capability of the white rot fungus *Irpex lacteus* to decolourise synthetic dyes such as RO16, RBBR and Bromophenol Blue, Anthraquinone, Triphenylmethane and Phthalocyanine etc., under different culture conditions like static, agitated, and immobilized cultures has also been studied by previous workers (Pointing, 2001; Kasinath *et al.*, 2003; Maximo and Costa-Ferreira, 2004; Novotny *et al.*, 2004a, b; Svobodova *et al.*, 2007; Tavcar *et al.*, 2006). In the present study, out of thirty six strains, two potential species *Irpex lacteus* and *Phanerochaete chrysosporium* giving promising results were selected for further studies.

The dye decolourisation ability of the fungi also depends upon the structure, type and the concentration of the dye used. At present, fungal decolourisation cannot be forecast on the basis of the chemical structure of dye. Similar dyes can be differently decolourised as it was already described by Knapp *et al.*, (1995). In the present study, all the dyes selected for the study are azo dyes and both the fungal strains efficiently decolourised and degraded all the dyes investigated. Previous works studying the decolourisation of chemically different dyes showed that azo dyes are more recalcitrant to the fungal transformation than anthraquinone dyes (Abadulla *et al.*, 2000; Jarosz-Wilkolazka *et al.*, 2002). Among Azo dyes, a large class of commercially produced dyes are not readily degraded by microorganisms (Jarosz-Wilkolazka *et al.*, 2002). As the azo dyes are not readily degraded and considered to be resistant to

decolourisation due to their chemical structure, easy decolourisation of these azo dyes by using white rot fungi is somewhat surprising (Wang and Yu, 1999; Abdulla *et al.*, 2000).

It has been reported that yellow and red azo dyes are more recalcitrant to the fungal decolourisation (Maximo *et al.*, 2003). In the present study also, Reactive Red HE8B required more time for its complete decolourisation. *Pleurotus sajor-caju* PS2001 is reported for complete decolourisation of Reactive Blue 220 (RB220), Acid Green 28 (AG28) and Acid Blue 80 (AB80) easily, while Reactive Red 198 (RR198) and Reactive Yellow 15 (RY15) were not fully decolourised until the mycelium had completely grown over the solid medium (Munari *et al.*, 2008). *Phanerochaete chrysosporium* totally decolourised Reactive Yellow 145 after 9 days (Minussi *et al.*, 2001) and Amaranth and Remazol Black took 10 days for complete decolourisation after fungal inoculation, while Reactive Blue and Tropaeolipn O were only faintly decolourised around the fungal colonies (Swamy and Ramsay, 1999). According to Minussi *et al.*, (2001), *Lentinus edodes* exhibited the highest decolourisation rate against Reactive Blue 19 (0.05%), than Reactive Red 195 (0.025%), Reactive Yellow 145 (0.05%) and Reactive Black 5 (0.05%), while *Trametes versicolor* and *Trametes villosa* showed 100% decolourisation in 12 days.

The identification of potent species for dye decolourisation requires a screening method based on the direct measurement of substrate transformation such as colour removal (Field *et al.*, 1993). Several studies of evaluation for decolourisation were performed using solid medium (Cripps *et al.*, 1990; Tekere *et al.*, 2001a, b; Dias *et al.*, 2003; Zouari-Mechichi *et al.*, 2006; Munari *et al.*, 2008). Available information indicates that the potential of white rot fungi for the solid plate (i.e. on plate) decolourisation of synthetic dyes differs with the complexity of dye structures. Tekere *et al.*, (2001a, b) studied the decolourisation of dyes such as Crystal violet, Bromophenol Blue, Cresol Red, Blue Dextran etc., on solid media. Jarosz-Wilkolazka *et al.*, (2002) also screened 115 strains of fungi for the decolourisation of two dyes by using solid medium.

and Ramsay, (1999) showed decolourisation of various dyes such as Amaranth and Remazol Black B, Reactive Blue and Tropaeolin O on solid plate by using *Phanerochaete chrysosporium*, *Trametes versicolor* and *Trametes hirsuta*. Available literature indicates that on plate decolourisation of the dyes is most suitable method for the screening of potent fungal species. In the present study also about thirty six strains were screened for on plate decolourisation of all the ten dyes. From these, two species viz. *Phanerochaete chrysosporium* and *Irpex lacteus* showed rapid decolourisation. Therefore, these two species were selected for detailed studies.

In the present study, on plate decolourisation of the dyes was observed by formation of clear zones around the fungal colonies (Figure 3.1 to 3.10) and the absolute decolourisation was assessed by the total disappearance of the colour from the plate. Both the strains (i.e. *Irpex lacteus* and *Phanerochaete chrysosporium*) completely decolourised all the ten dyes tested, with no absolute inhibitory effect on the growth of mycelia (Table 2.2). Dyes with five different concentrations (10, 50, 100, 250 and 500mg/l) were solidified on Malt Extract Agar medium in order to evaluate their effect on the growth of fungi and potential for decolourisation. In case of both the fungal strains, the mycelia started extending on malt agar medium from the 2nd day of inoculation whether the dye is present or not and the decolourisation rates of textile dyes varied according to their concentrations.

Irpex lacteus totally decolourised all the dyes (Reactive Orange 2R, Reactive Black B, Reactive Golden Yellow HR, Reactive Golden Yellow HRNL, Reactive Violet 5R, Reactive Magenta HB, and Reactive Yellow MERL) with the concentration of 10mg/l after the 11th day of inoculation except Reactive Yellow FG and Reactive Red ME4BL which required 13 days for complete decolourisation. Among all the ten dyes tested, Reactive Red HE8B is structurally more complex which took 18 days for complete decolourisation (Figure 3.11). On the other hand, *Phanerochaete chrysosporium* decolourised Reactive Orange 2R faster than the previous

species. It was completely decolourised on the 9th day of fungal inoculation, for which former species required 11 days. Complete decolourisation of all the other dyes (except Reactive Red HE8B) with the concentration of 10mg/l, was recorded only after 11th day of fungal inoculation. On the contrary, Reactive Red HE8B required 15 days for its complete disappearance from the plate (Figure 3.12). All the other four concentrations of dye tested in the present investigation were also been decolourised easily by both the strains. However, increase in concentration decreased the rate of decolourisation. Therefore, time required for the decolourisation of the dye increased gradually with the increase in concentrations from 10, 50, 100, 250 to 500mg/l.

As mentioned earlier that concentration of dye in the growth media plays important role to determine the time required for the complete decolourisation of dye from the media. It is reported that up to certain concentration of dye, there is no inhibitory effect of dye on fungal growth (Kim *et al.*, 1995; Selvam *et al.*, 2003; Eichlerova *et al.*, 2006). Exceeding particular concentration acts as an inhibitor for the fungal growth. This concentration of dye varies from species to species and the ability of the fungal species to decolourise it. In the present study, the concentration of the dyes up to 100mg/l was not detected to affect the mycelial growth of the fungi. But the increasing concentration led to the reduction in growth and decolourisation rate. Diameter of the decolourised zone (Figure 3.11 and 3.18) showed a positive correlation between the growth rate and the decolourisation ability of both the fungal species investigated. The colony diameter mostly exceeded the diameter of the decolourised zone with the reactive dyes. Eichlerova *et al.*, (2006) has also shown that decolourisation started very early even in media with a high concentration, but the total dye removal took the same or even a longer time.

Swamy and Ramsay, (1999) reported that *Phanerochaete chrysosporium* required 10, 13 and 19 days for decolouration of 10mg/l concentration of Remazol Black, Amaranth and Reactive Blue, respectively while *Trametes versicolor* took 7 days for decolourising

1.6 Bioremediation:

Bioremediation is a combination of two words – “Bio” and “Remediate”. It can be defined as any process that uses microorganisms or their enzymes to return the environment altered by contaminants to its original condition. Bioremediation is the ability of certain microorganisms, heterotrophic bacteria and fungi, to degrade hazardous organic materials to innocuous compounds such as carbon dioxide, methane, water, inorganic salts, and biomass (Anderson, 1995). As an ecological point of view, bioremediation is the use of microorganisms to degrade, sequester, or remove environmental contaminants (Milton and Nagabhushanam, 2005).

Bioremediation is potentially an environmentally safe, biologically effective, and low cost method to clean up xenobiotics from the environment. The goal of bioremediation is to reduce pollutant levels at least to undetectable, non-toxic or acceptable levels, i.e. within limits set by regulatory agencies (Pointing, 2001) or ideally completely mineralize the organopollutants to carbon dioxide. From an environmental point of view, the total mineralization is desirable as it represents complete detoxification (Gan and Koskinen, 1998). According to Alexander (1981), mineralization is nothing but the complete biologically mediated break down of organic compounds into water, CO₂ and other inorganic residue, which is also termed as biodegradation. However, bioremediation also provides a technique for discarding pollutants by enhancing the same biodegradation processes that occur in nature. Microorganisms use an organic substance as a source of carbon and energy which ultimately results into breakdown or decay of the material. Bioremediation involves detoxifying hazardous substances instead of merely transferring them from one medium to another. It is an urgent need of our planet for protection and restoration from toxic contaminants (Milton and Nagabhushanam, 2005). This process is essential to recycle the waste, so that the elements in them can be used again. Nature has mechanisms for

- 2

Cu-phthalocyanine and Poly R-478 on agar plates and in liquid culture at a relatively high concentration of 2 to 4 and 0.5 to 1g/l, respectively. On the other hand, Malachite Green and Crystal Violet were decolourised to a lower extent up to the concentration of 0.1g/l. Duygu *et al.*, (2005) reported that *Phanerochaete chrysosporium* partially decolourise Drimarene Blue X3LR and Remazol Brilliant Blue R (11–20%) within 10 days of its incubation period.

3.3.2 Decolourisation in liquid growth medium:

The decolourisation of ten reactive dyes by *Irpex lacteus* and *Phanerochaete chrysosporium* was measured as a decrease of visible light absorbance at the wavelength of maximum absorbance (λ_{max} , nm) of respective dyes. Fungal activity of both the strains can be seen as a colour change from the 3rd day of inoculation. Gradually, colour became faded and ultimately led to the complete disappearance of coloured dyes from the flask (Figure 3.13 to 3.17). Tekere *et al.*, (2001a, b) has also studied the decolourisation of dyes such as Crystal violet, Bromophenol Blue, Cresol Red, Blue Dextran on liquid media. Moreover, *Pleurotus sajor-caju* PS2001 was also exploited by Munari *et al.*, (2008) to test the decolourisation of industrial dyes in liquid cultures. Jia *et al.*, (2004) used *Schizophyllum* sp. F17, a local white rot fungus, which has previously shown potential for dye decolourisation in liquid culture.

Revankar and Lele, (2007) reported that azo dyes are recalcitrant for decolourisation and could be decolourised to a limited extent. However, Eichlerova *et al.*, (2006) stated that the difference between decolourisation of structurally different dyes is not easy to explain. In the present study, ten different reactive dyes with different structures were selected to check the potential and time required by the selected strain to degrade them. Majority of researchers used a dye concentration of 0.1 to 0.3g/l or lower in their studies (Chagas and Durrant, 2001; Hatvani and Mecs, 2001; Jarosz-Wilkolazka *et al.*, 2002). In the present study, the series of experiments were performed initially by using liquid culture method to

evaluate the rate of dye decolourisation. Different concentrations starting from 10mg/l to 500mg/l dye were checked and both the strains were found to be efficient degraders for all the ten dyes.

In previous studies, *Irpex lacteus* has shown efficient decolourisation of various synthetic azo dyes including RO16 (Robinson *et al.*, 2001; Novotny *et al.*, 2000; Maximo *et al.*, 2003; Novotny *et al.*, 2004a, b; Zhao and Hardin, 2002). In the present investigation, *Irpex lacteus* showed 100% decolourisation of Reactive Yellow FG, Reactive Violet 5R, Reactive Magenta HB, and Reactive Yellow MERL after the 11th day of inoculation, while Reactive Orange 2R, Reactive Red ME4BL, Reactive Black B, Reactive Golden Yellow HR, and Reactive Golden Yellow HRNL which took 13 days for its complete decolourisation. However, Reactive Red HE8B acquired only 97.89% of decolourisation after 13 days of fungal inoculation which indicates that Reactive Red HE8B is more difficult to be decolourised as compared to all other nine dyes (Figure 3.18). Various workers have reported that *Irpex lacteus* decolourise different dyes to various extents depending on the complexity of the dye (Novotny *et al.*, 2000; Robinson *et al.*, 2001a, b; Maximo *et al.*, 2003; Novotny *et al.*, 2004a, b; Zhao and Hardin, 2002). Maximo and Ferreira, (2004) observed about 50% decolourisation of Reactive Black B after 4 days which increased to 80% after 10 days of *Irpex lacteus* inoculation. Our results differ from the report made by Maximo and Costa-Ferreira, (2004) where complete decolourisation of Reactive Black B was achieved within 13 days of fungal inoculation. *Irpex lacteus* is considered to be one of the good decolourising strains because of its ability to decolourise all tested dyes up to 97-100% within 13 days. Novotný *et al.*, (2000) has also selected *Irpex lacteus* for its ability to decolourise all the tested dyes with an efficiency of 56–100% within 14 days.

On the other hand, *Phanerochaete chrysosporium* exhibited 100% decolourisation of all the reactive dyes tested on 11th day of inoculation, except Reactive Red HE8B, which gave only 83.7% decolourisation (Figure 3.19). Although *Phanerochaete chrysosporium* decolourised only 83.7% of

Reactive Red HE8B within 11 days, it is more efficient and faster than *Irpex lacteus* in decolourisation of all tested reactive dyes. Similar to our results, 83% of dye decolourisation by *Phanerochaete chrysosporium* in 11 days is also recorded by Swamy and Ramsay, (1999) and Maximo and Costa-Ferreira, (2004). It is well known fact that extent of dye decolourisation may vary depending on the species studied, for example Minussi *et al.*, (2001) has shown that the extent of decolourisation for *Phanerochaete chrysosporium* was 90%, while *Trametes versicolor* decolourised only 50% of the dye after 10 days. Similarly, *Datronia sp.* KAPI0039 reached its maximum i.e. 99.86% of colour reduction from 200mg/l RBBR solution within only 3 days of treatment, whereas 98.87% decolourisation from 1,000mg/l RBBR solution was achieved after 7 days of treatment (Vaithanomsat *et al.*, 2010). Similarly, Aksu *et al.*, (2007) also reported that *Trametes versicolor* took 8 days to reach its maximum (95%) colour reduction from 58.4mg/l RB5; whereas maximum 77% of colour reduction from 358.6mg/l RB5 was achieved within 14 days. *Serratia marcescens* decolourised about 90% of Ranocid Fast Blue (RFB) and Procion Brilliant Blue-H-GR (100mg/l final concentration) within 5 and 8 days at pH 7.0, respectively (Verma and Datta, 2003). Eichlerova *et al.*, (2006) found that *Dichomitus squalens* is the most intensive decolouriser of RBBR (0.5g/l concentration), which decolourises about 96 to 98% of the dye within 14 days of its inoculation.

3.3.3 Effect of carbon and nitrogen sources on decolourisation:

Growth of the fungi and production of enzymes depend upon the growth conditions and the nutrition provided to them (Sanghvi *et al.*, 2010). Any of the additional sources to the medium directly affect the dye decolourisation ability of the fungi. In the present investigation, five different carbon sources (Dextrose, Sucrose, Lactose, Maltose and Fructose) and five nitrogen sources (Ammonium sulphate, Urea, Asparagine, Sodium nitrate and Sodium nitrite) were tested for their effectiveness on the dye decolourisation on solid and in liquid medium

with *Irpex lacteus* and *Phanerochaete chrysosporium*. From all five carbon sources used, dextrose was found to be more efficient for enhancing the rate of dye decolourisation while supplementation of others carbon sources were found as less efficient. In case of all nitrogen sources used, asparagine was found to be very good source of nitrogen for inducing dye decolourisation while sodium nitrite is found to inhibit the fungal growth.

Earlier studies on application of various carbon sources suggest that glucose can serve as a carbon and energy source and could support the decolourisation of the dyes (Kim *et al.*, 1995). However, there is no unanimity about the role of carbon sources in the process of dye decolourisation. Carliell *et al.*, (1995) and Kapdan *et al.*, (2000) found that the presence of glucose increased decolourisation while others have observed no effect of it (Knapp and Newby, 1995; Özsoy *et al.*, 2001; Chen *et al.*, 2003). On the contrary, results obtained by Eichlerova *et al.*, (2006) did not show any direct relationship between the carbon sources and decolourisation capacity of the strains.

Supplementation of nitrogen in growth media not only influence the ligninolytic enzyme production by several white rot fungi, but also reported to play an important role in the process of dye decolourisation (Moldes *et al.*, 2004). Growth media containing higher source of nitrogen gave the highest laccase activity in *Lentinus edodes* and *Rigidoporus lignonus* (Gianfreda *et al.*, 1999). On the other hand, nitrogen limited media enhanced the production of the enzyme in *Pycnoporus cinnabarinus* and *Phlebia radiata* (Mester and Field, 1997; Gianfreda *et al.*, 1999). Machado *et al.*, (2006) has also reported that the nitrogen concentration in the culture medium influenced the growth of *Trametes villosa*. Levin *et al.*, (2010) studied *Trametes trogii*, *Trametes villosa* and *Coriolus versicolor* var. *antarcticus*, to investigate the effects of nitrogen sources (amino acids and complex fonts) and vitamins on their ligninolytic enzyme production and dye degradation capacity. In the present study, asparagine was found to be very good source of nitrogen compared to other nitrogen sources for inducing dye decolourisation. Available literature also indicates that there

are several species in which ligninolytic enzyme activity is suppressed rather than stimulated by nitrogen concentrations. *Phanerochaete chrysosporium* is the best known example of this type of regulation (Leatham and Kirk, 1983). In the present study also, both the fungal strains gave positive response to asparagine but sodium nitrite is found to show inhibitory effect. In contrast, with other species such as *Pleurotus ostreatus* (Leatham and Kirk, 1983) and *Trametes trogii* (Levin *et al.*, 2002), high nitrogen concentrations stimulated ligninolytic enzyme production. Likewise, the degradation of Congo Red by *Phanerochaete chrysosporium* is also inhibited by a high concentration of nitrogen (Tatarko and Bumpus, 1998).

Tekere *et al.*, (2001a, b) has determined the influence of carbon and nitrogen on the distribution of the enzymes and the enzyme production levels. According to them, *Lentinus velutinus*, *Thamnidium elegans*, *Trametes versicolor* and *Irpex* spp. had the highest manganese peroxidase activity under conditions of high nitrogen and low carbon concentrations. The effects of complex nitrogen sources on laccase and manganese peroxidase production have also been investigated in numerous white rot fungi (Kaal *et al.*, 1995; Galhaup *et al.*, 2002a, b; Dong *et al.*, 2005; Mikiashvili *et al.*, 2006). Levin *et al.*, (2004, 2007) studied eight isolates from 58 strains for their ability to produce ligninolytic enzymes in a synthetic liquid medium supplemented with glucose and asparagine as carbon and nitrogen sources respectively. Induced manganese peroxidase activity in *Phanerochaete chrysosporium* under carbon and nitrogen starvation is reported by Ascher, (1993) while *Irpex lacteus* showed suppressed activity of enzymes in presence of nitrogen sources (Svobodova *et al.*, 2008). On the other hand, Mester and Field, (1997) and Gianfreda *et al.*, (1999) noticed that some white rot fungi do not show any effect of carbon and nitrogen sources on ligninolytic enzyme production in the expected trend. Contrary to the previous investigations, our studies showed relatively improved effect of carbon and nitrogen sources on the decolourisation.

3.3.4 Influence of inoculum size on decolourisation:

Defining the effect of inoculum size on dye decolourisation is also an essential factor as there is a direct relationship between inoculum size and decolourisation of dye. The inoculation with lignocellulolytic microorganisms is a strategy that could potentially enhance the lignocellulose degradation (Zeng *et al.*, 2010). Therefore, considerable work has been carried out to study the effect of inoculum size during composting of lignocellulosic material (Higuchi, 1990; Schoemaker and Leisola, 1990; López *et al.*, 2007; Phil and Dan, 2007; Zeng *et al.*, 2007). However, no such studies related to the effect of inoculum size on the ligninolytic enzyme production were carried. ^{data} Therefore, the influence of inoculum size on the dye decolourisation was also investigated in the present study.

In case of solid plate decolourisation, four different inoculum sizes i.e. 1 to 4 agar plugs of 10mm diameter, were checked for their effect on the rate of decolourisation. Generally, it is expected that as the inoculum size increases, the growth becomes faster and should also increase the decolourisation rate. However, our study with solid plate decolourisation by *Irpex lacteus* and *Phanerochaete chrysosporium* revealed that on the 3rd day of inoculation, the decolourisation zone measured with all four inoculum sizes showed variation in increasing order with increase in inoculum size. However, after the 9th day of incubation, on plates decolourisation did not show any significant distinction between one plug and four plugs of inoculum size (Table 3.1 and 3.2).

Performance of fungal inoculum size on % decolourisation was also investigated. The inoculum sizes used in this study were varied at 3, 6, 9, 12, and 15 plugs of 10mm. For both the strains, fungal inoculum size was found to slightly affect the % decolourisation of all ten dyes tested. The rate of decolourisation was increased with inoculum size, but when the total % of decolourisation with all inoculum size was compared, the difference in % decolourisation with 6, 9, 12 and 15 plugs is very less

significant than 3 plugs. Therefore, the inoculum size of 3 plugs was found to be more efficient and significant (Table 3.3 and 3.4).

3.4 Determination of enzyme activity:

3.4.1 Production of ligninolytic enzymes by Solid State

Fermentation:

1992
(2009)

Solid state fermentation (SSF) involves fermentation process carried out on a solid material in absence of free flowing liquid (Pandey, 1999). SSF has been considered as an efficient method for enzyme production in biotechnological process due its potential advantages and high yield (Pandey *et al.*, 1999; Sanghvi *et al.*, 2010). In the present study, the potential of different agro-industrial wastes to produce all the three ligninolytic enzymes; manganese peroxidase, manganese independent peroxidase and laccase is evaluated. The production of ligninolytic enzymes using appropriate solid substrate is the key factor for the success of the SSF. Basidiomycetes (also referred as white rot fungi) are filamentous fungi, able to colonise lignocellulosic substrates in SSF due to their special enzymatic systems. Therefore, they may be used to convert cheap substrates into a valuable product (Rühl and Kües, 2007). Various types of oxidative enzymes are produced by white rot fungi in order to make use of lignocellulosic substrates for nutrition (Leonowicz, 1999; Hoegger, 2007). There are also few reports indicating the influence of the lignocellulose fermentation method on the enzyme production (Fenice, *et al.* 2003; Elisashvili, 2008).
R. Narsing
Narsing ref

Perusal of literature indicates that most of the studies describing ligninolytic system have been performed using liquid medium (Ardon, *et al.* 1996; Picard *et al.*, 1999). In liquid cultures *Irpex lacteus* was shown to produce all three main ligninolytic enzymes *viz.* lignin peroxidases, manganese peroxidases and laccases (Kasinath *et al.*, 2003; Novotny *et al.*, 2004; Shin *et al.*, 2005). In recent years, SSF has gained ground as a mean of enhancing enzyme production in fungi (Pant and Adholeya, 2007; Gupte

Novo

et al., 2007; Patel *et al.*, 2009; Sanghvi *et al.*, 2010, 2011). It is now accepted that SSF is the most economical process for ligninolytic enzyme production by fungi (Lwashita, 2002). Several studies emphasize the importance of working in solid state condition (Kerem *et al.*, 1992, 1995; Gupte, 1996; Gupte *et al.*, 1998; Arora, 2002; Shrivastava *et al.*, 2010).

Looking to the advantages of SSF, in the present investigation SSF mode of fermentation was chosen for production of ligninolytic enzymes. Galhaup *et al.*, (2002a, b) and Ramalho, (2005) reported that production of these enzymes is repressed by agitation in submerged liquid culture. Moreover, liquid culture does not provide the natural living conditions to the fungi. On the contrary, uses of agro-industrial waste provide the environment similar to natural habitat of fungi and offer the possibility of reusing and managing the agro-industrial waste fruitfully. Therefore, the SSF is considered as the most appropriate method for the cultivation of Basidiomycetous fungi and production of different enzymes produced by them (Pandey *et al.*, 1999), where lignocellulosic substrates such as wood, sawdust, straw or other natural substrates are used as medium (Orth *et al.*, 1993; Pandey *et al.*, 1999; Sanghvi *et al.*, 2010). Production of enzymes by using such substrates is inexpensive and they are easily available. Agro-industrial residues promote the excellent growth of fungi and enhance the enzyme activity by means of supplying the nutrients to the fungi. Thus, because of its low cost and the resulting high levels of enzyme production, SSF as a fermentation medium could be used to scale up the production of laccase, manganese independent peroxidase and manganese peroxidase (Laura *et al.*, 2007). Ligno-cellulosic material may contain specific compounds which stimulate the ligninolytic enzyme synthesis, for instance; the presence of extractive substances, derived from straw was essential for the production of manganese peroxidase by *Phanerochaete chrysosporium* (Kapich *et al.*, 2004). It was also proved by Elisashvili *et al.*, (2006), that the presence of lignocellulosic substrate is mandatory for manganese peroxidase production by *Pleurotus dryinus* IBB 903, since there was no enzyme production when the fungus was grown in the

synthetic medium with different carbon sources. Cullen, (1997) reported that production of manganese peroxidase and lignin peroxidase isoenzymes by *Phanerochaete chrysosporium* are strongly affected by medium composition. Kapich *et al.*, (2004) found a promoting effect of lignocellulose on the production of manganese peroxidase and lignin peroxidase by *Phanerochaete chrysosporium*. Above mentioned information indicates that not only the fungal species and its characteristics are important but also the substrates supporting the growth of fungi are also crucial factors for the production of enzyme.

3.4.1.1 Optimisation of different solid substrates:

In the present study, several agro-industrial wastes were studied in order to determine the most suitable substrate for the production of ligninolytic enzymes by *Irpex lacteus* and *Phanerochaete chrysosporium*. Solid supports like wheat straw, saw dust, ground nut shells, rice bran, sugarcane bagasse, and banana stems were used as a sole carbon source without any mineral supplementation. Solid state fermentation (SSF) was carried out at room temperature, where distilled water served as a moistening agent in the proportion of 1:10 (substrate: liquid). Among the different agro-industrial wastes tested, wheat straw was found to be one of the best lignocellulosic substrate, giving the promising growth and production of all three ligninolytic enzymes [Manganese Peroxidase (MnP), Manganese Independent Peroxidase (MIP), and Laccase], by both the fungal strains used in the present study. Both the fungi grow vigorously on sugarcane bagasse but did not promote notable enzyme activity and found to be the poorest substrate for enzyme production. *Irpex lacteus* produced 480.36, 440.12 and 195.19 IU/ml as the highest activity for manganese peroxidase, manganese independent peroxidase and laccase, respectively. *Phanerochaete chrysosporium*, when grown on wheat straw showed 487.9 IU/ml (manganese peroxidase), 475.92 IU/ml (manganese independent peroxidase), 177.32 IU/ml (laccase) as the

maximum productivity, while the other substrates were relatively less efficient (Figure 3.20 and 3.21).

Enzymes produced in lignocellulose-containing cultures are more likely to resemble the situation in the natural habitat of white rot fungi than the enzyme produced in defined liquid media. It is assumed that the variations in enzyme production by these fungi results due to adaptation to different natural culture conditions and substrates (Conesa *et al.*, 2002). Use of different agro-industrial wastes can be seen for the production of ligninolytic enzymes by using various white rot fungi (Gassara *et al.*, 2010). Pickard *et al.*, (1999) has reported increasing ligninolytic enzyme production of two white rot fungi, *Coriolopsis gallica* and *Bjerkandera adusta* by using cereal brans such as bran flakes, oat bran, wheat bran and rice bran. Sago hampas was also used for laccase production by using *Pycnoporus sanguineus* in SSF (Vikineswary *et al.*, 2006). Use of corncob is a very common SSF substrate and is used by several researchers for enhanced enzyme production (Vares *et al.*, 1995; Couto and Raatto, 1998; Cabaleiro *et al.*, 2002; Oliveira *et al.*, 2006). Niku-Paavola *et al.*, (1988, 1990) found that production of these ligninolytic enzymes maximal in solid state culture of *Phlebia radiata* using wheat straw as a medium. On the other hand, *Pleurotus ostreatus* produces manganese peroxidase isoenzymes on sawdust which is different from those in defined culture media (Giardina *et al.*, 2000, Kamitsuji *et al.*, 2004). Chedchant *et al.*, (2009) showed that *Datronia* sp. KAPI0039 was cultivated on solid agar containing sawdust or rice straw also produced extracellular laccase and manganese peroxidase.

It is well known fact that wheat straw is one of the best substrate for the production of enzyme and it is the most common among all the various substrates that have been employed for this purpose (Pickard *et al.*, 1999; Aikat and Bhattacharyya, 2000; Valaskova and Baldrian, 2006). Maximum production of ligninolytic enzymes during wheat straw degradation by fungi has already been reported by earlier workers (Arora *et al.*, 2002; Rodrigues *et al.*, 2006, Zhang *et al.*, 2008; Shrivastava *et al.*,

200571
(343)

2010). The highest manganese peroxidase activity of *Phlebia radiata* and *Pleurotus spp.* was also recorded in solid-state cultures containing wheat straw (Vares *et al.*, 1995; Burlat, 1998). Manganese peroxidase is the major protein produced during growth of some white rot fungi on wheat straw (Golovleva *et al.*, 1993; Vyas *et al.*, 1994; Hofrichter *et al.*, 1997). The use of wheat straw for the production of laccases has been reported widely from fungal as well as Actinomycetes strains (Berrocal, 1997; Rodriguez, 2005). Gupte *et al.*, (2007) found that wheat straw as the best substrate followed by wheat bran, rice bran, corn bran and coconut coir for production of ligninolytic enzymes by *Irpex lacteus* and *Phanerochaete chrysosporium*. In the present study also, compared to other substrates used wheat straw was proved to be the best substrate for the production of ligninolytic enzymes. Therefore, it is necessary to select fungus specific growth substrate for the maximal production of targeted enzymes.

3.4.1.2 Optimisation of particle size:

Along with the substrate, its concentration also plays an important role in the enzyme production. Gupta *et al.*, (2009) found that an increase in concentration of substrate lead to a decrease in enzyme activity. Declined enzyme production may be due to the fact that a high substrate concentration led to increased viscosity, which influenced medium components and oxygen transfer (Gupta *et al.*, 2009; Sanghvi *et al.*, 2010). As the growth of fungi and production of the enzyme is clearly dependent on the particle size of the substrate used, optimisation of the wheat straw as an agro-industrial waste should be followed by determining the effect of different particle sizes on ligninolytic enzyme production. Use of wheat straw as a substrate becomes more exponential when the appropriate particle size of the substrate is used (Sanghvi *et al.*, 2010). Nine different particle sizes (<1, 1, 1.5, 2, 2.5, 3, 3.5, 4 and >4mm) were examined in order to determine the production of the highest enzyme activity. *Irpex lacteus* and *Phanerochaete chrysosporium* both produced highest manganese peroxidase, manganese independent peroxidase and laccase

with 1mm sieve size particles. The production of the highest titre of all three enzymes by *Irpex lacteus* was 480.36 IU/ml (MnP), 440.12 IU/ml (MIP) and 195.19 IU/ml (Laccase), where as *Phanerochaete chrysosporium* exhibited 487.9, 475.92 and 177.32 IU/ml activity for MnP , MIP and laccase production, respectively (Table 3.5 and 3.6).

Effect of particle size on enzyme production may be associated with the surface area available to the fungus (Sanghvi *et al.*, 2010). These findings also confirmed that the size of the carbon source is an important factor in production of enzymes by using SSF method (Kalogeris *et al.*, 1998). In solid culture, the particle size of the substrate determines the void space which is occupied by air (oxygen). Since the rate of oxygen transfer into the void space affects growth, the substrate should contain particles of suitable sizes to enhance mass transfer (Pandey, 1992). In the present study also, particles with 1mm sieve size gave highest production of manganese peroxidase, manganese independent peroxidase and laccase. Production of these enzymes was less at the particle size smaller than 1mm sieve size. Reduced enzyme production may be associated with increased viscosity and poor aeration (as the small particles are very closely arranged) to the organism growing on it (Sanghvi *et al.*, 2010; 2011).

3.4.1.3 Optimisation of incubation time:

Production of the enzymes is attributed to the duration of the culture conditions provided to the growth medium. In general, many Basidiomycetes initiate the production of enzymes after 2 or 3 days of growth, and decline within 2 to 3 weeks. The approach used for the isolation may be improved by constant monitoring of the production of the extracellular enzymes of interest, rather than using a set (Jordaan, 2003). In the present study, the ligninolytic enzyme activity was determined after every three days of interval for 18 days to conclude the optimum incubation period for maximum enzyme production. Production of all three ligninolytic enzymes by both the fungal strains (*Irpex lacteus* and

Phanerochaete chrysosporium) started from the 3rd day of the fungal inoculation. In case of *Irpex lacteus*, manganese peroxidase, manganese independent peroxidase and laccase attained their peak activity on the 6th day of inoculation at 35°C. It was then declined gradually after the 6th day of incubation. Thereafter, increased incubation period did not improve enzyme production; rather it resulted into decreased enzyme production (Table 3.7). On the other hand, *Phanerochaete chrysosporium* showed the highest production of ligninolytic enzymes on the 9th day of incubation at 35°C. Similar to former species, decline in enzyme production was observed after 9 days of incubation and thereafter it declines with increasing incubation time (Table 3.8). It is well documented that after a certain limit, enzyme production could decrease because of depletion of nutrients due to the enhanced biomass which would result in a decreased metabolic activity (Kashyap *et al.*, 2002). Therefore, 6th and 9th day of incubation periods were taken as optimum for the maximum ligninolytic enzyme production by both *Irpex lacteus* and *Phanerochaete chrysosporium*, respectively.

Available literature indicates that incubation time for maximal production of these enzymes varies from species to species. Tekere *et al.*, (2001a, b) showed that the manganese peroxidase and laccase production starts after 3rd day of culture growth and the highest amounts of extracellular enzymes may be recorded on 28th day (Levin *et al.*, 2010). Vaithanomsat *et al.*, (2010) showed that *Datronia* sp. KAPI0039 produced laccase and the highest MnP after 8 days of cultivation. Schlosser *et al.*, (1997) documented that in SSF when wheat straw was used as a substrate, *Trametes versicolor* produced the highest titre of ligninolytic enzymes within 14 days of incubation while Collins and Dobson, (1997) recorded the maximum enzyme yield on the 10th day by using same fungal strain i.e. *Trametes versicolor*. According to Arora *et al.*, (2002) and Zhang *et al.*, (2008), the highest production of manganese peroxidase and laccase occurs after 10 days of *Trametes versicolor* incubation while Shrivastav *et*

al., (2010) recorded that production of enzyme by *Trametes versicolor* reached its peak on 5th day of incubation.

In the present work, *Irpex lacteus* revealed peak enzyme activity on the 6th day of solid state fermentation, whereas *Phanerochaete chrysosporium* shown the potential activity after 9 days of cultivation. On the basis of available results, it appears that though the fungal strain may produce all three ligninolytic enzymes, their maximum production may vary within same species or may be in another species. ^{between?} ✓

3.4.2 Production profile of ligninolytic enzymes:

Perusal of literature suggests that production of ligninolytic enzymes may vary from species to species. Some white rot fungi produce all three enzymes, some only two, and a few, apparently, only one (Eriksson *et al.*, 1990; Orth *et al.*, 1993; Hatakka, 1994). Both the strains selected in the present study produce all three enzymes (Manganese Peroxidase, Manganese Independent Peroxidase and Laccase). Among these enzymes laccase and manganese peroxidase are considered to be the most common ligninolytic enzymes produced by white rot fungi (Nerud and Misurcová, 1996). *Pycnoporus cinnabarinus* produce laccase as the sole ligninolytic enzyme, which enables the fungi to degrade lignin (Eggert *et al.*, 1996). In many fungi, the main role in lignin degradation is ascribed to lignin and Mn-dependent peroxidases (Leonowicz *et al.*, 1999) and several workers obtained MnP-laccase combination as the most common group of enzymes in the white rot fungi (Pelaez *et al.*, 1995; Nerud and Misurcova, 1996). Banyan/cult
Biology
Gorb?

According to Wesenberg *et al.*, (2003), the most common ligninolytic peroxidases produced by almost all white rot Basidiomycetes and by various litter-decomposing fungi are manganese peroxidases (MnPs). Vaithanomsat *et al.*, (2010) concluded that *Datronia* sp., KAPI0039 though produced both laccase and manganese peroxidase enzymes, production of manganese peroxidase was maximal as compared to laccase. In the

present investigation, *Irpex lacteus* produced 560.6 IU/ml manganese peroxidase, 534.4 IU/ml manganese independent peroxidase and 263.22 IU/ml laccase while *Phanerochaete chrysosporium* showed 607.35 IU/ml manganese peroxidase, 539.27 IU/ml manganese independent peroxidase and 263.03 IU/ml laccase. When the resulting activity of *Irpex lacteus* and *Phanerochaete chrysosporium* was compared, it was observed that among all the three enzymes, production of manganese peroxidase was highest. Moredo *et al.*, (2003) found *Phanerochaete chrysosporium* to produce 1070–1230 U/l on 11th day of incubation using grape seeds and barley bran. Villas-Bôas *et al.*, (2002) utilized *Candida utilis* for the production of ligninolytic enzymes such as pectinase, manganese-dependent peroxidase, cellulase and xylanase by using apple pomace and reported very low yield of manganese-dependent peroxidase (19.1U/ml). Gupte *et al.* (2007) observed the highest production of manganese peroxidase (20.2 U/ml) after 10 days of incubation with *Phanerochaete chrysosporium* in media containing wheat straw. On the other hand, Hailei *et al.*, (2009) recorded the highest manganese peroxidase activity (1913±59U/l) on 5th day of incubation with *Phanerochaete chrysosporium*. mistake
ref

Available literature indicates that production of manganese peroxidase and laccase by different white rot fungal strains are more common and predominant (Vyas *et al.*, 1994; Hofrichter *et al.*, 1999; Tekere *et al.*, 2001; Arora *et al.*, 2002; Laura *et al.*, 2010). On the contrary, our results show a general predominance of manganese peroxidase and manganese independent peroxidase enzymes. Moreover, the biosynthesis of MnP by some Basidiomycetes needs a comparatively high content of manganese (Tekere *et al.*, 2001) and the same is found with *Irpex lacteus* and *Phanerochaete chrysosporium* in the present work. Additionally, *Trametes versicolor* is also known to produce manganese peroxidase (Johansson *et al.*, 1990) as do many other fungi in the genus *Trametes* (Vares and Hatakka, 1997).

As per previous findings, *Irpex lacteus* belongs to the group of white rot fungal species that are able to produce lignin peroxidase, manganese

peroxidase (Cajthaml *et al.*, 2008) and laccase (Novotný *et al.*, 2000), in which it resembles *Phlebia radiata* and *Trametes versicolor* (Hatakka, 1994). Tereke *et al.*, (2001) have reported that *Irpex* spp. had the highest manganese peroxidase activity under conditions of high nitrogen and low carbon, while Gupte *et al.*, (2007) and Kasinath, (2002) reported that *Irpex lacteus* lack manganese peroxidase activity. According to Novotný *et al.*, (2001), *Irpex lacteus* has yielded very low level of manganese peroxidase. However, our results disagree with the earlier reports due to production of manganese peroxidase as a dominant enzyme by *Irpex lacteus*. Recently, Sklenar *et al.*, (2010) have also reported that *Irpex lacteus* is a source for the production of manganese peroxidase as compared to strains of white rot fungi that are producing other ligninolytic enzymes. In the present investigations, *Irpex lacteus* was detected as the best producer of manganese peroxidase than that of manganese independent peroxidase and laccase but if compared with *Phanerochaete chrysosporium*, it is found to be secondary. The presence of low laccase activity agreed with the finding that; even though *Irpex lacteus* was found to produce extracellular laccase (Novotný *et al.*, 2000), the enzyme activity measured in the culture medium was usually low (Kasinath *et al.*, 2003; Svobodová *et al.*, 2007).

Phanerochaete chrysosporium is also used for the production of several extracellular enzymes, such as manganese peroxidase (MnP), lignin peroxidase (LiP) and laccase that are capable of degrading lignin (Hatakka, 1994). Lignin peroxidase and manganese peroxidase have been the most intensively studied extracellular enzymes of *Phanerochaete chrysosporium*, and several reviews have summarized their biochemistry (Higuchi, 1990; Schoemaker and Leisola, 1990). The manganese peroxidase and lignin peroxidase are the main extracellular ligninolytic peroxidases from *Phanerochaete chrysosporium* (Tien and Kirk, 1984; Tang *et al.*, 2006). Earlier workers have also reported that *Phanerochaete chrysosporium* to produce the highest manganese peroxidase activities (Reid and Deschamps, 1990; Valmaseda *et al.*, 1991; Vyas *et al.*, 1994;

Moldes *et al.*, 2003); which appears to be very much true in case of our study. Lankinen, (2004) and Gupte *et al.*, (2007) reported the absence of laccase in *Phanerochaete chrysosporium*. We disagree with the reports of Lankinen, (2004) and Gupte *et al.*, (2007), it is true that production of laccase is relatively less as compared to other enzymes but it is not completely absent. Gnanamania *et al.*, (2006) reported that *Phanerochaete chrysosporium* requires inducer to produce Laccase.

In the present investigation, manganese peroxidase, manganese independent peroxidase and laccase were produced by *Irpex lacteus* and *Phanerochaete chrysosporium* on solid state fermentation by using wheat straw as a substrate. The production profile of manganese peroxidase was higher than that of manganese independent peroxidase and laccase activity. In case of both the strains, partial purification of crude enzymes was carried out by using ammonium salt purification method. Therefore, it was essential to undertake all the purification steps at 4°C in order to ensure the purity of the final product of enzyme. About 90% of proteins in the crude extract were filtered/separated out in the 80% saturation by ammonium sulphate. The enzyme activities determined from these all the saturated fractions are mentioned in Figure 3.22 and 3.23.

3.4.3 Molecular weight determination:

The ammonium sulphate fractions (20-80% saturation) containing about 90% of manganese peroxidase was subjected to molecular weight determination. From all 20, 40, 60 and 80% saturated fractions of crude enzyme, *Irpex lacteus* showed maximum (560.6 IU/ml) MnP activity with 40% saturated fraction, while *Phanerochaete chrysosporium* was well exhibitor of optimum MnP activity with 60% saturation. These fractions were dialysed with the membrane having 12000 to 14000 Da cut off value. These dialysed fractions when subjected to gel electrophoresis, the enzymes appeared as distinct bands on SDS-PAGE. *Irpex lacteus* yielded 58.3 kDa MnP molecular mass, whereas, the molecular weight (MW) of

MnP produced by *Phanerochaete chrysosporium* was 52.8 kDa (Figure 3.24).

Hofrichter (2002) revealed that MnPs of white rot fungi usually have a MW of 45 kDa. Shin *et al.*, (2005) isolated MnP from *Irpex lacteus* with the molecular mass of 53.2 kDa, while Baborová *et al.*, (2006) exhibited the 37.5 kDa MnP from *Irpex lacteus*, which is very less compared to our results. Molecular weight of MnP obtained from *Phanerochaete chrysosporium* is recorded 46 kDa (Glenn and Gold, 1985; Rüttimann-Johnson *et al.*, 1994; Matsubara *et al.*, 1996; Takano *et al.*, 2004) while in the present study it is found to be 48.3 kDa and 45 kDa in case of *Phanerochaete crassa* and *Phanerochaete sordid*, respectively. The four different isoenzymes of *Flavodon flavus* MnP showed 43, 52, 78.5, and 99 kDa bands (Raghukumar *et al.*, 1999). Cheng *et al.*, (2007) reported 47.7 kDa molecular weight of MnP isolated from *Schizophyllum* sp. F17, which falls within the range of the MnP family (38-50 kDa). This result was similar to *Dichomitus squalens* MnP₁ and MnP₂ exhibiting 48 kDa and 48.9 kDa, respectively (Perie *et al.*, 1996; Fakoussa *et al.*, 1999). MnP from a white rot fungus *Nematoloma frowardii* has 44 kDa of molecular weight (Schneegass *et al.*, 1997; Steffen, 2003). The molecular mass (MW) value (44 kDa) of the purified MnP obtained from *Collybia dryophila* are in the typical range for MnPs from white rot fungi and other litter decomposers (Hatakka, 2001; Steffen *et al.*, 2002). The MW of MnPs produced by *Stropharia rugosoannulata* ranged from 41-44 kDa, while the MnP of *Agaricus bisporus* has MWs of 40 kDa which are in the same range of the MnPs from *Stropharia coronilla* and *Stropharia rugosoannulata* (Steffen, 2003). The observations were also recorded for MnP produced by *Trametes* sp., having typically 45 kDa molecular mass (Jenness, 2007).

3.5 Effect of Physico-chemical factors on enzyme activity:

Some factors, such as reaction time, pH, metal ion and temperature exert significant influence on the activity of enzymes.

3.5.1 Influence of reaction time:

Time required for the reaction of enzyme and the substrate used as chromogen, directly influences the enzyme activity. It is very necessary for the reaction mixture to get the appropriate time to react, at which the determined enzyme activity would be optimum. In the present investigation, the range of time period from 5 to 45 minutes was checked in order to find out the maximum enzyme activity. The promising results were obtained in 10 minutes of reaction and the optimum manganese peroxidase, manganese independent peroxidase and laccase activities noted were 560.6 IU/ml, 534.4 IU/ml and 263.22 IU/ml with *Irpex lacteus*, respectively; whereas *Phanerochaete chrysosporium* showed 607.35 IU/ml manganese peroxidase, 539.27 IU/ml manganese independent peroxidase and 263.03 IU/ml laccase (Table 3.9 and 3.10).

HO
discuss it
?

3.5.2 Influence of pH:

Enzymes are considered to be highly sensitive to pH. It is an important factor to control the activity of manganese peroxidase and lignin peroxidase (Silva *et al.*, 2008). In the present study, activity of the ligninolytic enzymes by *Irpex lacteus* and *Phanerochaete chrysosporium* under different pH showed considerable variation (Figure 3.25 and 3.26). *Irpex lacteus* showed the highest amount of manganese peroxidase, manganese independent peroxidase and laccase activity at pH 5, whereas with *Phanerochaete chrysosporium*, the highest titre of all three ligninolytic enzymes (manganese peroxidase, manganese independent peroxidase and laccase) production was recorded at pH 5.5. Value of hydrogen ion concentration beyond and below 5 and 5.5 resulted in declined activity of all the three enzymes obtained from *Irpex lacteus* and *Phanerochaete chrysosporium*, respectively. This may be attributed to the fact that change in the pH may alter the three-dimensional structure of the enzymes (Shulter and Kargi, 2000).

Most enzymes are (best) active in the lower pH range i.e. pH 2 to 4 (Baldrian, 2006; Kilaru, 2006). Extracellular MnP production under alkaline conditions has been reported in *Aspergillus terreus* (Kanayama *et al.*, 2002). MnP activity of *Irpex lacteus* was maximal at pH 5 when analysed at 25°C (Sklenar *et al.*, 2010), which is very much similar to our results. Baldrin, (2004) has also found that the optimum pH for Mn²⁺ oxidation of *Agaricus bisporus* was pH 5 which is typical for fungal MnPs. According to Glenn *et al.*, (1986), MnP of *Irpex lacteus* and *Phanerochaete chrysosporium* have a broad pH range (4 to 7.6). Baborová *et al.*, (2006) has detected 5.5 as optimum pH for the enzyme produced by *Irpex lacteus*, which is slightly higher than that of other MnPs purified so far. As reported by earlier workers that *Phanerochaete chrysosporium*, *Ceriporiopsis subvermispora* and *Pleurotus ostreatus*, has the optimum pH range between 4.5 and 5.5 (Glenn and Gold, 1985; Becker *et al.*, 1993; Tapia and Vicuna, 1995). Lundell *et al.*, (1990) suggested that pH range between 4.5 and 5.5 favours the release of extracellular enzymes. Silva *et al.*, (2008) has also reported pH 5 is optimum for the recovery of MnP produced by *Phanerochaete chrysosporium*. On the other hand, Gassara *et al.*, (2010) found no effect of pH on production of MnP. There are reports that most of the white rot fungi displayed much higher laccase activity at acidic pH and high temperature (Eggert *et al.*, 1996b; Calvo, 1998; Saparrat *et al.*, 2002; Jordaan *et al.*, 2004; Baldrian, 2004, 2006; Hildén, 2007; Litthauer *et al.*, 2007). Our results are in agreement with the previous reports that maximum laccase production by *Irpex lacteus* and *Phanerochaete chrysosporium* was exhibited within the acidic pH range. *Daedalea quercina* required 1.8 and 2 pH for the maximum laccase production (Baldrin, 2004), which is very much far away to our findings.

3.5.3 Influence of incubation temperature:

Temperature is one of the significant parameter for the determination of the growth of the fungi, enzyme production and its activity. This is because during the fermentation there is general increase

in the temperature of the fermenting mass due to respiration (Niladevi *et al.*, 2007). In the present investigation, optimisation of the temperature for attaining the excellent enzyme activity was carried out within the range of 5 to 45°C. The variation in the temperature showed the fluctuation in the activity as it directly affects the growth of the fungi. *Irpex lacteus* and *Phanerochaete chrysosporium* (both) exhibited the maximum enzyme activity at 35°C and then increase in the temperatures led to the decline of enzyme activity. For further optimisation, 35°C was considered as optimum temperature for maximum ligninolytic enzyme activity (Figure 3.27 and 3.28). The result indicates that the production of enzyme is related to the growth of fungi at particular temperature.

missy
ref.

Available literature suggests that manganese peroxidase has an optimal activity between 23 and 40°C (Aitken *et al.*, 1989; Forrester *et al.*, 1990; Shin *et al.*, 2005) while Baborová *et al.*, (2006) isolated highest titre of MnP isoenzymes at 50 to 60°C. Recently, Sklenar *et al.*, (2010) has also shown the reasonable temperature range up to 50°C for the production of MnP by *Irpex lacteus*. In support to the values reported in the present study, Hestbjerg *et al.*, (2003) and Couto *et al.*, (2006) has mentioned that *Phanerochaete chrysosporium* has a high temperature requirement (30 to 37°C) for growth and production of ligninolytic enzymes. Tien and Kirk, (1988) and Vyas *et al.*, (1994) found 39°C as the optimum temperature for the growth of *Phanerochaete chrysosporium* and production of spores which is slightly higher if compared with our results. Svobodova *et al.*, (2008) noted that temperature optimum for the mycelium-bound *Irpex lacteus* enzyme to be 50°C and noted that the enzyme activity was lost rapidly at temperatures higher than 60°C.

Many previous studies had considered the impacts of temperature on laccases activities (Jordaan and Leukes, 2003; Kimet *et al.*, 2008). The optimum temperature value reported for the laccase is 55 to 60°C for *Botrytis cinerea* (Zouari *et al.*, 1987). However, laccase obtained from *Fomes fomentarius*, requires an optimum temperature of 52°C (Rogalski *et al.*, 1991), and for *Chaetomium thermophile*, an optimum temperature is

missy
reference

reported between 50 and 60°C (Chefetz *et al.*, 1998). Many researchers have showed the optimum laccase activity between 50 and 70°C (Eggert *et al.*, 1996a, b; Saparrat *et al.*, 2002; Jordaan. *et al.*, 2004; Baldrian, 2004, 2006). Contrary to these all, Jordaan *et al.*, (2003) recorded that *Trametes versicolor* exhibits a high level of laccase activity at temperature values 30 to 40°C. It is very well corresponding with our results of *Irpex lacteus* and *Phanerochaete chrysosporium* where both the strain produced the highest laccase activity at 35°C.

3.5.4 Influence of metal ions:

The effect of metal ions on enzyme production concluded that some microelements conferred a significant impact on enzyme activity (Baldrian *et al.*, 2005). In the present study, five different metal ions Mn^{2+} , Zn^{2+} , Cu^{2+} , Ca^{2+} , and Mg^{2+} were examined for their ability to affect the enzyme activity. Several chemicals, e.g., copper sulphate, veratryl alcohol, and 2,5-xylidine etc., have been found to have an inducing effects on laccase production in numerous white rot fungi (Eggert *et al.*, 1996; Palmieri *et al.*, 2000; Saparrat *et al.*, 2002) recorded significant effect of Mn^{2+} on manganese peroxidase activity of *Irpex lacteus* (Susla and Svobodova, 2007) and *Phanerochaete chrysosporium* (Bonnarme and Jeffries, 1990; Mester and Field, 1997). Verma and Datta, (2003) also observed that the supplementation of Mn^{2+} to media increased decolourisation rates and enzyme activities. The requirement for manganese in the culture medium to increase MnP activity is characteristic for most of the white rot fungi (Bonnarme and Jeffries, 1990, 1991; Scheel *et al.*, 2000). It is known fact that supplementing cultures with manganese and aromatic compounds can stimulate the MnP activity, acting as inducers, enhancers or mediators (Hofrichter *et al.*, 1997). In wood, Mn^{2+} occurs at very low concentrations thus determines the effect of Mn^{2+} on enzyme production at low Mn^{2+} concentrations in the medium (Tereke *et al.*, 2001). Hars and Huttermann, (1983) and Sutherland *et al.*, (1983) have also revealed that Mn^{2+} may be responsible for higher production of MnP activity by

Phanerochaete chrysosporium. Unlike previous study, no effect of these metal ions is observed in the present study.

Zouari-Mechichi *et al.*, (2006) showed that the presence of Mn^{2+} slightly increases the laccase activity levels in the cultures of *Trametes trogii*. They have also investigated the effect of Cu^{2+} on production of laccase and reported that Cu^{2+} acts as strongest inducer of laccase. Copper as an inducer of fungal laccases has also been reported in other fungal species by earlier workers (Collins and Dobson, 1997; Garzillo *et al.*, 1998; Galhaup *et al.*, 2002a, b; Couto *et al.*, 2004; Ozsoy *et al.*, 2005). Rosale *et al.*, (2007) found that *Trametes hirsuta* grown on orange peels supplemented with 1mM copper sulphate under solid-state conditions increases laccase production. The highest laccase activity (3-fold increase than the media without inducer) is reported by Couto *et al.*, (2009) by adding 0.5mM Cu^{+2} to the culture medium. These results clearly showed the positive effect of copper sulphate as an inducer of laccase activity (Gassara *et al.*, 2010).

In the present study, the activity of MnP, MIP and Laccase are not affected by the presence of metal ions in enzyme reaction mixture. However, there are no unanimous opinions about the role of metal ions on the production and activity of various ligninolytic enzymes. Baldrian *et al.*, (2005) showed that the MnP activity was less affected in the presence of Mn, Cu, and Pb; although the average MnP activity in the presence of Mn was lower than the media without Mn. The manganese peroxidase levels produced by *Pleurotus eryngii* were highest in the absence of Mn^{2+} (Mester and Field, 1997). Similarly, Svobodova *et al.*, (2008) has also found that the addition of laccase inducers (copper sulphate or 2, 5-xylidine) to *Irpex lacteus* cultures did not influence the biomass growth nor the secretion of laccase in the liquid culture. Our results are in agreement with Svobodova *et al.*, (2008) and herewith we reconfirmed that *Irpex lacteus* do not show any effect of inducer on enzyme production.

3.6 FTIR (The Fourier Transform Infrared Spectroscopy)

White rot fungi constitute a diverse eco-physiological group comprising mostly Basidiomycetous fungi capable of aerobic lignin depolymerisation and mineralisation, playing a central role in the global Carbon cycle (McMullan *et al.*, 2001; Wesenberg *et al.*, 2003). White rot fungi attract growing attention for its use in bioremediation processes since these organisms have the ability to degrade a broad range of environmental pollutants, including highly recalcitrant synthetic dyes and a wide range of xenobiotics (Paszczynski and Crawford, 1995; Fu and Viraraghavan, 2001; Pointing, 2001; Van der Zee, 2002; Rabinovich *et al.*, 2004; Novotný *et al.*, 2004a, b; Resmies *et al.*, 2010). The xenobiotic compounds include a wide variety of recalcitrant synthetic compounds, like chlorinated organic compounds, dioxins, polycyclic aromatic hydrocarbons (PAHs), polychlorinated biphenyls (PCBs), synthetic polymers and also synthetic dyes (Paszczynski and Crawford, 1995; Reddy, 1995; Pointing, 2001; Robinson *et al.*, 2001a, Wesenberg *et al.*, 2003; Forgacs *et al.*, 2004; Rabinovich *et al.*, 2004). Degradation of these various xenobiotic compounds including dyes directly entails the ligninolytic system of white rot fungi. The ability of the white rot fungi to degrade a wide range of recalcitrant dyes has generally been associated with the non-specific nature of their lignin modifying enzymes (Field *et al.*, 1993; Goszczynski *et al.*, 1994). For the confirmation of biodegradation of these compounds by ligninolytic enzymes, FTIR analysis was carried out by earlier workers (Parshetti *et al.*, 2006; Kalme *et al.*, 2007; Dhanve *et al.*, 2009; Ghodake *et al.*, 2009). In the present investigation, the FTIR spectra of all ten tested control and treated dyes showed the specific peaks in specific region (4000 to 500 cm^{-1}). The stretching vibration at 3456 cm^{-1} represented the -N-H stretching which indicates the nature of aromatic amine group present in the parent dye compound. Azo dyes are aromatic compounds with one or more azo bonds (-N=N-). The presence of -C-H and -N=N- stretching confirmed the azo groups present in the dye, while -SO_2 stretch represented the presence of sulphur group in the dye

structure. These all the stretchings confirm the structures of the dyes. When the spectrum of control and treated dyes were compared, changes in the positions of these peaks were observed. Shifting of these peaks to another position from their original position indicates degradation of original structure of the dye. Similar changes in the peak of different dyes has already been reported by earlier workers (Field *et al.*, 1993; Goszczynski *et al.*, 1994; Parshetti *et al.*, 2006; Kalme *et al.*, 2007; Dhanve *et al.*, 2009; Ghodake *et al.*, 2009). The FTIR spectral comparison between control dye and samples treated with ligninolytic enzymes of *Irpex lacteus* and *Phanerochaete crysosporium* showed degradation of all the ten dyes tested (Figure 3.29 to 3.38).

?
What change

II. Histological study

3.7 RESULTS

3.7.1 ALIANTHUS EXCELSEA Roxb.

Wood Decay by Inonotus hispidus:

Appearance of decay: In humid condition, the outer dead bark gets exposed, due to mechanical injuries such as pruning, cut branch stubs, wood boring insects and beetles became main source of infection. Insects make holes/tunnels into sapwood through the bark of healthy or stressed trees (Figure 3.39A, B). When such infected stems and branches were debarked, they usually exhibited areas of wood which showed the infected and healthy portion of wood. Naturally infected wood can be easily recognized macroscopically by black lines or bands produced by fungi in the decayed wood while fungal infection due to beetle attack showed dark rings encircling the tunnels (Figure 3.39A, B). Naturally infected wood stained dirty whitish-grey to yellowish brown colour. However, variations in wood colour or pattern of lines/patches were characteristics to individual fungal species. When these samples were carefully cut within the same wood block and inoculated on Potato Dextrose Agar media, it

was found that these demarcating lines/patches were colonies of individual fungal species such as *Inonotus hispidus*, *Fusarium* sp., *Chaetomium* sp., *Alternaria alternata*, *Penicillium* sp., etc.

Histology of decay: As mentioned earlier, fungal infection by *I. hispidus* is associated with branch stubs, pruning wounds or tunnels made by wood borer insects. Fungal hyphae were ~~the~~ most abundant within the lumina of vessels, xylem rays and fibres (Figure 3.39C, D). They were 1 to 2 μm in diameter and septate. Fungal hyphae attacked all the cell types of secondary xylem but vessel members were found to be relatively resistant to fungal attack (Figure 3.39F), preferential degradation of xylem fibres resulted in a distinct degradation pattern (Figures 3.39F, 3.40A).

Sections passing through the borer holes, branch stubs and pruning wounds showed that mycelia travelled through vessel lumen via rays and infected all the cell types of secondary xylem. Fungal hyphae invades neighbouring cell through the pits present on the lateral walls (Figure 3.39F). In the advanced stage of decay, wood became completely eroded, and soft; light in weight and lost its original colour. At cellular level, cell walls also lost their integrity and several cavities of various shapes and size developed in the cell walls (Figure 3.40A). In the wood fibres, hyphae entered from the adjacent vessels via rays (Figure 3.40B, C) by cell wall erosion (Figure 3.40D). Hyphal growth was mostly confined to the secondary walls of fibres, where the majority of hyphae and their associated bore hole were around $1\mu\text{m}$ in diameter (Figure 3.40D). The hyphae had frequently grown transversely through the cell walls of fibres and often diverted within secondary walls around lumina of fibres (Figure 3.39F, 3.40A). The cell walls of xylem rays and vessels showed no visible signs of fungal attack (Figure 3.40E), but fibres showed the first sign of structural alterations, which were typical of soft rot attack. Although, hyphae were also visible within the fibre lumen, cell wall degradation was only apparent where hyphal tunnelling had occurred within the cell walls (Figure 3.40F).

The degradation pattern of *I. hispidus* resembled selective delignification i.e. at an early stage of decay, degradation commenced in the corner of fibres, along the middle lamellae without any pronounced effect on the primary and secondary wall layers (Figure 3.41A). Sections stained with safranin and Astra blue showed that the discoloured inner secondary wall was delignified and stained blue due to absence of lignin. As the decay progressed further, localized degradation of lignin, hemicellulose and cellulose resulted in the formation of small cavities within S₂ layer of secondary wall of libriform fibres (Figures 3.40F, 3.41B). Single cavities were 2 to 4 µm in tangential diameter but the most of the times 2 to 3 cavities fused together to form a relatively larger one. (Figure 3.41C, D). These cavities were consistently separated from one another by radial structure (Figure 3.40F).

Transverse sections showed hyphal growth and formation of tunnels within S₂ layers by branches or extension of hyphae penetration into xylem fibres (Figure 3.40A, 3.41D). These hyphae changed their direction to grow inside the cell wall after crossing the S₂ layer. This type of attack by *I. hispidus* resembled the characteristic features of soft rot with a typical 'L-bending' of hyphae (Figure 3.41E). In advanced stages of decay, several small cavities were merged to form tunnels of indefinite length and shape (Figure 3.40A, F). These tunnels may be oval, circular (Figure 3.41C, E, F), irregular (Figures 3.40D, 3.41D), 'C' shaped or half-moon shaped (Figures 3.40A, 3.42D) and 'L' or 'T' shaped (Figure 3.41C, E). In addition to cavities formed by hyphae within the cell wall, discrete notches of cell wall erosion by hyphae lying within the lumina were also observed frequently in the cell walls of the xylem fibres (Figure 3.41E).

As compared to fibres, vessels were relatively resistant to the fungal attack and degradation of their cell walls was very slow. Although, several fungal hyphae ramified on the inner walls through the vessel lumen (Figures 3.39C, F, 3.40E), it was markedly delayed and structural alterations commenced only after complete degradation of adjacent of

fibres (Figure 3.40F, 3.42D). Unlike xylem fibres, vessel walls showed progressive delignification in the secondary wall from the lumen to middle lamellae rather than formation of cavities. Delignification of middle lamellae eventually resulted in the separation of cell walls (Figures 3.41C, 3.42D).

At an advanced stage of decay xylem fibres^{walls} became completely degraded (Figure 3.39G) and lost their integrity and rigidity (Figure 3.42A, B), whereas vessel lumens were filled with sclerotic tissue formed by fungal hyphae (Figure 3.42E, F). These sclerotic tissues were the main source of fruiting bodies that came out from the injured stem and branch stubs.

3.7.2 AZADIRACHTA INDICA (L.) DEL.

Structure of wood: Secondary xylem of *Azadirachta* was diffused porous with indistinct growth rings. Annual increment of the xylem may be discerned by wide bands of axial parenchyma between two successive rings. The secondary xylem was composed of vessels, fibres, axial and ray parenchyma cells. Vessels were mostly solitary but radial multiples of 2 to 6 vessels were also seen frequently. Xylem rays were uni-multiseriate, compound and heterocellular.

Histology of Wood Decay by *Irpex lacteus*: After 30 days of fungal inoculation, there was no appreciable weight loss of wood block, but the fungal mycelia invaded all the cell types of the secondary xylem. Initially fungal mycelia began to ramify on wood block and ultimately covered the whole block within 15 days. In the beginning, mycelial invasion was observed through the lumen of both large and small vessels (Figure 3.43A, B). From the vessels, hyphae traversed into the neighbouring rays and vessels associated axial parenchyma cells (Figure 3.43C). These fungal mycelia gradually extended in all directions including xylem fibres and adjacent axial parenchyma cells (Figure 3.43C, D). Vessels and axial parenchyma was observed as the main path for vertical movement and

invasion of wood tissue (Figure 3.43D, E), while xylem rays acted as main path for the radial dispersal of fungal mycelia (Figure 3.43F). At this stage, no visual damage was observed in the cell walls. Fungal mycelia moved from one cell to the next through the pits present on their walls. Presence of fungal mycelia in all the cell types of xylem adjacent to vessel elements was a common feature in all the samples studied.

Decay fungi	% Weight loss (60 days)	% Weight loss (90 days)	% Weight loss (120 days)
<i>Irpex lacteus</i>	18.09 (+ 4.23)	23.37 (+ 5.48)	29.79 (+ 5.67)
<i>Phanerochaete chrysosporium</i>	21.97 (+ 5.73)	29.08 (+ 4.94)	37.73 (+ 6.39)

Table 3.11: Average percent weight loss of *Azadirachta* wood during each incubation period

Wood samples exposed to fungi for 60 days showed that almost all the cell types of secondary xylem were invaded by fungal mycelia (Figure 3.44A). At this stage, wood blocks showed about 18.09 % of weight loss (Table 3.11) and sign of selective delignification were much distinct in all the cell types. Delignification can be very easily detected in xylem fibres i.e. by defibration due to ligninolytic activity of fungal enzymes. In transverse view, many of them showed concentric delignification starting from middle lamellae towards lumen. As a result, the secondary wall adjacent to the middle lamellae stained blue with astra blue instead of red by safranine. This feature was initially observed in the fibres adjacent to the rays, axial parenchyma cells and vessel elements. The middle lamellae that were stained blue, began to lose the integrity and individual cells became separated from each other (Figure 3.44B, C). As the degradation progressed further, complete separation of fibres was a common feature and it was observed in most of the sections (Figure 3.44C). Except defibration, no much visual damage was observed in the axial elements but the radial system showed considerable variations and alterations in

the cell walls. Pits of the ray and axial parenchyma cells became more pronounced and became larger in size and irregular in shape. At the same time, formation of several bore holes on the lateral walls of the rays was a common feature (Figure 3.44D). Compared to axial elements, ray cells were more affected showing advanced thinning of the cell walls. Ray cell walls also showed separation from each other due to dissolution of middle lamella (Figure 3.44E) while vessels just began to separate from each other (Figure 3.44F). Though, dissolution of middle lamella resulted in the separation of vessels, there was no much cell wall damage observed.

Wood blocks after 90 days of incubation showed more pronounced effect on the cell wall of all xylem elements. As the degradation progressed further, complete separation of fibres was a common feature in most of the sections observed studied. Due to delignification, pits on the lateral walls of the fibres became more prominent and became larger in size, irregular in shape and showed blue staining on pit margin with the astra blue (Figure 3.45A). At the same time, formation of several bore holes on the lateral walls of the fibres was also observed very frequently in the samples exposed to *Irpex lacteus* for 90 days (Figure 3.45B). At this stage, xylem rays were severely affected with the fungal attack. Fungal hyphae not only travelled through the lumina of the ray cells (Figure 3.45E, F) but they also moved through the intercellular spaces of the ray cells, which ultimately resulted into dissolution of middle lamella (Figure 3.45C, D). Thus, corners of the adjacent rays showed blue staining on rim of the pit with the astra blue (Figure 3.45C, D). Formation of bore holes in the ray cell walls became a common feature and observed frequently in all the samples after 90 days of incubation (Figure 3.45D).

Wood samples exposed to fungi for 120 days showed extensive damage to all the cell types of secondary xylem. Compared to other cell types, ray cells were relatively less resistant to the fungal invasion. Irregularly arranged, several oval to oblong erosion pits/boreholes of various sizes were formed on the lateral walls which completely damaged the ray cells (Figure 3.45E, F). At this advanced stage of decay, other

xylem derivatives such as xylem fibres also showed severe effect of mycelial action. In longitudinal sections, fibres showed several boreholes (also referred as round erosion pits) of various sizes measuring from 3 to 5 μm in diameter (Figure 3.46A, B). These bore holes were formed by the erosion activity by fungal mycelia, which completely broke the cell walls (Figure 3.46C). Similar to the ray cells, axial parenchyma cells were also highly susceptible to the ligninolytic activity of the fungal enzymes. Several cavities/boreholes of irregular size were formed on the lateral walls (Figure 3.46D). Single cavity was 3 to 5 μm in tangential diameter but the most of the times 2 to 3 cavities fused together to form a relatively larger one (Figure 3.46D). At this stage wood blocks lost their original colour and became pale yellowish-white. They were relatively lighter and lost about 29.79 % of weight.

Histology of Wood Decay by *Phanerochaete chrysosporium*: Like former fungal species, even after 30 days, there was no appreciable weight loss of wood block incubated with *Phanerochaete chrysosporium*. Fungal mycelia entered into all the cell types of the secondary xylem and showed presence of mycelial growth in the cell lumen. These mycelia invaded the wood block and completely covered it before completion of 30 days. In the initial stage, mycelial invasion began through the vessel lumen and the most abundant hyphae were observed in its lumina and in the xylem rays and fibres. From the vessels lumen, hyphae entered into the neighbouring rays and gradually dispersed in all directions including xylem fibres and adjacent axial parenchyma cells. No visual damage was observed at this stage in the cell walls. Like former species, fungal mycelia moved from one cell to the next through the pits present on their lateral walls. Presence of fungal mycelia in all the cell types of xylem adjacent to vessel elements was a common feature in all the samples studied. Xylem rays although showed presence of mycelia but no appreciable alterations were observed in most of the sections. However, initiation of cell wall separations at the cell junctions was observed occasionally in some of the sections.

Wood blocks exposed to *Phanerochaete chrysosporium* for 60 days showed sign of selective delignification. Though the signs were not that distinct in all the cell types, but can be easily observed in fibres. In transverse view, many of them showed concentric delignification starting from middle lamellae towards lumen. As a result, the secondary wall adjacent to the middle lamellae stained blue with astra blue instead of red by safranin. This feature was initially observed in the fibres adjacent to the rays, thereafter it gradually dispersed into adjacent axial parenchyma and vessel elements. Separation of the cell walls due to ligninolytic activity of fungal enzymes was the only characteristic feature of axial system. However, ray cells showed significant alterations in the cell wall structure. Pits present on lateral wall became more distinct, larger in size and irregular in shape due to the action of fungal enzymes. Occasionally, separation of rays was also observed in some of the samples studied. Similar to rays cells, axial parenchyma cells also showed variations in the size and shape of the pits while formation of several boreholes on its wall by mycelial activity was observed in most of the samples studied.

Wood blocks after 90 days of incubation with *P. chrysosporium* revealed relatively more marked effect on the cell wall of all xylem elements. In transverse view, the fibres were separated from the middle lamella (Figure 3.47A). Fungal mycelia travelled through lumen, which grew on the inner secondary wall (S₂) surrounding the cell lumina (Figure 3.47B). Due to the enzymatic action of the fungus, erosion troughs appeared and the dye reaction of the secondary wall with safranin and astra blue changed from red to blue, indicating the preferential degradation of lignin (Figure 3.47B). Similar to previous species, pits on the lateral walls of the fibres became more distinct and became larger in size, irregular in shape due to delignification and showed blue staining on pit margin with the astra blue indicating absence of lignin. Along with these pits, several boreholes were also observed on the walls of the rays and axial parenchyma cells.

mycelia
not
seen
in figure

After 120 days of incubation with the fungus, all the derivative cells of xylem were severely damaged by formation of boreholes on the lateral walls owing to the enzyme activity of the fungal hyphae. Vessels were the most resistant cell types while rays were most susceptible cells among all the xylem elements (Figure 3.47C).^{D?} Though, vessel elements were not much affected with fungal invasion but most of them arranged in the form of radial or tangential multiples were found to be separated due to the dissolution of middle lamella (Figure 3.47D). As reported for previous species (i.e. *Irpex lacteus*), several boreholes of irregular size and shape were formed on the walls of ray and axial parenchyma cells due to fungal enzymes. Size of these boreholes was measured about 3 to 5 μm in tangential diameter but sometimes 2 to 3 such bore holes fused together to form a relatively larger one (Figure 3.47E). In case of xylem fibres and lignified parenchyma cells, pits present on their lateral wall also became larger, irregular in size and stained with astra blue due to absence of lignin (Figure 3.47F).

vessels
not in
fig 3.47C

3.7.3 *TECTONA GRANDIS* L. f.

Wood structure: Secondary xylem of *Tectona grandis* L.f. was ring porous with distinct growth rings and generally conspicuous to naked eyes. Sapwood was pale yellow to golden colour while heartwood was light golden brown in fresh and brown to dark brown in dry wood, often with darker streaks of growth rings. The secondary xylem was composed of vessels, tracheids, fibres, axial and ray parenchyma cells. Vessels were enclosed in parenchymatous tissue forming an aliform to confluent arrangement. In early wood they were large, distinctly visible to naked eyes, vessel diameter decreases gradually showing distinct ring porous arrangement. Vessels mostly solitary, oval in outline and partly filled with tyloses. Gradually, vessels became smaller towards the late wood, mostly solitary or in radial pairs and round to oval in outline. Parenchyma formed thin sheath around the vessels, which were distinct in early wood

cells

but visible only with hand lens in latewood. Rays were uni-multiseriate with oval to polygonal ray cells.

Wood colonisation and cell wall degradation: Both the fungal strains *Irpex lacteus* and *Phanerochaete chrysosporium* showed similar modes of wood colonization and cell wall degradation. Though, there was no appreciable weight loss, the blocks were completely invaded after 30 days of incubation with both the strains (Table 3.12). Thereafter, weight loss was rapid in the succeeding days and showed 34 to 39% weight loss after 120 days of inoculation (Table 3.12). Initially, fungal mycelia completely ramified over the wood blocks within 10 to 12 days of inoculation. Mycelia of both the strains entered into the wood cells through the vessel lumen, vessel associated axial parenchyma (Figure 3.48A, B) and invaded all the cell types of the secondary xylem within 30 days. From the vessels, hyphae traversed into the neighbouring rays and gradually extended in all directions including xylem fibres and adjacent axial and ray parenchyma cells. No visual damage was observed in the cell walls within 15 days of incubation. Fungal mycelia traversed from one cell to the next through the pits present on their walls and formed a mycelia mat in the ray cells (Figure 3.48C). While passing from one cell to the next, the mycelia adjusted its diameter with the relatively narrow pit diameter (Figure 3.48D). Presence of fungal mycelia in all the cell types of xylem adjacent to vessel elements was a common feature in all the samples studied.

Decay fungi	% Weight loss (60 days)	% Weight loss (90 days)	% Weight loss (120 days)
<i>Irpex lacteus</i>	16.05 (+ 6.23)	26.37 (+ 4.84)	34.17 (+ 4.97)
<i>Phanerochaete chrysosporium</i>	23.97 (+ 6.41)	32.11 (+ 4.94)	39.37 (+ 5.89)

Table 3.12: Average percent weight loss of *Tectona* wood during each incubation period

Histology of Wood Decay by *Irpex lacteus*: At the end of 30 days, wood blocks inoculated with *I. lacteus* showed no much appreciable alterations in the cell wall except some of the fibres located at the periphery of the block showed separation of the fibres and ray cells from the middle lamellae (Figure 3.48E). As a result, the portion of secondary walls exposed to ligninolytic enzymes produced by the fungi degraded lignin present in the cell wall. Therefore in absence of lignin, cell walls were stained blue with astra blue instead of red by safranin (Figure 3.48E). This feature was initially observed in the fibres adjacent to the rays, axial parenchyma cells and vessel elements. Thereafter, it gradually invaded neighbouring cells of the secondary xylem. In the beginning, mycelial invasion was observed through the vessel lumen. From the vessels, hyphae traversed into the neighbouring rays and gradually extended in all directions including xylem fibres (Figure 3.48F) and adjoining axial parenchyma cells. Thus, presence of fungal mycelia in all the cell types of xylem adjacent to vessel elements was a common feature in all the samples studied. Even after 30 days of incubation with *Irpex lacteus*, cell walls of xylem rays and vessels showed no visible signs of fungal attack but fibres showed the first sign of structural alterations, which were typical of selective delignification i.e. separation of fibres from the middle lamella were noticed due to its dissolution. Separation of xylem cells was more frequent in those cells which were adjacent to the rays (Figure 3.48E). At this stage, delignification was mostly restricted to the cells located at the periphery of wooden blocks.

At the end of 60 days, blocks inoculated with *I. lacteus* were relatively more delignified than the blocks observed after 30 days of fungal inoculation. Unlike previous stage (i.e. 30 days), delignification was scattered more uniformly throughout the wooden blocks. In transverse view, many of the fibres showed concentric delignification starting from middle lamellae towards lumen. As a result, the secondary wall adjacent to the middle lamellae stained blue with astra blue. Except separation of the fibres, no appreciable effect was observed on its morphology in both

transverse and longitudinal plane. At this stage, ray also showed separation of ray cells from the middle lamella due to the ligninolytic activity of the fungal enzymes (Figure 3.49A).

Compared to vessels, rays became more vulnerable to fungal attack and the effect was more prominent on xylem rays (Figure 3.39F). In ray cells, degradation commenced at the cell corners along the middle lamellae without any marked effect on the primary and secondary wall layers (Figure 3.49A). Cell corners became discoloured due to absence of lignin and stained blue with astra blue. Gradually ray cells were separated from each other due to the dissolution of middle lamella, consequently resulting into collapse of the cell walls (Figure 3.49A).

Wood samples exposed to fungi for 90 days showed separation of vessel elements without any significant effect on their cell walls. Not only wider vessel elements were separated but narrow vessel elements also exhibited dissolution of middle lamella and separation of vessel walls (Figure 3.49B). All the cell types of secondary xylem showed distinct effect of delignification on their wall material. Defibrillation was a common feature and it was observed frequently in all the samples studied. At this stage, xylem cells showed characteristic of simultaneous rot, the walls were partially bleached and showed erosion troughs across the cell walls (Figure 3.49C). Therefore, simultaneous degradation of all cell wall components resulted into breaking of the cell walls (Figure 3.49C). Erosion troughs formed in response to mycelia activity were irregular in shape and size. In some instances, the erosion troughs reached the middle lamella completely removing the cell wall in a localized area (Figure 3.49D). As the degradation progressed further, pits of the ray and axial parenchyma cells became more distinct, larger in size and irregular in shape. At the same time, formation of several boreholes on the lateral walls of the rays was observed commonly (Figure 3.49E).

Wood blocks exposed to fungi for 120 days showed more marked effect of delignification of all the cell types of secondary xylem (Figure

3.50A). Fibre walls showed distinct erosion troughs across the cell walls from the lumen towards the middle lamella, they were completely bleached and stained blue coloured with astra blue due to loss of lignin (Figures 3.49F, 3.50A). In the advancement stage of decay, the xylem fibres were not only completely separated from each other but also lost their rigidity due to removal of lignin from the cell walls. Formation of several boreholes on the lateral walls of many ray cells resulted into partial or complete disintegration of rays. Like *Azadirachta*, in *Tectona* also vessels were more resistant as compared to fibres and axial parenchyma while rays were found to be more susceptible.

Histology of Wood Decay by *Phanerochaete chrysosporium*: Like former fungal species, there was no appreciable weight loss of wood block by *P. chrysosporium* after 30 days of its inoculation (Table 3.12). Fungal mycelia invaded the wood blocks and completely covered them within few days after inoculation. In the initial stage, mycelial invasion was seen through the vessel lumen and hyphae were most abundant within the vessels lumina, fibres axial and ray parenchyma cells. From the vessels lumen, hyphae entered into the neighbouring rays and gradually spread in all directions including xylem fibres and adjacent axial parenchyma cells. At this stage, no visual damage was observed in the cell walls. Fungal mycelia moved from one cell to the next through the pits present on their walls. Presence of fungal mycelia in all the cell types of xylem adjacent to vessel elements was a common feature in all the samples studied. Xylem rays although showed presence of mycelia but no significant alterations were observed in most of the sections. However, initiation of cell wall separations at the cell junctions was observed occasionally in some of the sections (Figure 3.50B).

After 60 days of inoculation, the degradation pattern of *P. chrysosporium* resembled selective delignification i.e. at an early stage of decay, degradation commenced in the fibre walls, along the middle lamellae without any marked effect on the primary and secondary wall layers. Xylem fibres began to separate from each other by dissolution of

middle lamella (Figure 3.50C). As reported for previous fungal species, this feature was initially observed in the fibres and axial parenchyma cells adjacent to the rays. Sections stained with safranin and astra blue showed that the discoloured secondary wall was delignified and stained blue due to absence of lignin while portion of the cell wall with lignin was stained red in colour (Figure 3.50C). As the decay progressed further, localized degradation of lignin, hemicellulose and cellulose resulted in the formation of boreholes on the lateral walls of the rays. Pits on the walls of the ray cells became more prominent and larger in size and irregular in shape.

After 90 days, separation of xylem fibres was more distinct, due to dissolution of middle lamella (Figure 3.50D). The middle lamellae that were stained blue began to lose the integrity and individual cells became separated from each other. Due to delignification, pits of the ray and axial parenchyma cells became evident due to increase in their size and irregular in shape. At the same time, formation of several boreholes on the lateral walls of the rays became more frequent (Figure 3.50E, F). Compared to axial elements, ray cells were more affected and stained blue in colour with astra blue while fractions of the cell wall in which lignified part was relatively unaffected stained red in colour with safranin. Though vessel elements were not much affected with fungal invasion but most of them were separated from the middle lamella due to its dissolution. Compared to pits of the ray cells, bordered pits on the lateral walls of the vessels were relatively less affected and their rim stained blue coloured but not much visual damage of cell walls as well as bordered pits was observed.

Wood blocks exposed to *P. chrysosporium* for 120 days showed more pronounced effect of delignification on all the cell types of xylem. Xylem fibres were completely bleached and not only stained blue coloured with astra blue due to loss of lignin but also showed complete disintegration of cells due to loss of rigidity and integrity (Figure 3.51A). In advance stage of decay, pits of the ray and axial parenchyma cells became more marked,

larger in size and irregular in shape. At the same time, formation of several boreholes on the lateral walls of the rays was a widespread feature (Figure 3.51B). Size of these boreholes was measured about 3 to 5 μm in tangential diameter but sometimes 2 to 3 such boreholes fused together to form a relatively larger one. It is evident from the Figure 3.51C that with the advancement of decay, many of the ray cells were either partially or completely disintegrated and underwent collapse. In case of xylem fibres and axial parenchyma cells, pits present on their lateral wall also became larger, irregular in size and stained blue with astra blue due to delignification. As the fungal activity progressed further, these fibres became separated gradually from each other due to the dissolution of middle lamella which led to collapse of the cell walls (Figure 3.51D).

3.8 DISCUSSION

The most visible role of plant cell walls is to determine the size and shape of cells. By differentially resisting and yielding turgor pressure, the plant cell wall prescribes the growth and shape of the cells (Taiz, 1984). It is also the first obstacle that a pathogen needs to overcome in order to penetrate the plant cell. As the plant cell wall is such an important interface between the plant cell and the pathogen, no much information is available on the histological aspects of cell wall degradation on tropical timber species (Lagaert, ^{et al.} 2009). However, a group of fungi referred as rot fungi has the ability of differential degradation of cell wall components. On the basis of micro-morphological and chemical characteristic of decay produced by these fungi, wood degradation is classified into (1) white rot (members of Basidiomycota), subdivided into simultaneous rot and selective delignification (2) brown rot (members of Basidiomycota) and (3) soft rot (members of Ascomycota and Deuteromycota). Some species have the capacity to preferentially remove lignin whereas; others remove lignin along with varying amounts of cellulose and hemicelluloses (Eriksson *et al.*, 1990). In brief, white rot fungi can be defined as; Hymenomycetes that degrade the lignin leaving behind the cellulose and hemicellulose are

known as white rot fungi due to the bleached appearance of wood decayed by these fungi (Jenness, 2007).

It is well known fact that white rot fungi have a very high ligninolytic potential and are adapted to degrade more complex structure of angiosperm wood, thus resulting into wide range of degradation modes (Schwarze and Fink, 1998; Koyani *et al.*, 2010, 2011). In the past, two broad divisions of white rot have been widely accepted: i) selective delignification and ii) simultaneous rot (Schwarze and Fink, 1998; Schwarze and Baum, 2000; Schwarze 2007; Lehringer *et al.*, 2010; Koyani *et al.*, 2010, 2011). In addition to these types Schwarze and Engels, (1998) have reported an unusual type of cavity formation reminiscent of soft rot followed by selective delignification for a range of host-fungus combinations. In the present study, three fungal species viz. *Inonotus hispidus*, *Irpex lacteus* and *Phanerochaete chrysosporium* were utilised to investigate the pattern of wood decay and structural alterations induced in the cell wall of wood elements.

A number of species of fungi live in or on wood, and as a result of their growth, anatomical changes may be induced in wood cell walls. These changes occur in several patterns that can be readily distinguished from one another, and that apparently result from quantitative or qualitative differences in the enzyme complement of the organisms in each group. The patterns resulting from the fungus action tend to correlate closely with taxonomic groupings based upon the morphology of the fungal thallus, micro-morphological and chemical characteristics of decay, which results in different pattern of attack on the middle lamella, S₁, S₂ and S₃ layers. In the present investigation, *Inonotus hispidus* showed soft rot pattern, although it belongs to Basidiomycetes. Available information indicates that *Inonotus hispidus* can cause a soft rot in addition, or alternatively, to their more typical mode of attack, i.e. soft rot (Schwarze, 1995; Schwarze *et al.*, 1995; Koyani *et al.*, 2010), while other two fungal strains *Irpex lacteus* and *Phanerochaete chrysosporium* characteristically

showed white rot with dual mode of decay pattern i.e. selective delignification and simultaneous rot.

Inonotus hispidus is one of the most frequently occurring fungi that affect trees like ash, apple, London plane, walnut, elm, sycamore and lime etc., (Schwarze and Engels, 1998). It is often classified as heart rot fungus (Nutman, 1929), but in the present study, fruiting bodies are also observed on the relatively young branches of 5 to 7 inches in diameter. Earlier studies had shown that *I. hispidus* has the capacity to attack young sapwood of relatively thick stems (McCracken and Toole, 1974). In the early stages of infection, initial sign of decay is yellowish brown patches that are delimited by brown reaction zone. Such reaction zones commonly contained tyloses and result in blocking lumina of vessels. Tyloses are an outgrowth of adjacent ray or axial parenchyma cells into a lumen of vessels that block the vessel lumen partially or completely. It is a common feature and reported by several earlier workers (Shain, 1967, 1979; Pearce, 1996).

Light microscopic studies have revealed that *I. hispidus* causes soft rot in addition or instead of its white rot pattern (Schwarze *et al.*, 1995; Schwarze and Fink, 1997). Such soft rotting activity may commonly precede white rotting, when the fungus invades previously unaffected zones of xylem in which moisture content is supra-optimal (Schwarze, 1995, 1997; Schwarze *et al.*, 1995). In *Ailanthus*, infection by *I. hispidus* initiates during the monsoon when the moisture content is very high and the cut branch stubs are also exposed to rain (Koyani *et al.*, 2010).

On the basis of degradation pattern, these rot fungi are usually separated into three main types viz. white rot, brown rot and soft rot (Liese, 1970; Blanchette, 1991; Eaton and Halle, 1993; Schwarze and Fink, 1998). 1) In white rot, all cell constituents are degraded by the fungus and are broadly classified into: a) selective delignification and b) simultaneous rot. In selective delignification hemicellulose and lignin are preferentially degraded first, especially in the early stages. The most

remarkable anatomical effect is separation of fibres by dissolution of middle lamella. In simultaneous rot, lignin and structural polysaccharides are attacked more or less at the same time (Worrall *et al.*, 1997; Schwarze and Fink, 1998).

Degradation of wood by *I. hispidus* in *Ailanthus* shares both white and soft rot pattern. In the initial stages, it resembles selective delignification especially at an early stage of decay; degradation commences at the cell corners of the middle lamellae within the xylem fibres without any distinct effect on the primary and secondary wall layers. Similar pattern of wood degradation is reported for London plane by *I. hispidus* (Schwarze *et al.*, 1995; Schwarze and Fink, 1997). It is well established that various species of *Inonotus* cause selective delignification (Nutman, 1929; McCracken and Toole, 1974; Schwarze *et al.*, 1995; Schwarze and Fink, 1997; Schwarze and Engels, 1998). However, it appears to be a temporary phase, because the structure of the cavities and the formation of multiple L-bending by the associated hyphae were typical of soft rot type. Such pattern of intra-wall branching and associated cavity formation within cell walls by *I. hispidus* is reminiscent of soft rot fungi. The particular pattern of cell wall degradation is assigned to form group '13' by Courtois, (1963). It is characteristic pattern of soft rot in which cavities resembling tunnels are formed along the orientation of cellulose microfibrils in the secondary wall (Courtois, 1963). In the present investigation, *I. hispidus* made similar cavities along the cellulose microfibrils in the secondary walls of xylem fibres. It was generally not recognised in the past that soft rot is a common feature which has been described for a range of wood decaying Basidiomycetes (Nilsson and Daniel, 1988; Daniel *et al.*, 1992; Worrall *et al.*, 1997; Schwarze and Fink, 1997, 1998).

Characteristic feature of soft rots is their pattern of development, which involves "T" branching or "L" bending and hyphal tunnelling inside lignified cell wall. This distinctive mode of attack was described in the mid-century by Schacht (1863) and was elucidated by Savory (1954), who

proposed the term soft rot. Discrete notches of cell wall erosion by hyphae lying within the lumina, in addition to cavities formed by hyphae within the cell wall are also frequently found in wood degraded by soft rot fungi. These erosion troughs, which are indistinguishable from those of white rot fungi, have been attributed to a category of soft rot known as type 2, whereas internal cavity formation is typical of type 1 attack (Corbett, 1965; Hale and Eaton, 1985a, b). Soft rot have generally been attributed to Deuteromycetes and Ascomycetes fungi and not to Basidiomycetes (Blanchette, 1992).

In nature, white rot fungi are more commonly found on angiosperms than on gymnosperm wood (Gilbertson, 1980). In these fungi, degradation is usually localized to cells colonized by fungal hyphae and substantial amounts of undecayed wood remains even after an advanced decay has occurred. A progressive erosion of the cell wall occurs when components are degraded simultaneously or a diffuse attack of lignin may occur by species that preferentially remove lignin. Strength losses are not significant until late stages of decay. Moreover, affected wood shows normal shrinkage and usually does not collapse or crack across the grain as seen in brown rot damage. However, wood invaded by white rot fungus loses its strength gradually until it becomes spongy to touch. Sometimes, white rot fungi cause thin, dark lines around decayed areas, referred as zone lines. In the present study also, wood portions collected from the wood logs at the time collection showed presence of such zone lines (Gilbertson, 1980). White rot fungi usually attack hardwoods, but several species of them can also cause decay to softwoods.

Both the white rot fungal strains characteristically showed dual mode of decay pattern i.e. selective delignification and simultaneous rot: 1). Simultaneous decay, in which degradation of cellulose, hemicellulose and lignin occur simultaneously. Erosion troughs beneath hyphae extend deeply into the secondary wall, degrading the S₁, S₂ and S₃ layers in succession (Liese, 1970; Rayner and Boddy, 1988; Eriksson *et al.*, 1990; Koyani *et al.*, 2010, 2011). Many white rot fungi colonize cell lumina and

cause cell wall erosion. This type of rot is referred to as non-selective or simultaneous rot (Blanchette, 1995). 2) Selective decay or preferential delignification, where species preferentially remove lignin from wood leaving pockets of white, degraded cells that consist entirely of cellulose (Blanchette, 1984b, 1995; Otjen and Blanchette, 1987). There are reports that some white rot fungi are capable to cause both types of decay in the same wood or in different wood species (Blanchette, 1984a, b, 1991). In the present study, both the fungal species investigated showed both types of decay pattern.

Initially both the strains (*Irpex lacteus* and *Phanerochaete chrysosporium*) showed selective delignification pattern and the most remarkable effect is defibration by dissolution of the middle lamella. Both, *Azadirachta* as well as *Tectona* wood inoculated with *Irpex lacteus* and *Phanerochaete chrysosporium* showed selective delignification i.e. separation of all the cell types of secondary xylem from the middle lamella. In *Azadirachta* wood, along with the separation, xylem ray cells also showed formation of boreholes by *Irpex lacteus* after 60 days of its inoculation while similar type of boreholes on lateral walls of fibres were observed after 90 days of *Phanerochaete chrysosporium* inoculation. On the other hand, in case of *Tectona* wood formation of boreholes on the ray cell walls were observed after 90 days of incubation of both the fungal species. During this period, formation of erosion trough and borehole tunnels in xylem fibres and in axial parenchyma cells were also recorded in both the timber species investigated in the present study.

The axial alignment of tracheids, vessels and fibres and, the radial arrangement of the xylem ray parenchyma facilitate access into the wood and allow widespread distribution of hyphae within the xylem (Rayner and Boddy, 1988; Schwarze *et al.*, 2004). Access to adjacent cells occurs via pit apertures, or direct penetration may take place directly through the cell wall. Initially, both the fungal strains (*Irpex lacteus* and *Phanerochaete chrysosporium*) entered into the wood cells through the vessel elements. Thereafter, hyphal invasion occurred into the adjacent

cells through the pits on lateral walls. In the beginning of fungal attack, mycelia entered into the ray cells through the pits on lateral walls but during the advanced stage of decay, several boreholes were observed on the lateral walls of the rays of both the timber species. However, formation of boreholes in the fibres was observed only in *Azadirachta* wood invaded by both the fungal strains. Fungal mycelia also travelled through the intercellular spaces of the ray cells. As the decay progressed further, it showed separation of the ray cells due to the ligninolytic activity of the fungal enzymes. Separation of ray cells in response to ligninolytic enzymes produced by fungi is also reported in earlier studies (Schwarze *et al.*, 1995; Schwarze and Fink, 1997; Schwarze, 2007; Koyani *et al.*, 2010, 2011).

In the present study, light microscopy observations revealed that all the three species viz. *Inonotus hispidus*, *Irpex lacteus* and *Phanerochaete chrysosporium* caused different patterns of decay. This may be evidenced by the presence of distinctive anatomical features and by the staining technique. Initially, all the fungal strains studied here produced a selective delignification of the xylem tissue, which was manifested by cell separation. Separation of xylem cells owing to the dissolution of middle lamella is considered to be the best indicator of the selective type of decay (Anagnost, 1998; Luna *et al.*, 2004). The staining technique contributed also to separate the selective delignification from the simultaneous decay, as proposed by Srebotnik and Messener, (1994). Delignified tissue of *Ailanthus*, *Azadirachta* and *Tectona* wood stained blue with astra blue due to absence of lignin while portion of relatively unaffected cell wall stained red with safranin. Our earlier study also demonstrated similar feature to distinguish the delignified xylem cells in *Ailanthus* and *Azadirachta* (Koyani *et al.*, 2010, 2011). new?

Compared to xylem fibres, vessels are found to be more resistant to decay caused by *I. hispidus*. In hardwoods, vessels walls are considered to be resistant to degradation by white rot Basidiomycetes as has been described in details by Blanchette *et al.*, (1987). The persistence of lignin rich vessel elements in *Ailanthus excelsa* (Mahaneem) wood decayed by

Inonotus hispidus, and *Azadirachta* (Neem) and *Tectona* (Teak) wood inoculated with *Irpex lacteus* and *Phanerochaete chrysosporium* may be due to the high percentage of guaiacyl lignin. Degradation ability of the secondary xylem is considered to be associated with the lignin composition of individual cell type. The libriform fibres and xylem ray parenchyma reported to have relatively high syringyl monomer content (Nakano and Meshitsuka, 1978; Iiyama and Pant, 1988) and it show peak UV-absorbance at short wave length (Fergus and Goring, 1970a, b). In contrast, fibre-tracheids have high guaiacyl monomer content and show their peak UV-absorbance at longer wave length. Among the vessels also, narrow vessels were relatively more resistant to fungal attack as compared to wider ones. Wood samples invaded by all three fungi showed that there was no appreciable change in the cell wall of narrow vessels except their separation. On the contrary, wider vessels collapsed completely and became deformed in all the samples studied. It is considered that hardwood vessel walls are resistant to degradation by white rot Basidiomycetes (Nakano and Meshitsuka, 1978; Blanchette *et al.*, 1987, 1988a,b; Iiyama and Pant, 1988). Similar observations are also reported in the present study on naturally infected *Ailanthus excelsa* by *Inonotus hispidus* and artificially infected wood of Neem and Teak. The persistence of lignin rich vessel elements in *Azadirachta* wood inoculated with *T. harzianum* and *C. asperatum* may be due to high percentage of guaiacyl monomer content as reported in earlier investigations (Blanchette *et al.*, 1987, 1988a; Schwarze *et al.*, 2000; Koyani *et al.*, 2010, 2011). Available literature indicates that there are some fungal species which leave the vessels of angiosperm trees largely undegraded, even at a relatively advanced stage of decay (Blanchette *et al.*, 1988). This is apparently due to the high lignin:carbohydrate ratio of vessel walls, together with their morphology and the monomeric composition of their lignin (Blanchette *et al.*, 1988). In the present investigation also, vessels in *Azadirachta* and *Tectona* remain unaltered even at the advance stage of decay by *I. lacteus* and *P. chrysosporium*.

messw
ref

In angiospermous wood, white rot fungi showed a tendency to colonize cells via apertures of simple pits or bordered pits which are subsequently enlarged and mistaken for boreholes. It is evident from the Figures 3.44D; 3.45A, B, E; 3.46A-D; 3.47F and 3.51B that the boreholes shown on the lateral walls of fibres, ray and axial parenchyma in the present investigation are formed in response to enzyme activity of inoculated fungi and not as the pits. Morphology, size and distribution of these boreholes are other indications that they are the boreholes and not the pits on their walls. Similar results are reported in *Fomes fomentarius* which induces abundant boreholes in colonized wood of beech and pedunculate oak (Schwarze, 2007). Formation of boreholes by specialized cell wall degrading hyphae has been described in the literature (Liese, 1970; Schwarze *et al.*, 2004). These holes were initiated by fine penetration hyphae, less than 0.5 mm diameter, which penetrated the cell wall by means of ligninolytic enzymes, which were released at the hyphal tips (Schwarze *et al.*, 2004). Subsequently, boreholes progressively enlarged by the secretion of enzymes from the general surface of the hypha. At a more advanced stage of decay, cracks often developed between adjacent boreholes in the radial cell walls, and the boreholes eventually coalesce (Schwarze *et al.*, 2004). In the present study also 2 to 4 adjacent boreholes fuse together and formed a larger one.

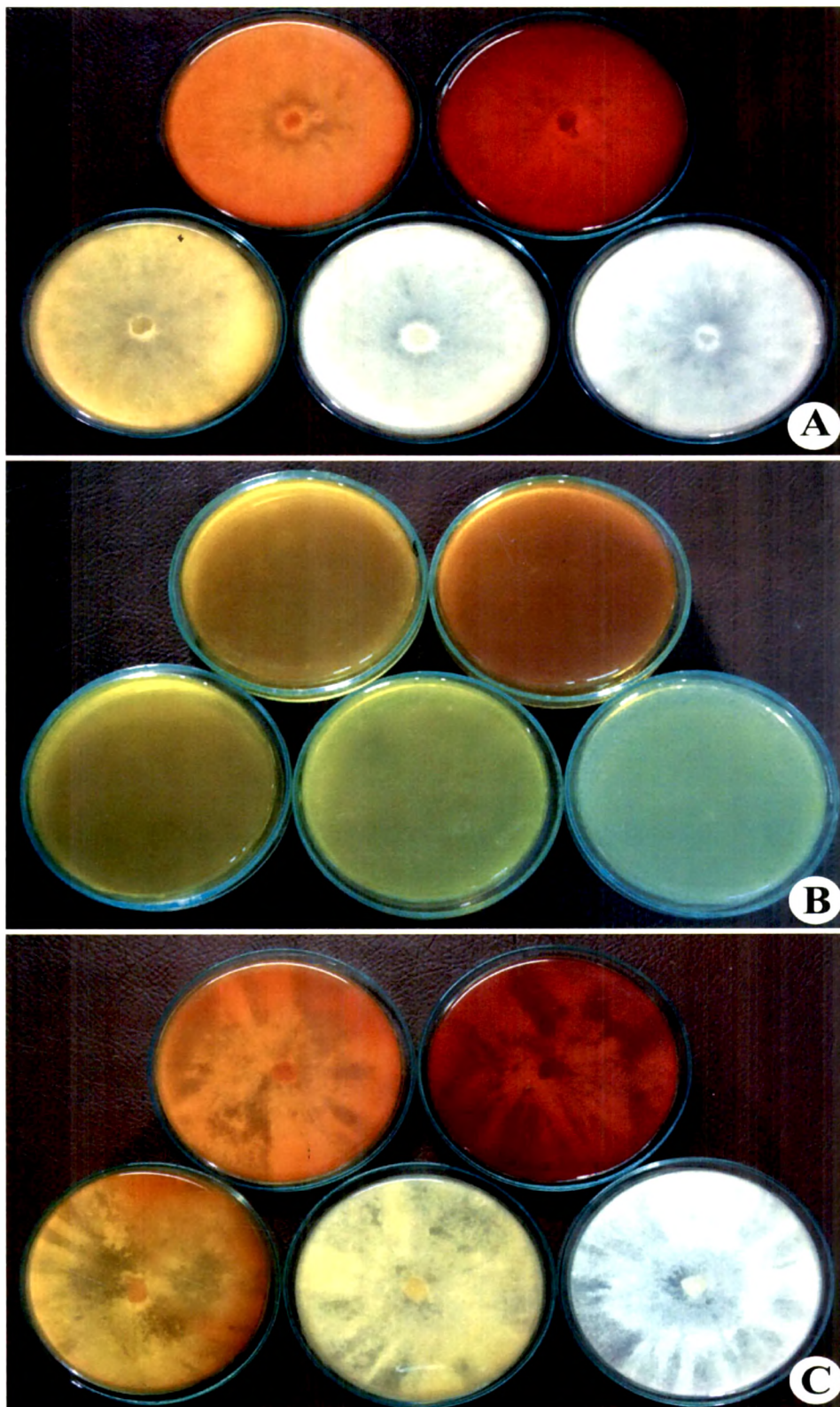


Figure 3.1: On plate decolourisation of Reactive Yellow FG by *Irpex lacteus* (A), *Phanerochaete chrysosporium* (C) and Control dye (B).

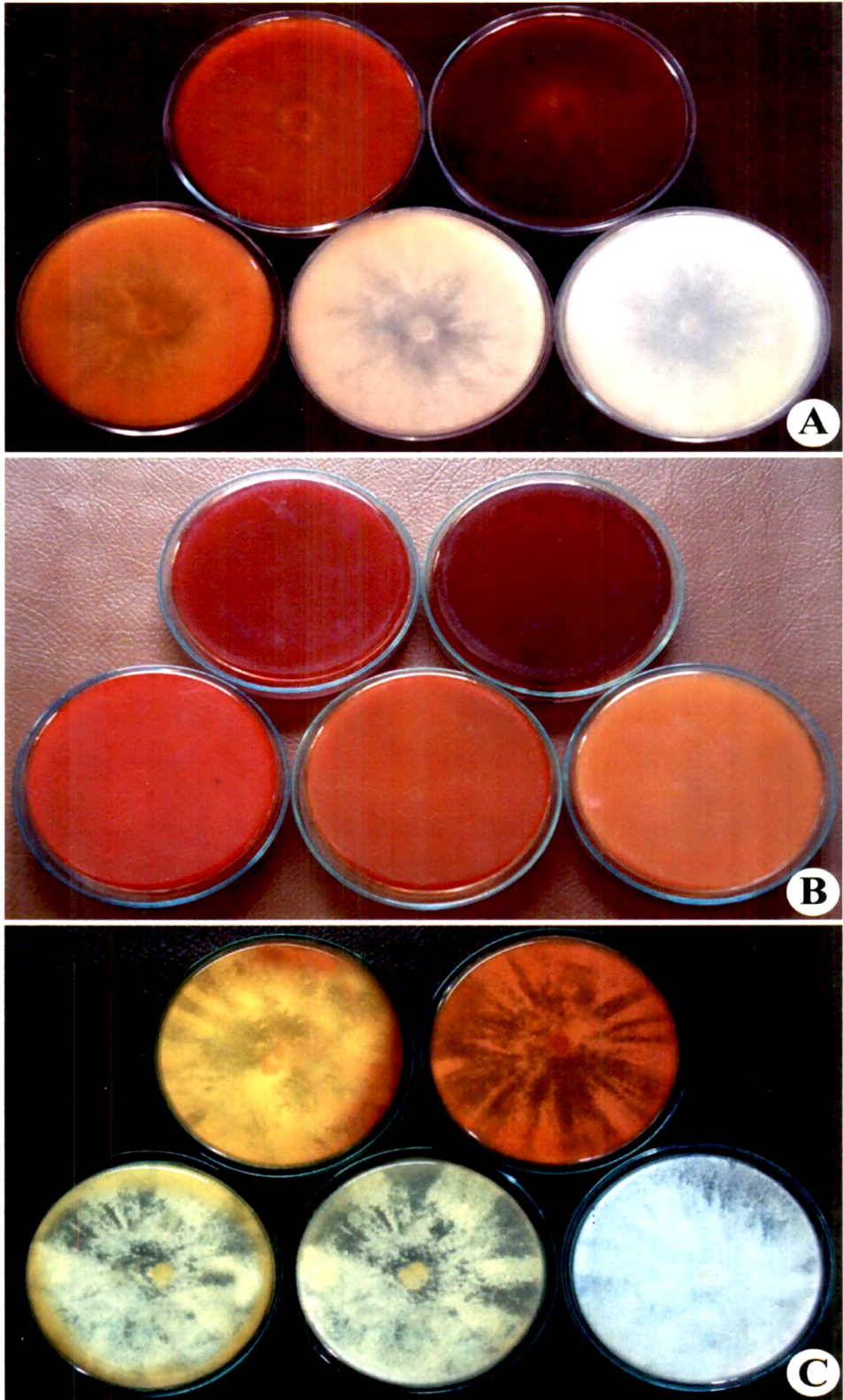


Figure 3.2: On plate decolourisation of Reactive Orange 2R by *Irpex lacteus* (A), *Phanerochaete chrysosporium* (C) and Control dye (B).

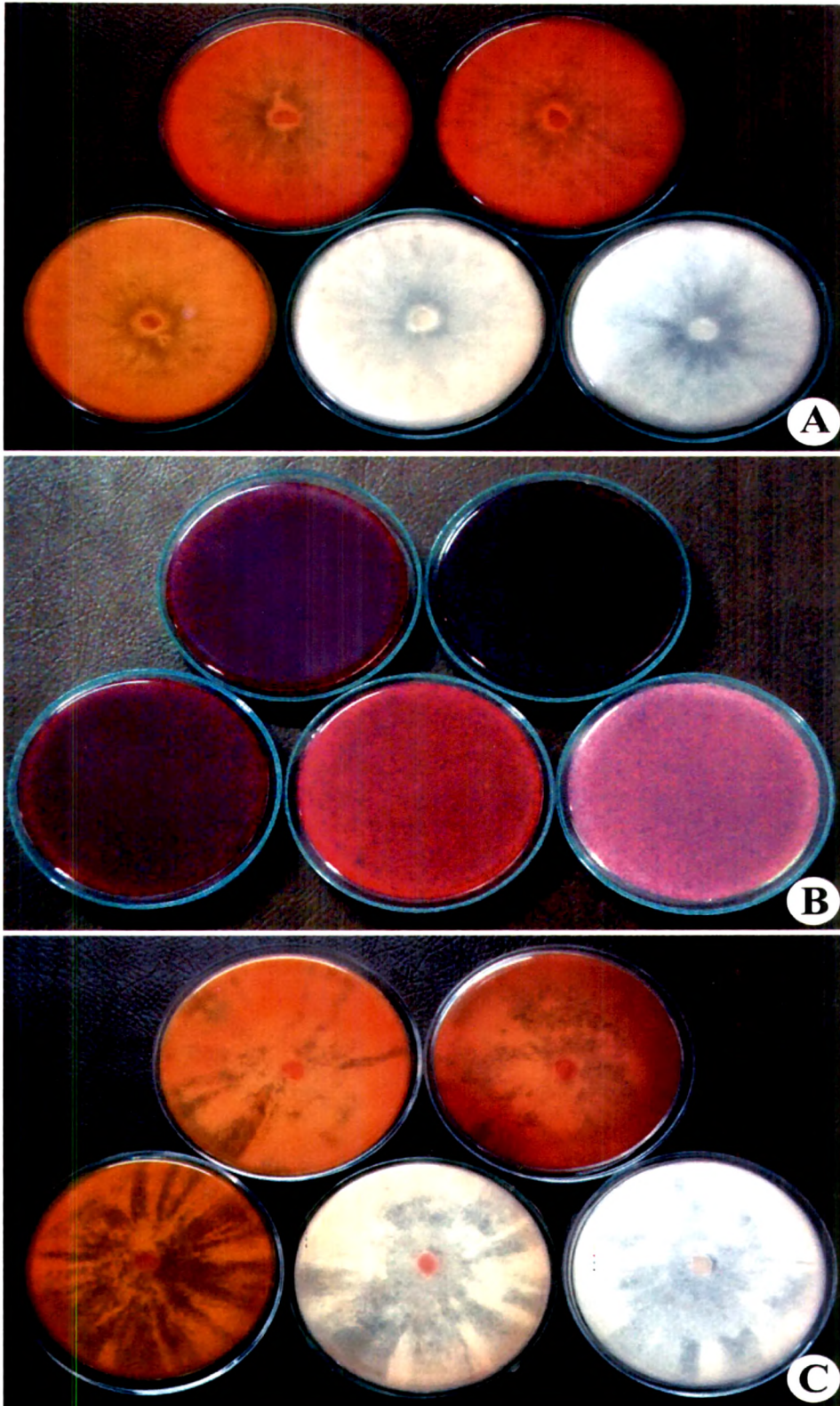


Figure 3.3: On plate decolourisation of Reactive Red ME4BL by *Irpex lacteus* (A), *Phanerochaete chrysosporium* (C) and Control dye (B).

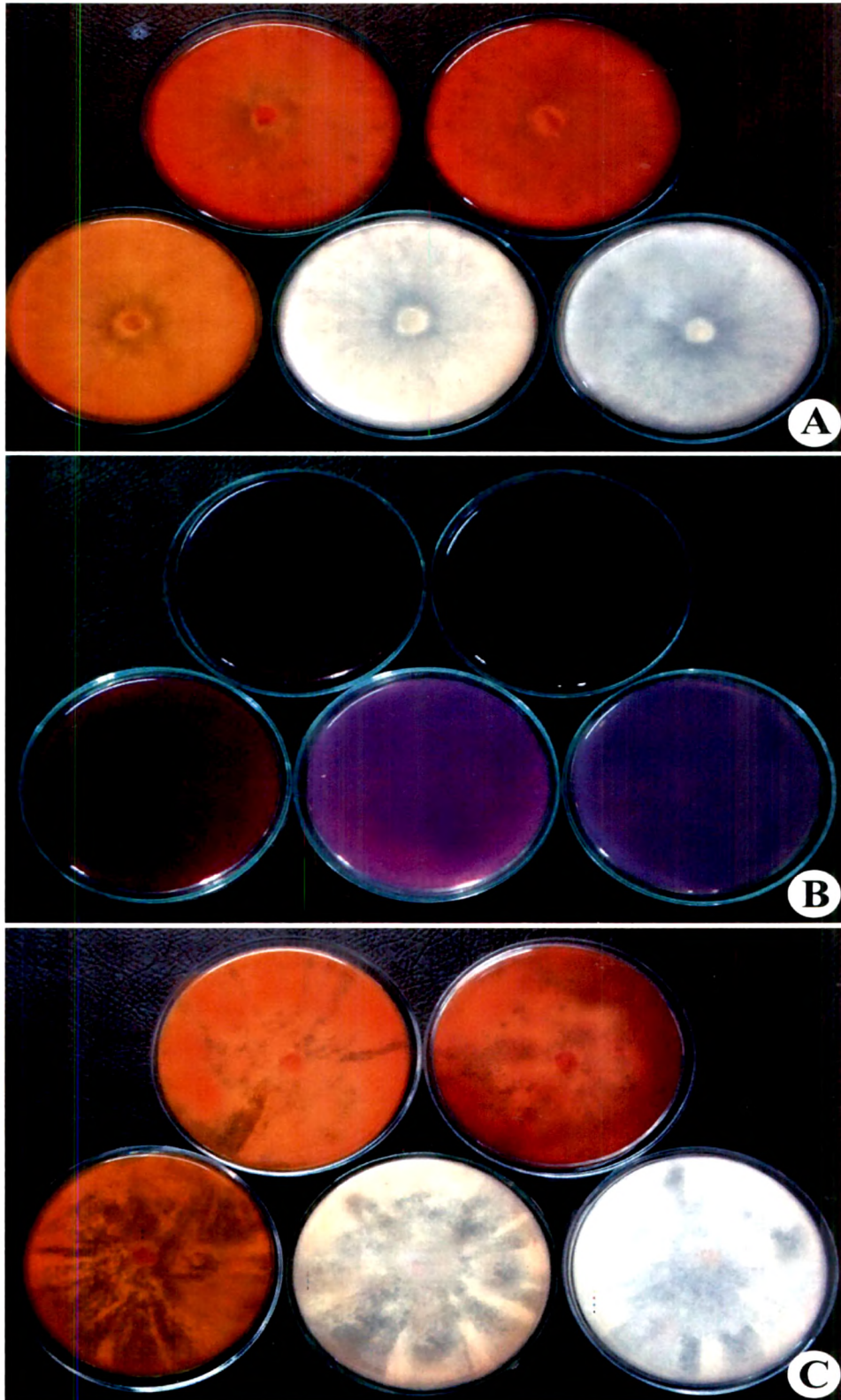


Figure 3.4: On plate decolourisation of Reactive Red HE8B by *Irpex lacteus* (A), *Phanerochaete chrysosporium* (C) and Control dye (B).

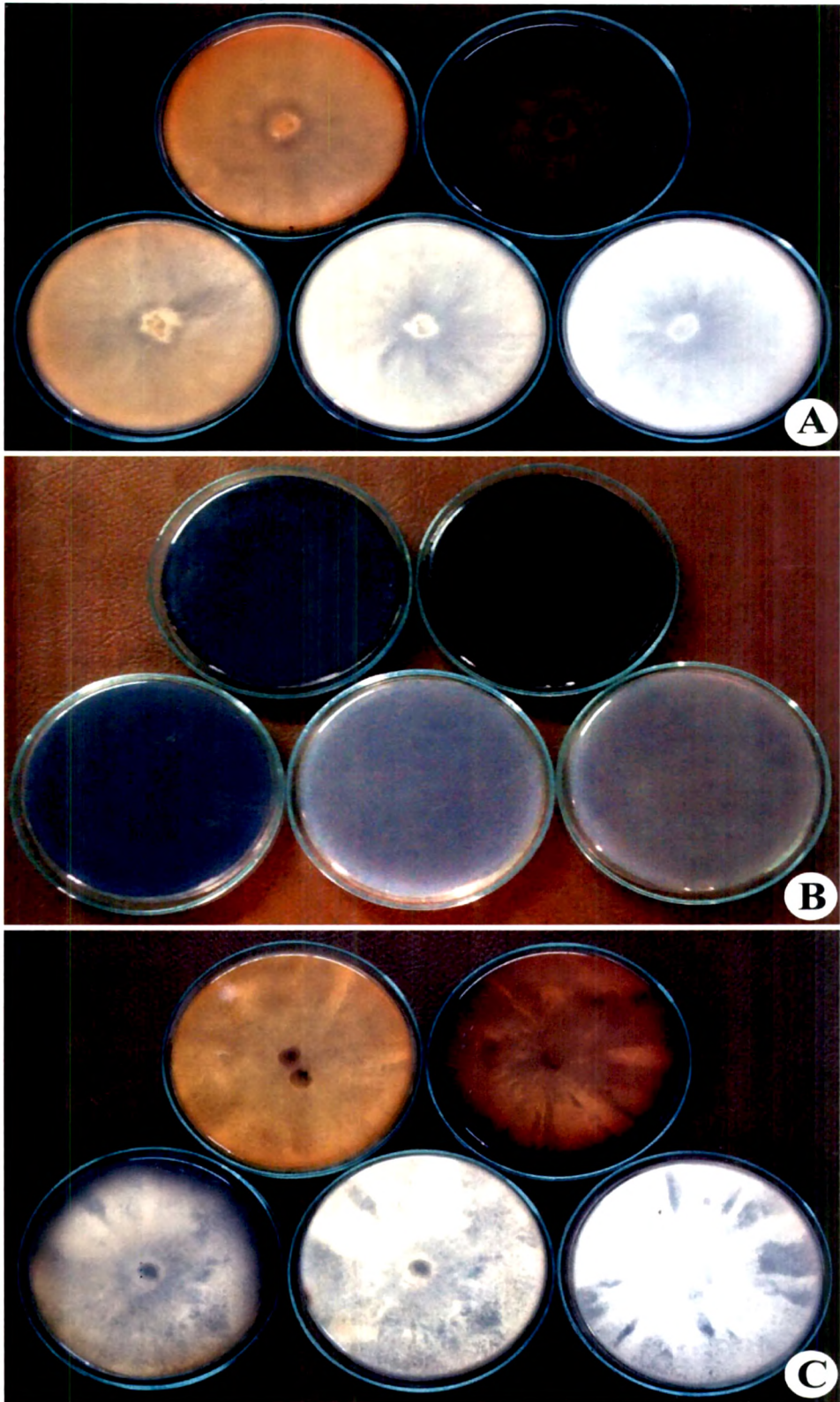


Figure 3.5: On plate decolourisation of Reactive Black B by *Irpex lacteus* (A), *Phanerochaete chrysosporium* (C) and Control dye (B).

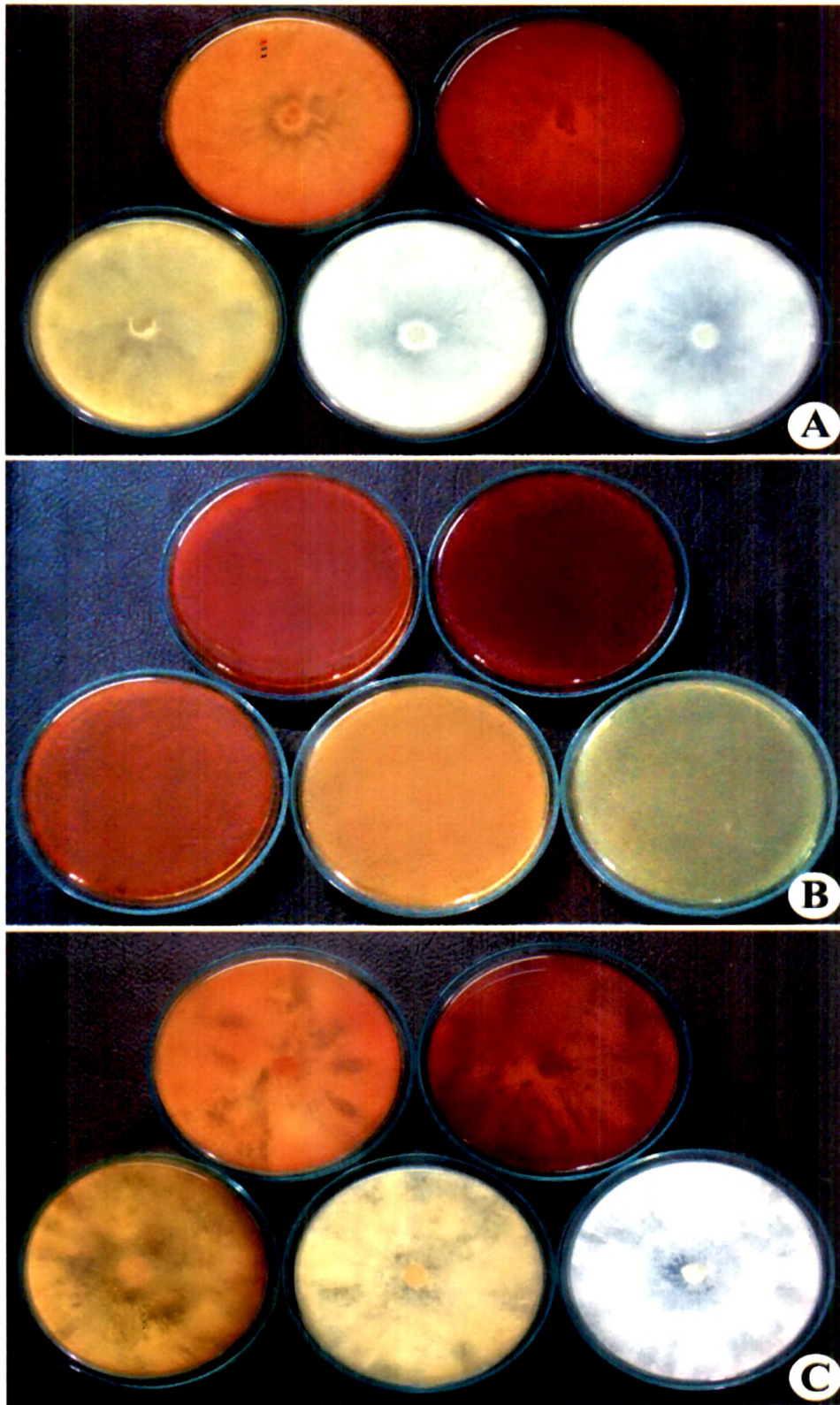


Figure 3.6: On plate decolourisation of Reactive Golden Yellow HR by *Irpex lacteus* (A), *Phanerochaete chrysosporium* (C) and Control dye (B).

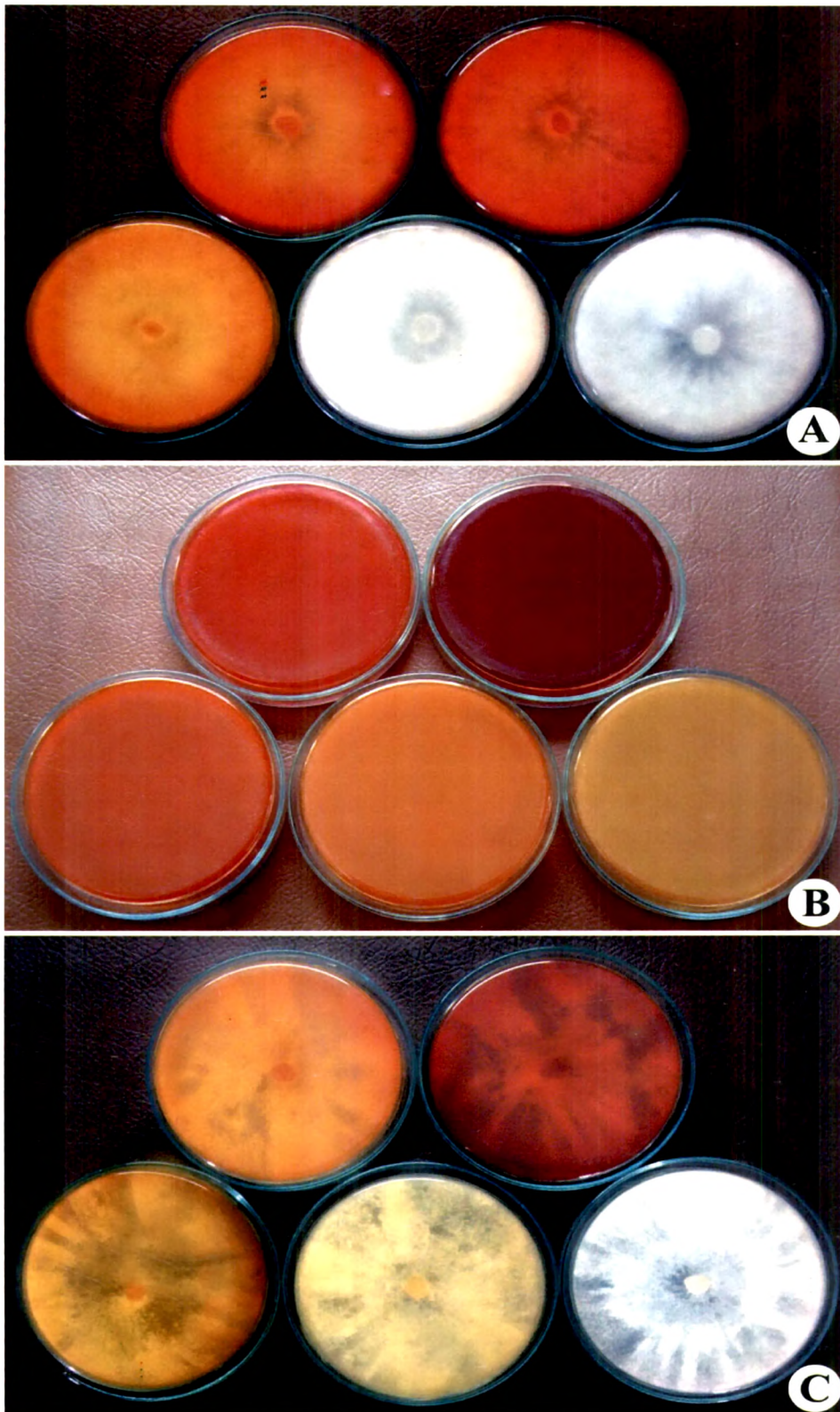


Figure 3.7: On plate decolourisation of Reactive Golden Yellow HRNL by *Irpex lacteus* (A), *Phanerochaete chrysosporium* (C) and Control dye (B).

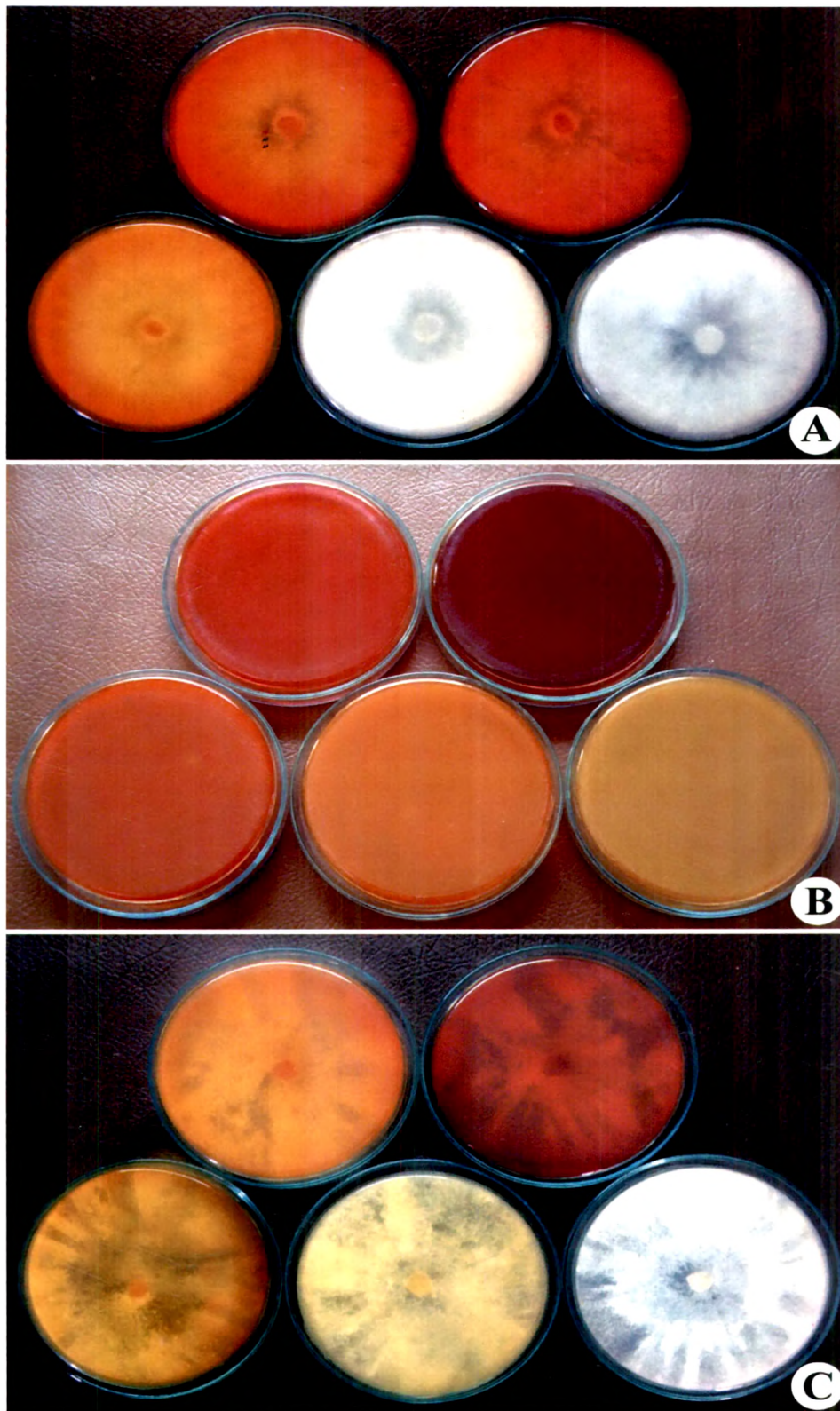


Figure 3.8: On plate decolourisation of Reactive Violet 5R by *Irpex lacteus* (A), *Phanerochaete chrysosporium* (C) and Control dye (B)

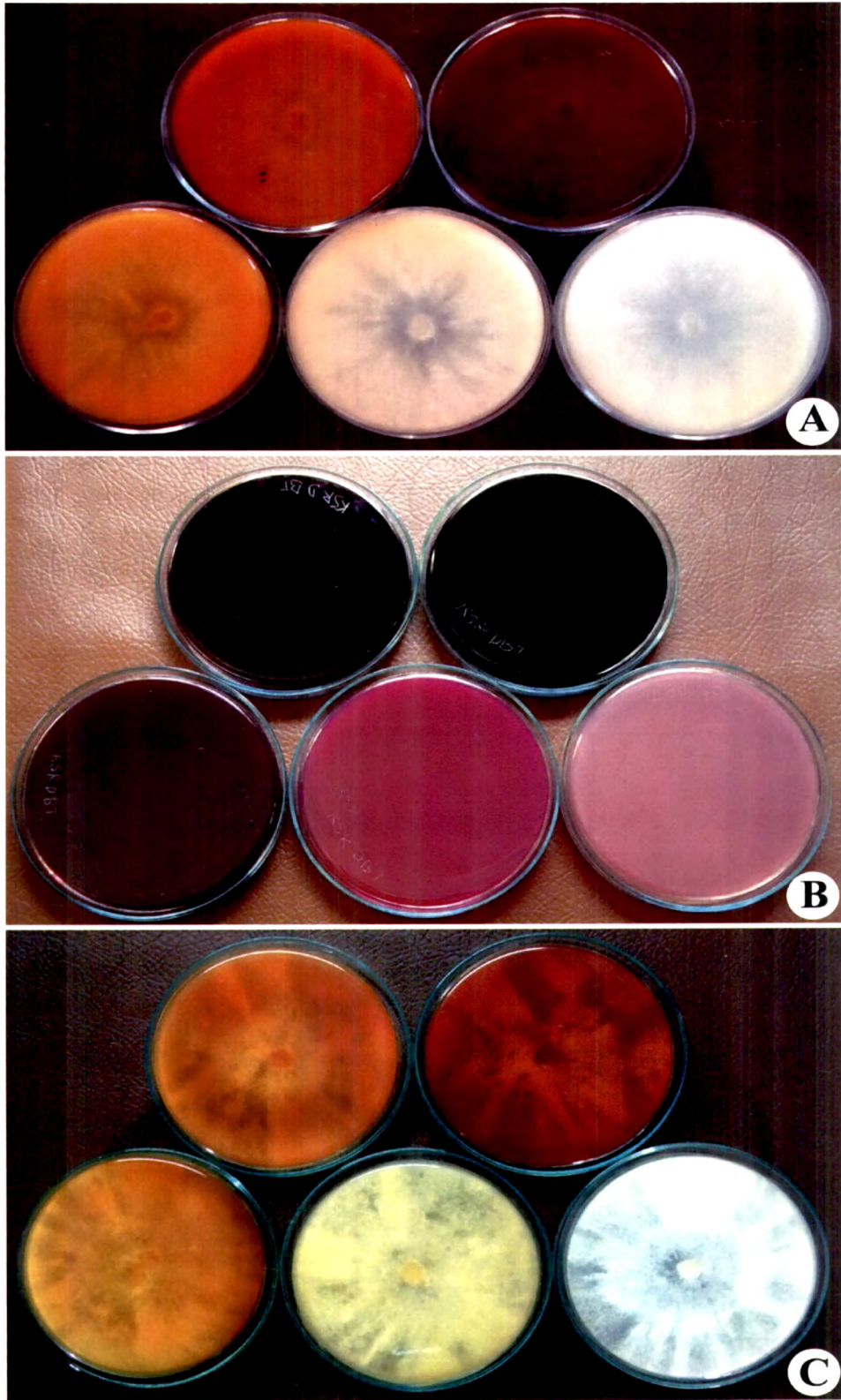


Figure 3.9: On plate decolourisation of Reactive Magenta HB by *Irpex lacteus* (A), *Phanerochaete chrysosporium* (C) and Control dye (B).

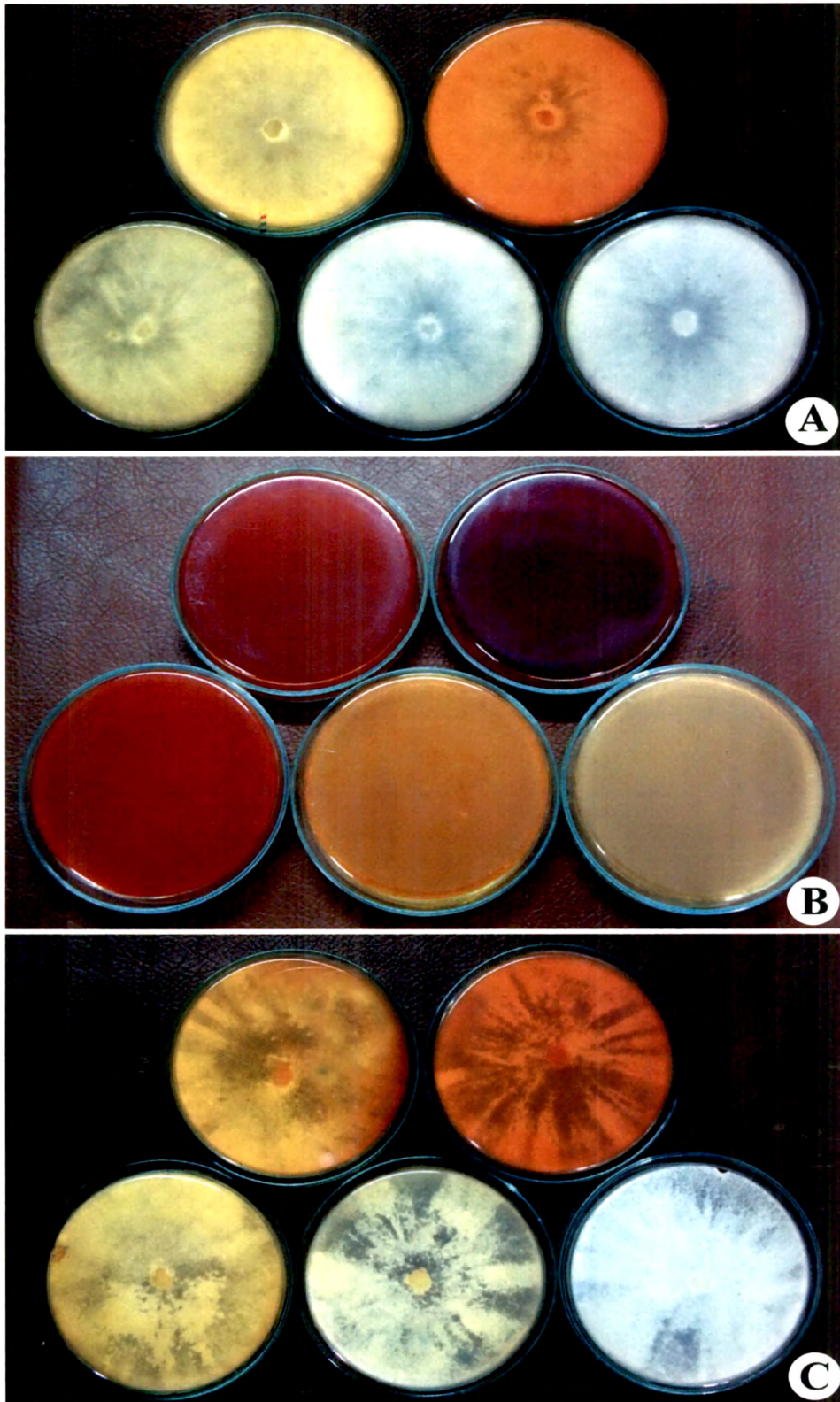


Figure 3.10: On plate decolourisation of Reactive Yellow MERL by *Irpex lacteus* (A), *Phanerochaete chrysosporium* (C) and Control dye (B).

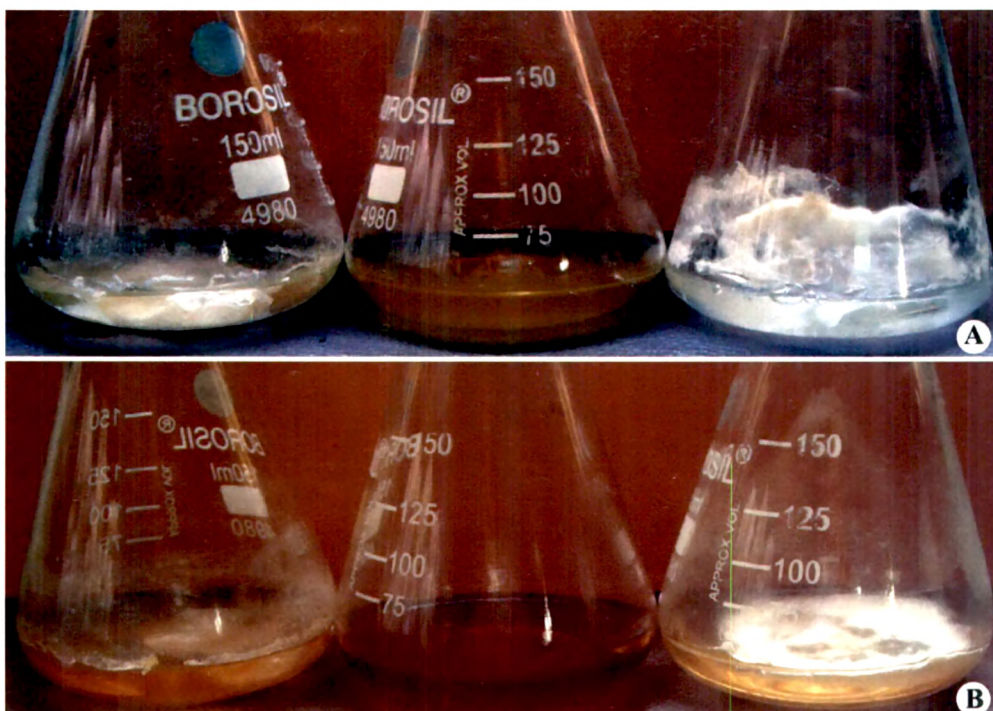


Figure 3.13 Decolorization of Reactive Yellow FG (A) and Reactive Orange 2R (B) in liquid medium: *Irpex lacteus* (Right), Control (Middle) and *Phanerochaete chrysosporium* (Left).

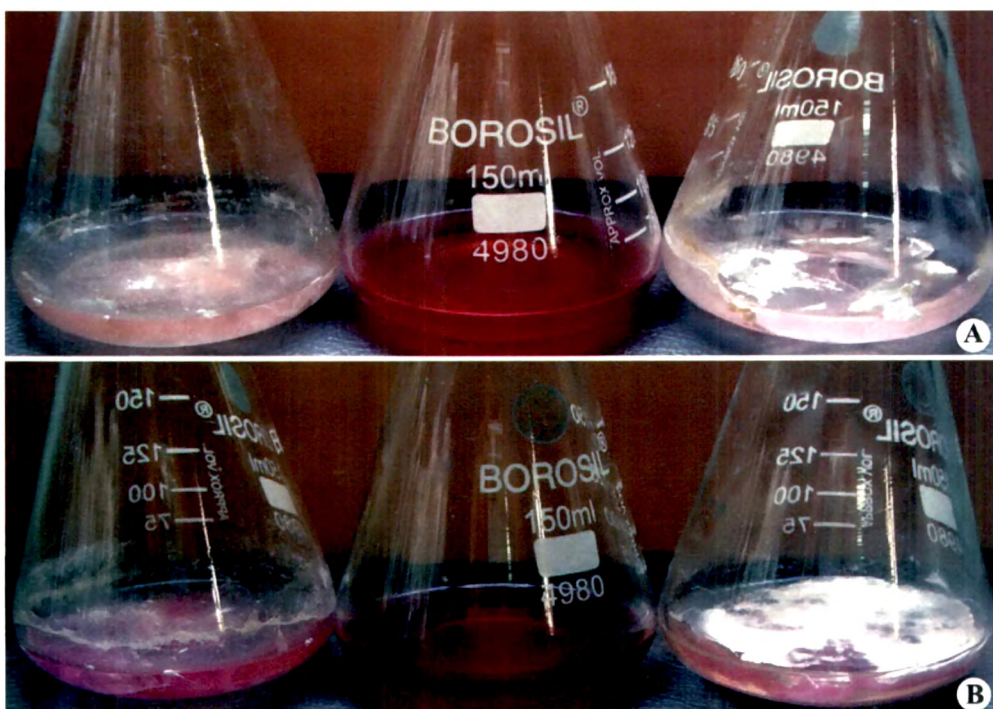


Figure 3.13 Decolorization of Reactive Red ME4BL (A) and Reactive Red HE8B (B) in liquid medium: *Irpex lacteus* (Right), Control (Middle) and *Phanerochaete chrysosporium* (Left).



Figure 3.13 Decolorization of Reactive Black B (A) and Reactive Golden Yellow HR (B) in liquid medium: *Irpex lacteus* (Right), Control (Middle) and *Phanerochaete chrysosporium* (Left).

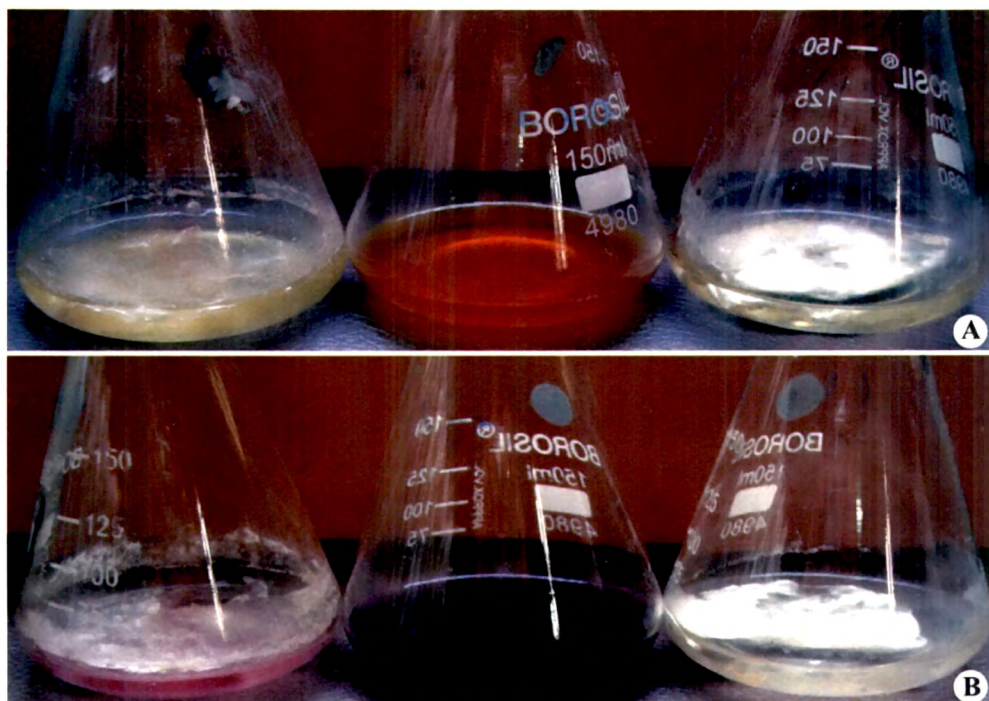


Figure 3.13 Decolorization of Reactive Golden Yellow HRNL (A) and Reactive Violet 5R (B) in liquid medium: *Irpex lacteus* (Right), Control (Middle) and *Phanerochaete chrysosporium* (Left).

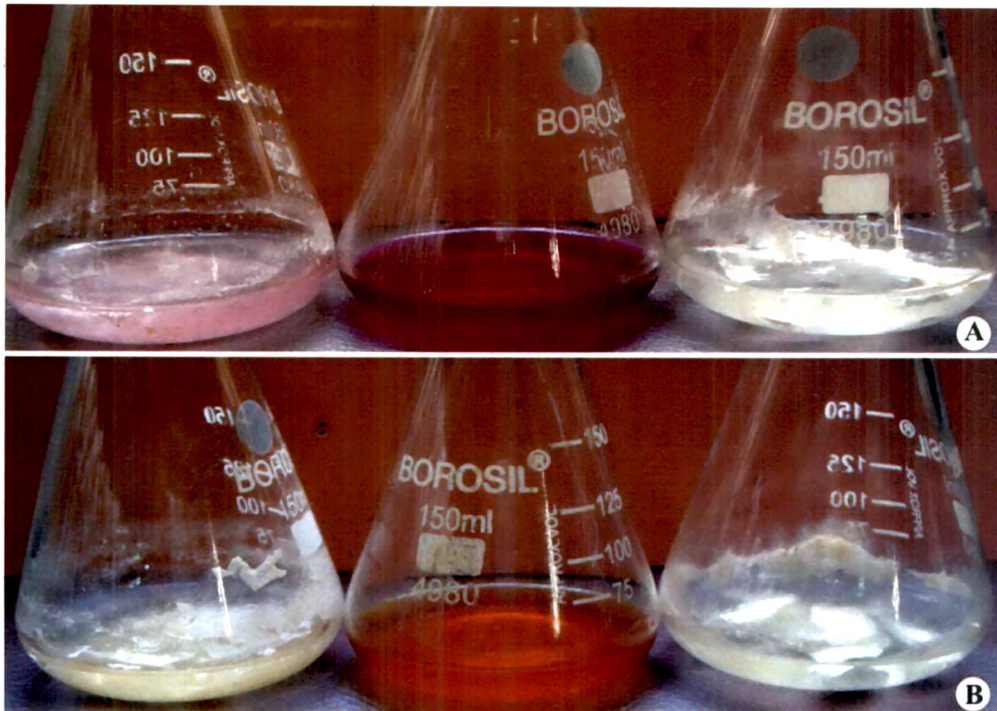


Figure 3.13 Decolorization of Reactive Magenta HB (A) and Reactive Yellow MERL (B) in liquid medium: *Irpex lacteus* (Right), Control (Middle) and *Phanerochaete chrysosporium* (Left).

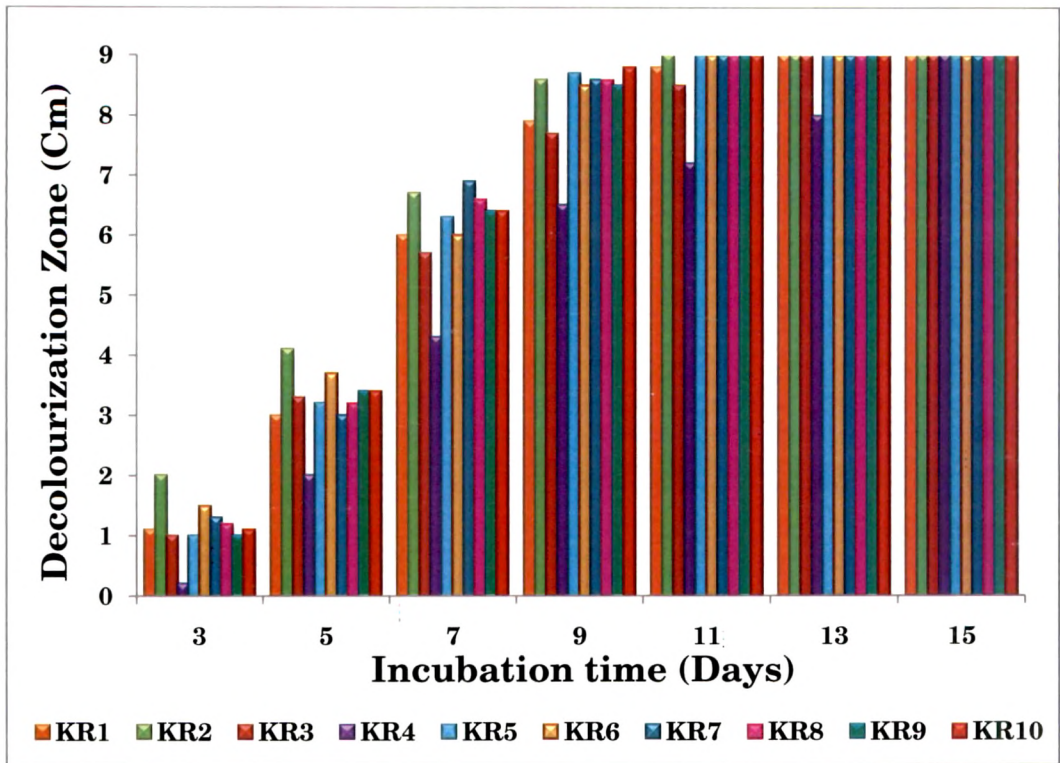


Figure 3.11: Solid plate dye decolorization by *Irpex lacteus*

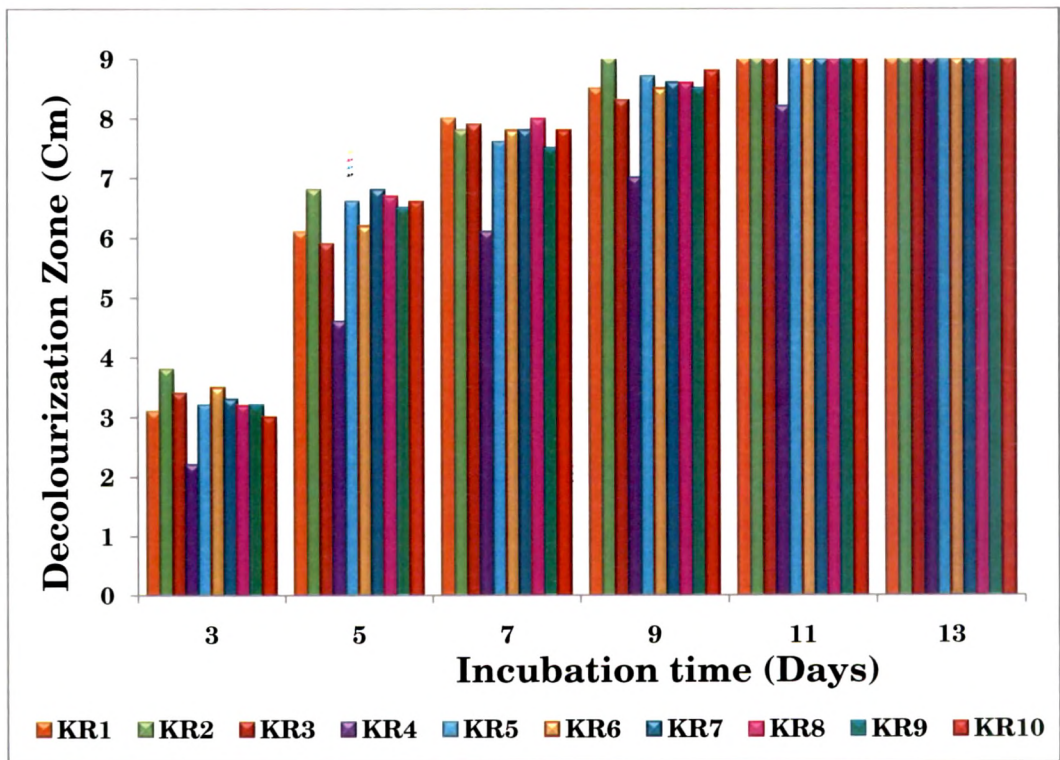


Figure 3.12: Solid plate dye decolorization by *Phanerochaete chrysosporium*

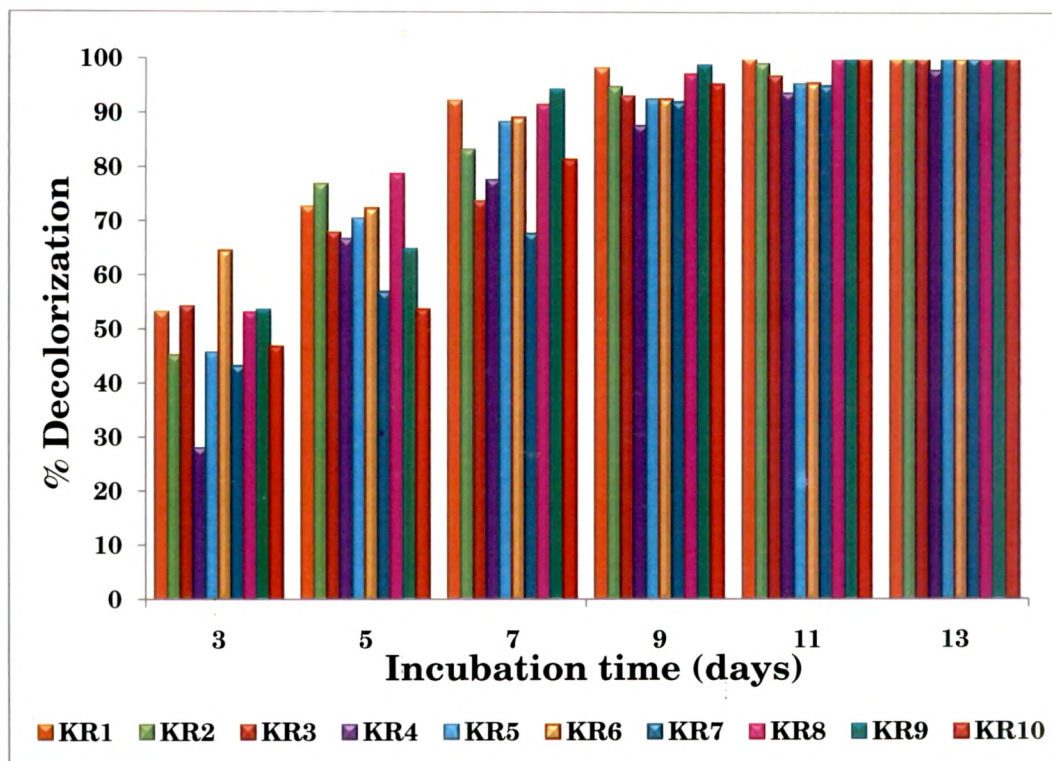


Figure 3.18: %Decolorization of ten reactive textile dyes by *Irpex lacteus*

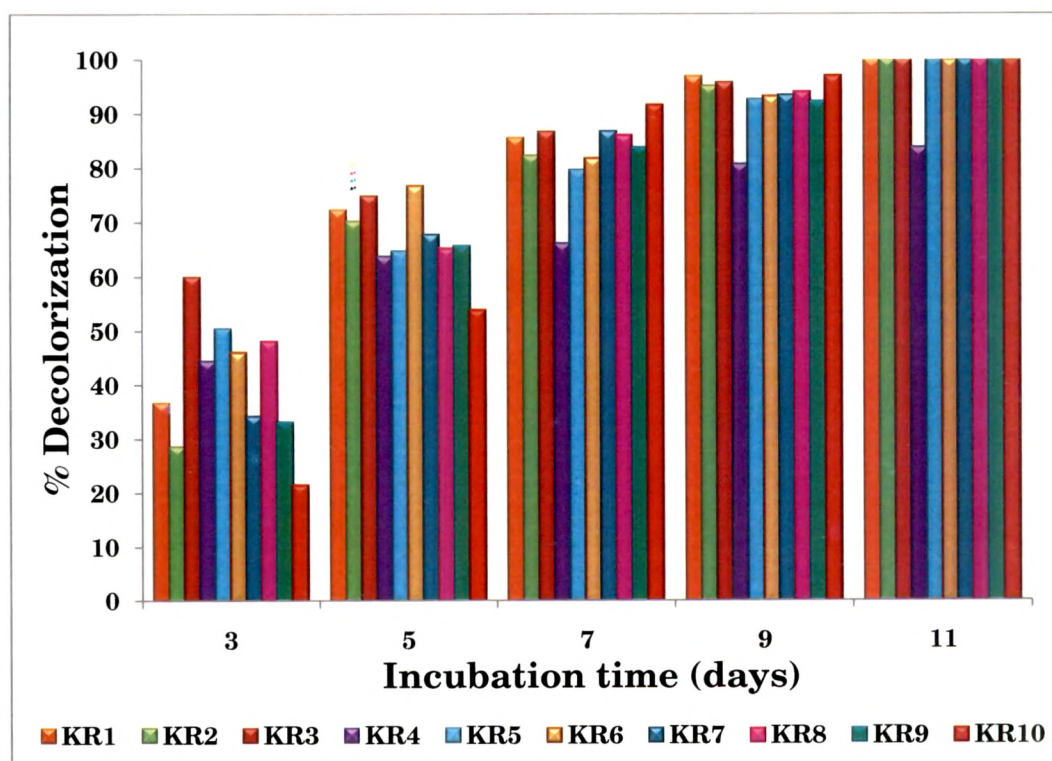


Figure 3.19: %Decolorization of ten reactive textile dyes by *Phanerochaete chrysosporium*.

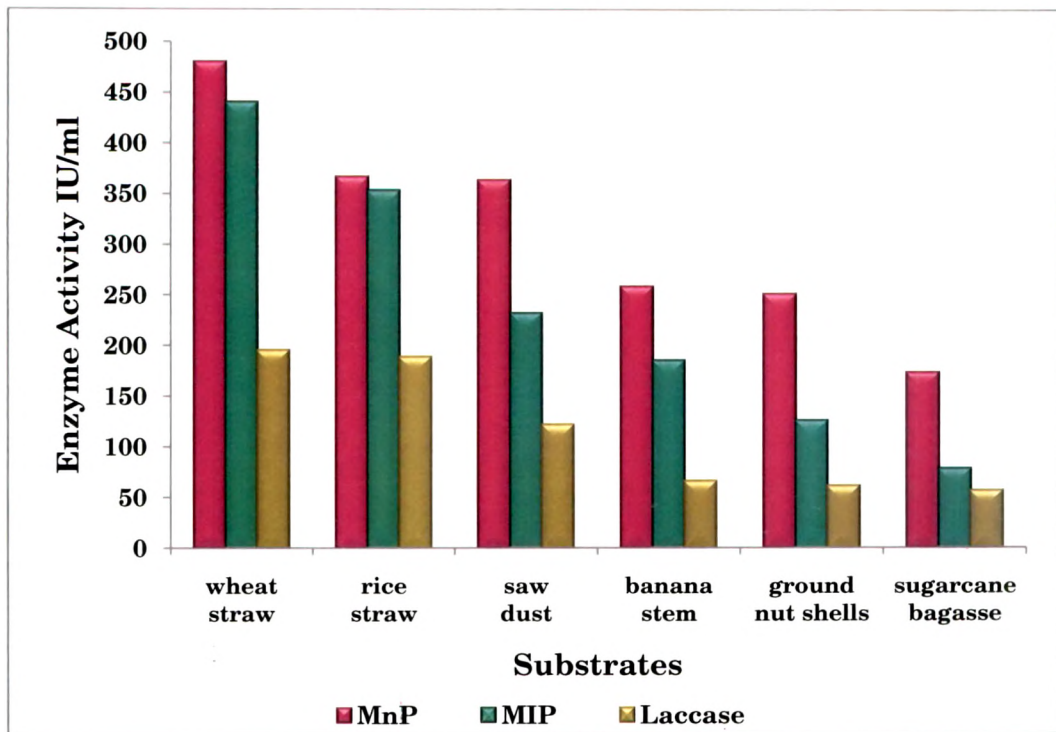


Figure 3.20: Optimisation of different solid substrates for ligninolytic enzyme production by *Irpex lacteus*

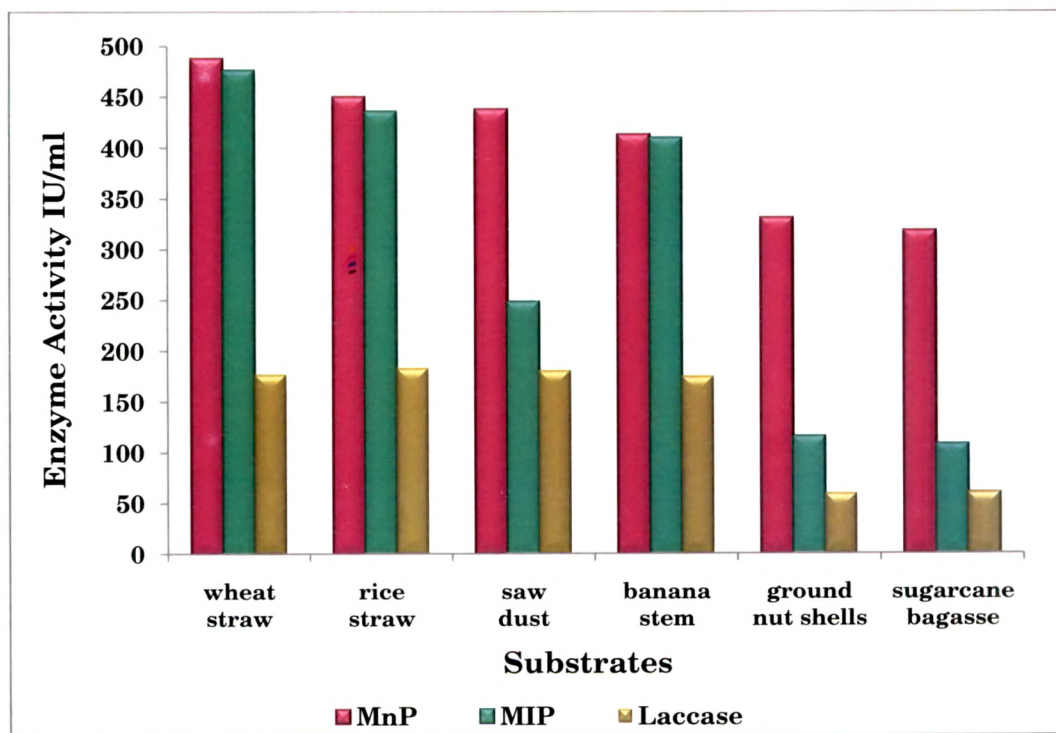


Figure 3.21: Optimisation of different solid substrates for ligninolytic enzyme production by *Phanerochaete chrysosporium*

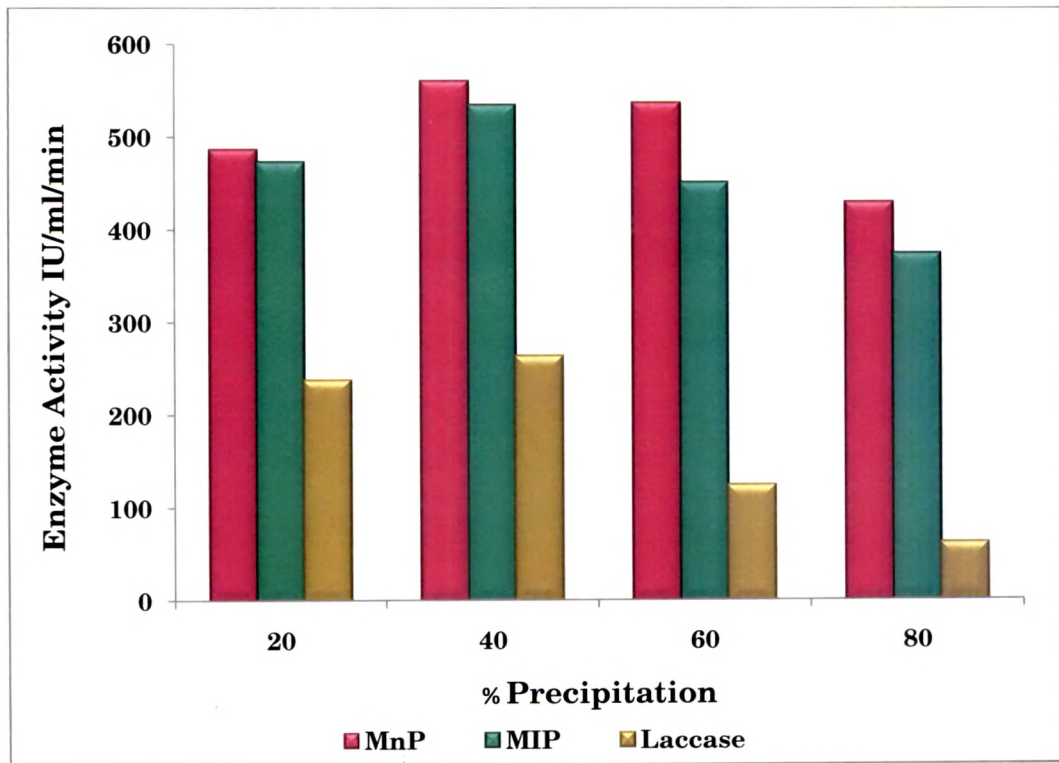


Figure 3.22: Production profile of ligninolytic enzymes produced by *Irpex lacteus*

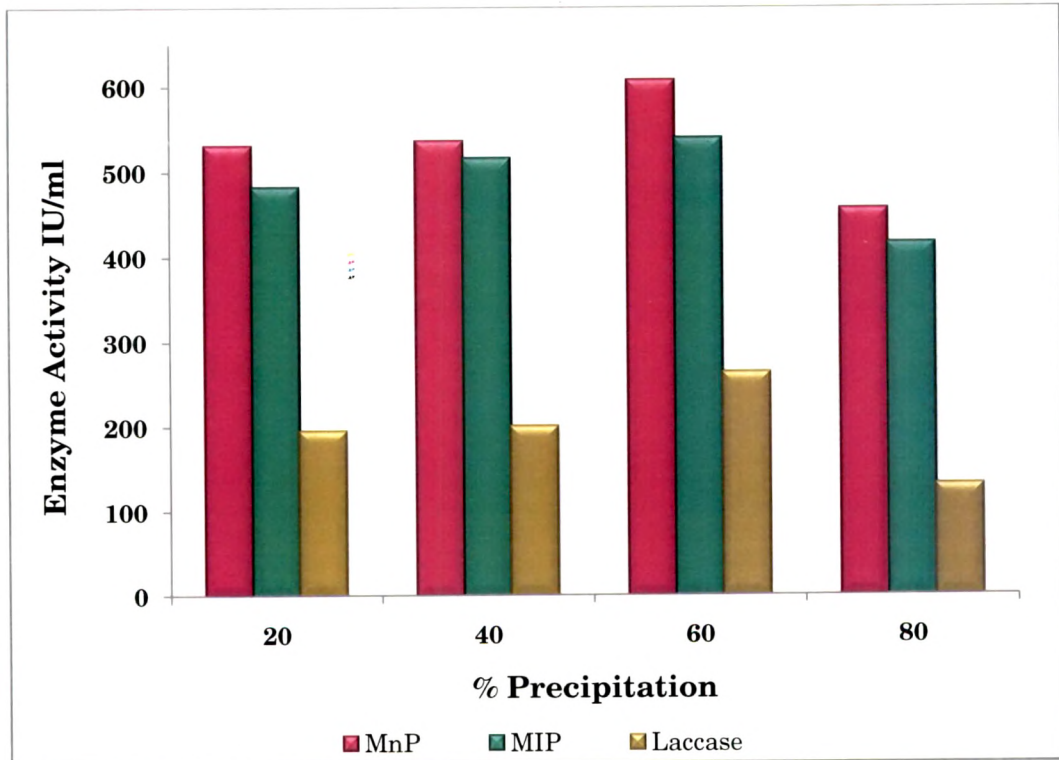


Figure 3.23: Production profile of ligninolytic enzymes produced by *Phanerochaete chrysosporium*

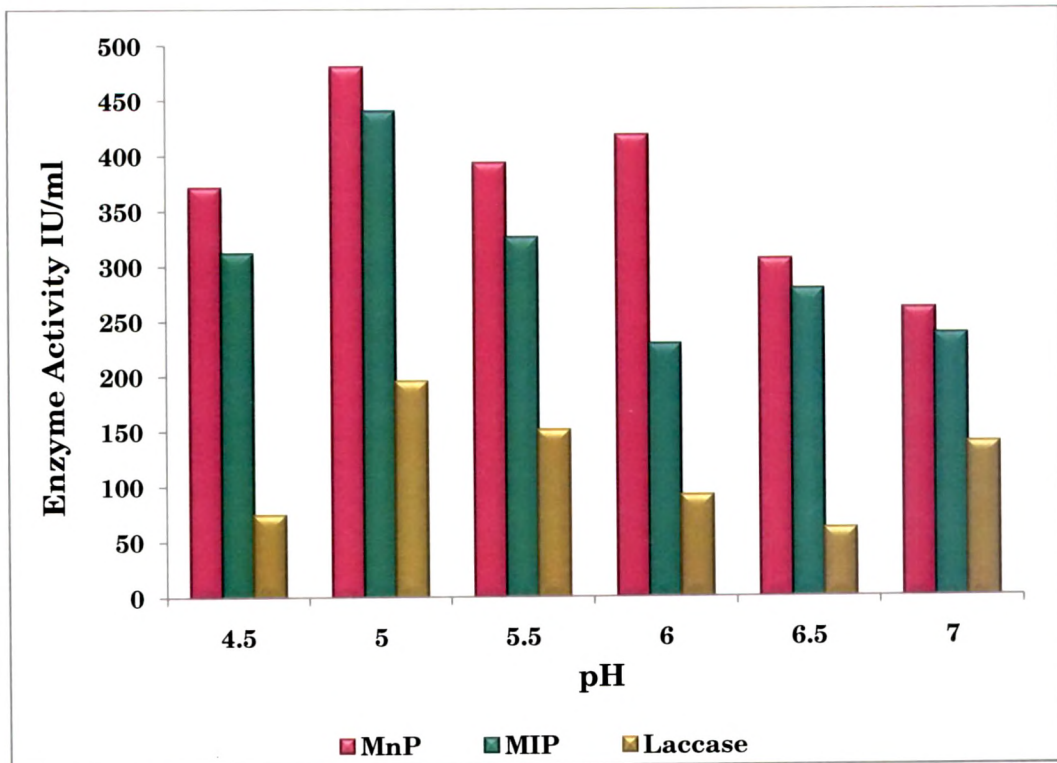


Figure 3.25: Influence of pH on ligninolytic enzyme activity produced by *Irpex lacteus*

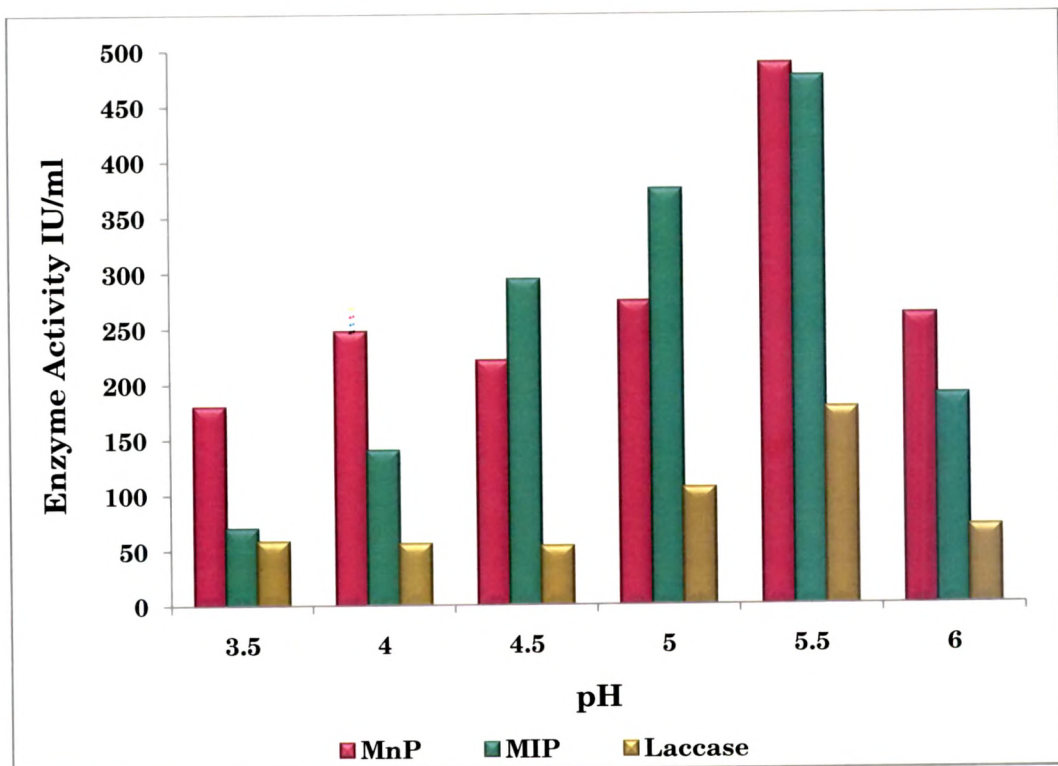


Figure 3.26: Influence of pH on ligninolytic enzyme activity produced by *Phanerochaete chrysosporium*

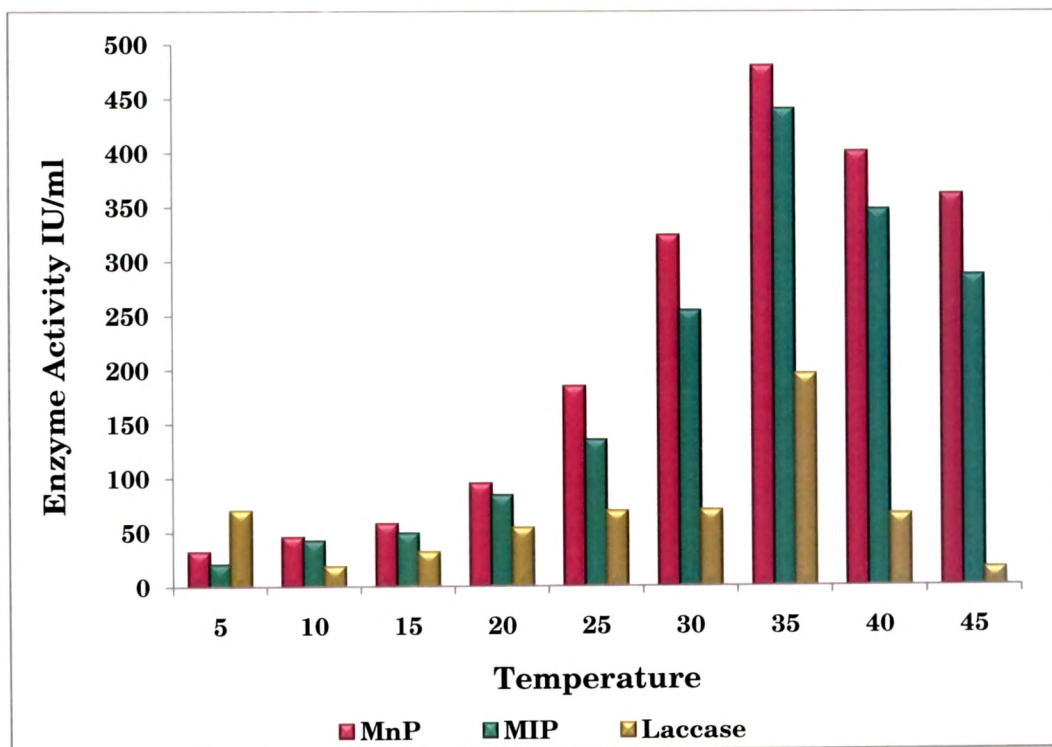


Figure 3.27: Influence of incubation temperature on ligninolytic enzyme activity produced by *Irpex lacteus*

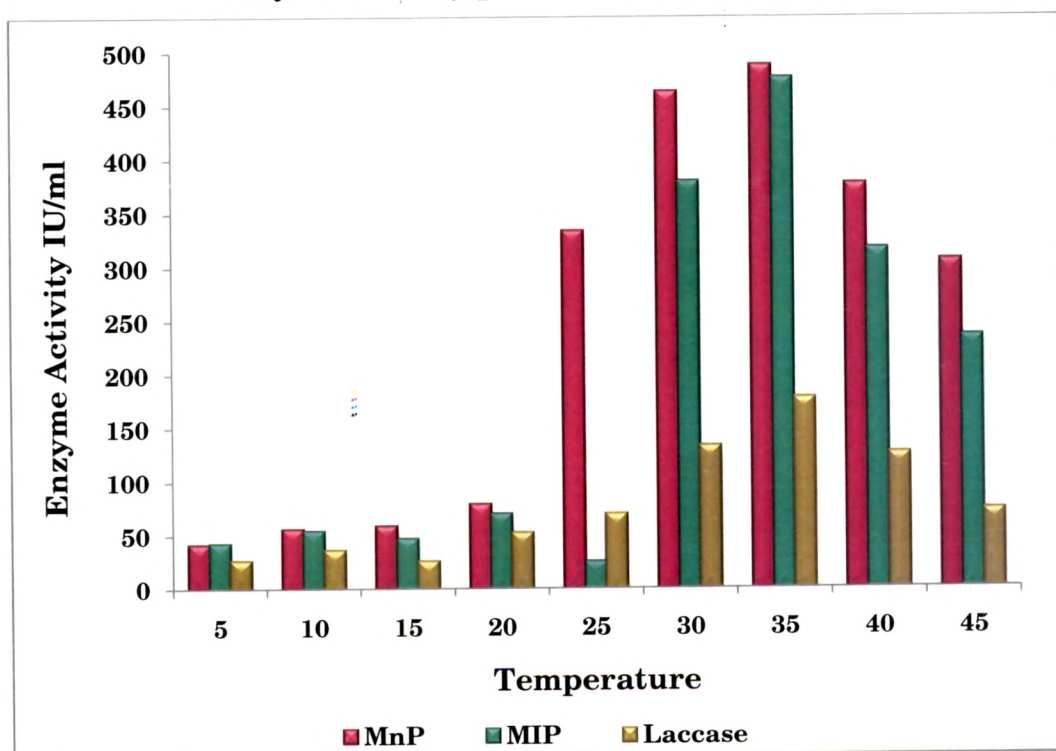


Figure 3.28: Influence of incubation temperature on ligninolytic enzyme activity produced by *Phanerochaete chrysosporium*

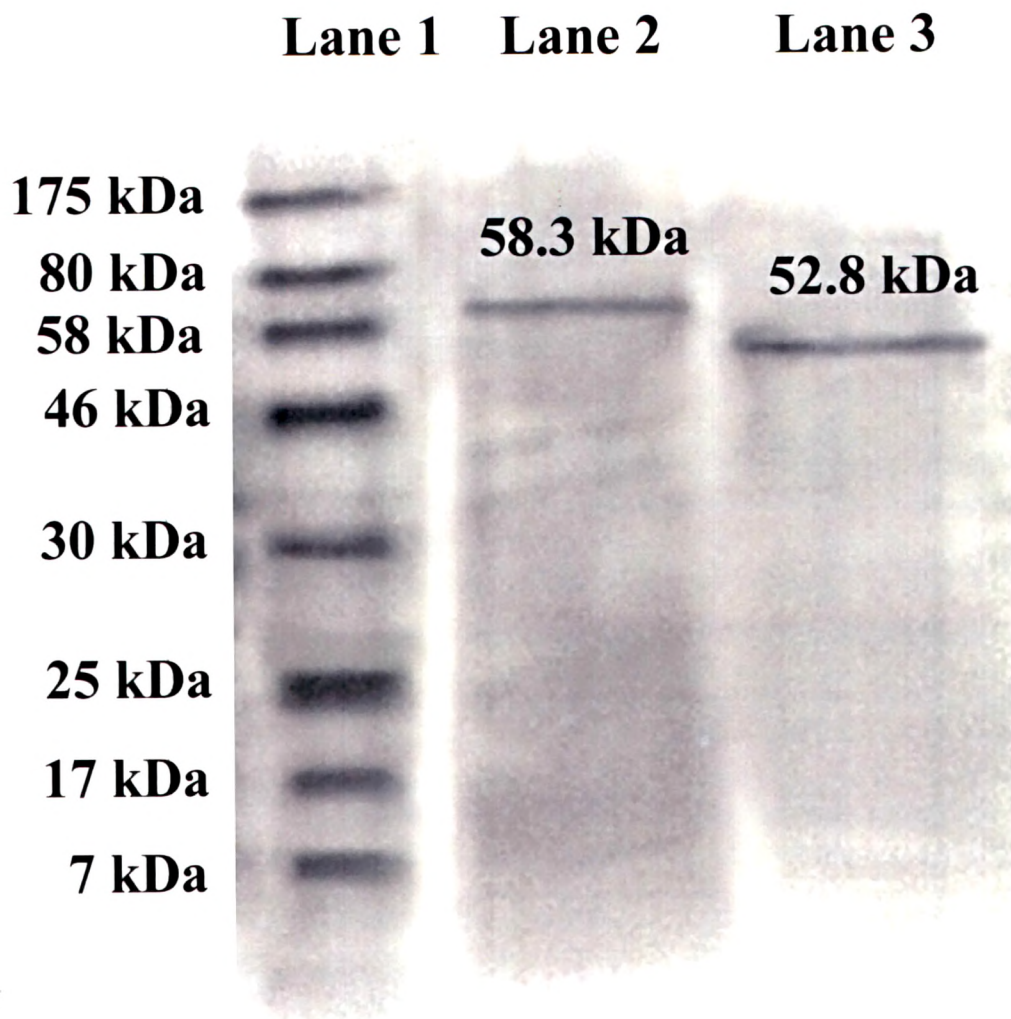


Figure 3.24: Electrophoretic analysis (SDS-PAGE) of the purified MnP from *Irpex lacteus* (Lane 2) and *Phanerochaete chrysosporium* (Lane 3). Lane 1 indicates standard marker (NEB # P7708).

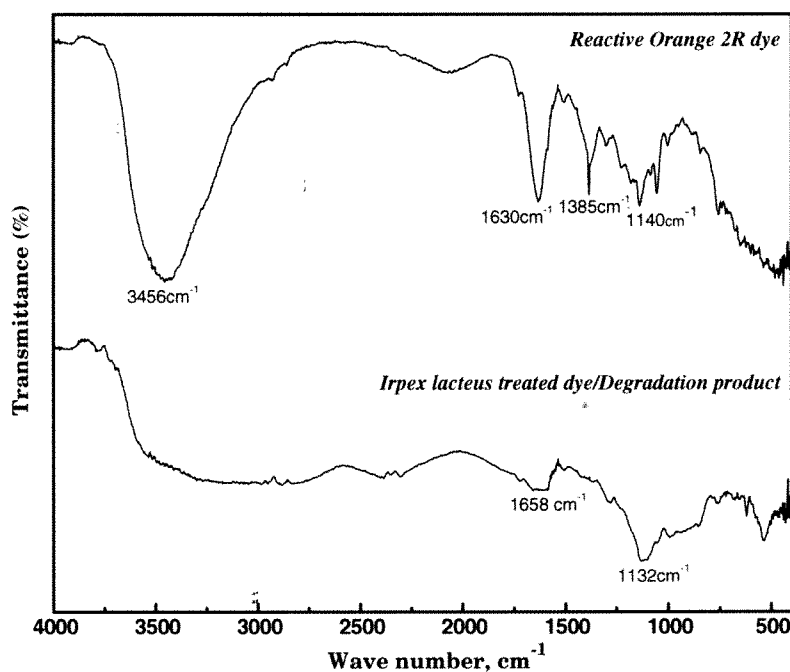
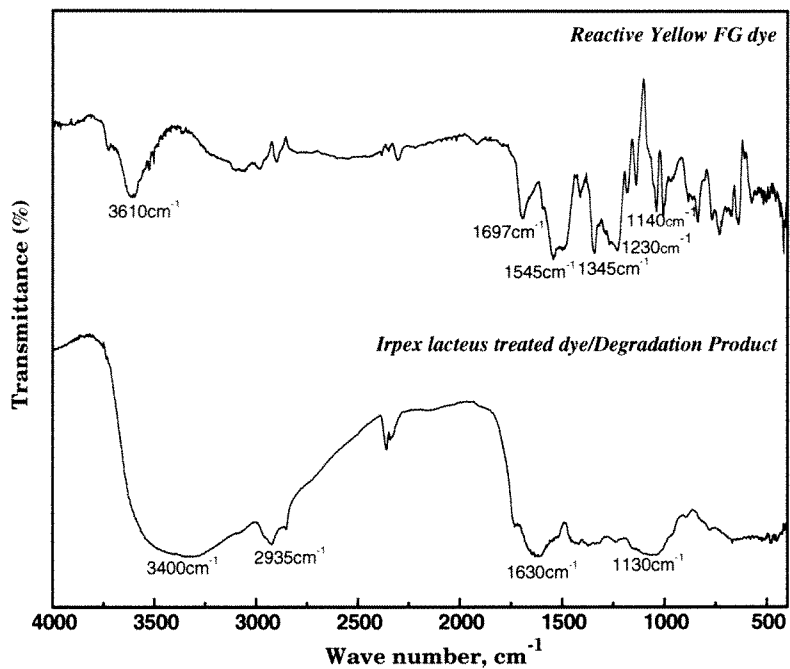


Figure 3.29: Comparison of the FTIR spectra of control dyes a) Reactive Yellow FG; b) Reactive Orange 2R, and their degradation products extracted after 48 hours of reaction with *Irpex lacteus* MnP.

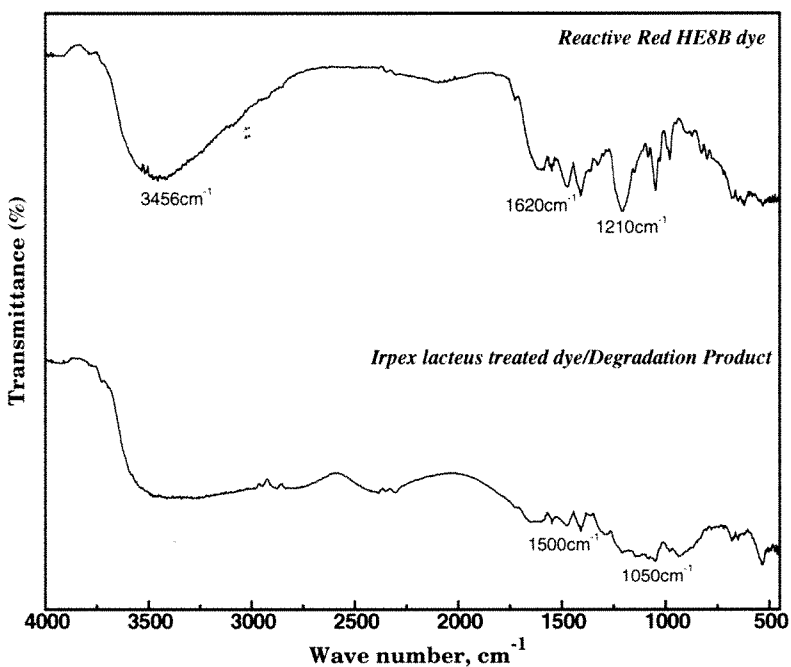
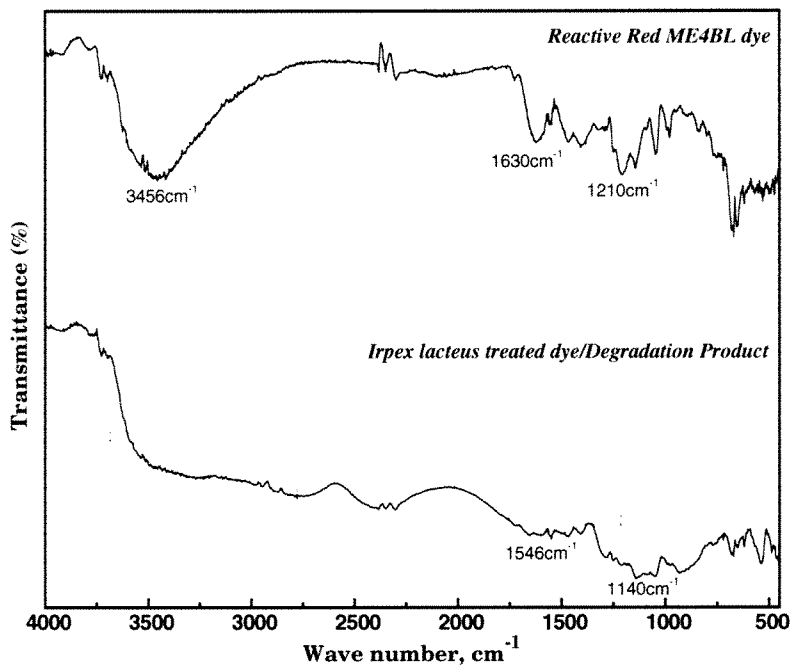


Figure 3.30: Comparison of the FTIR spectra of control dyes a) Reactive Red ME4BL; b) Reactive Red HE8B, and their degradation products extracted after 48 hours of reaction with *Irpex lacteus* MnP.

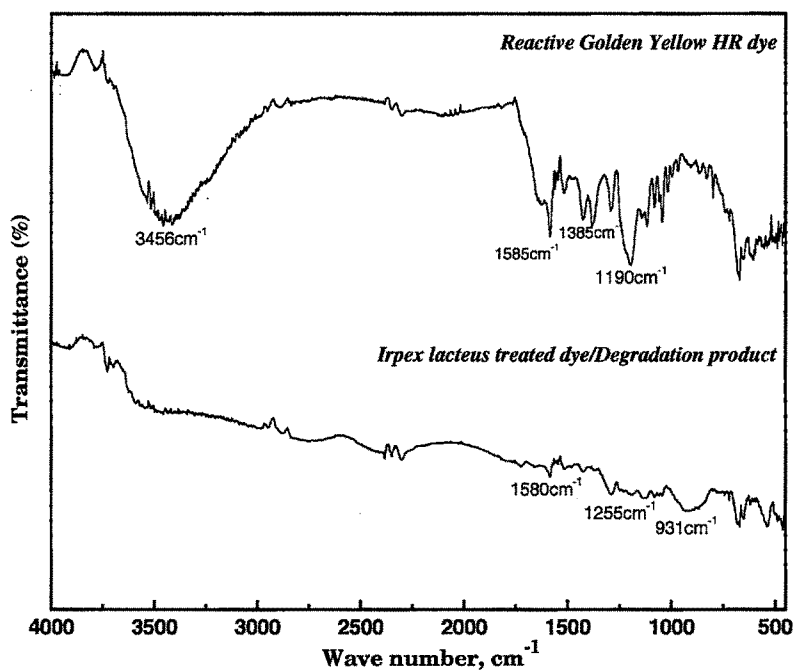
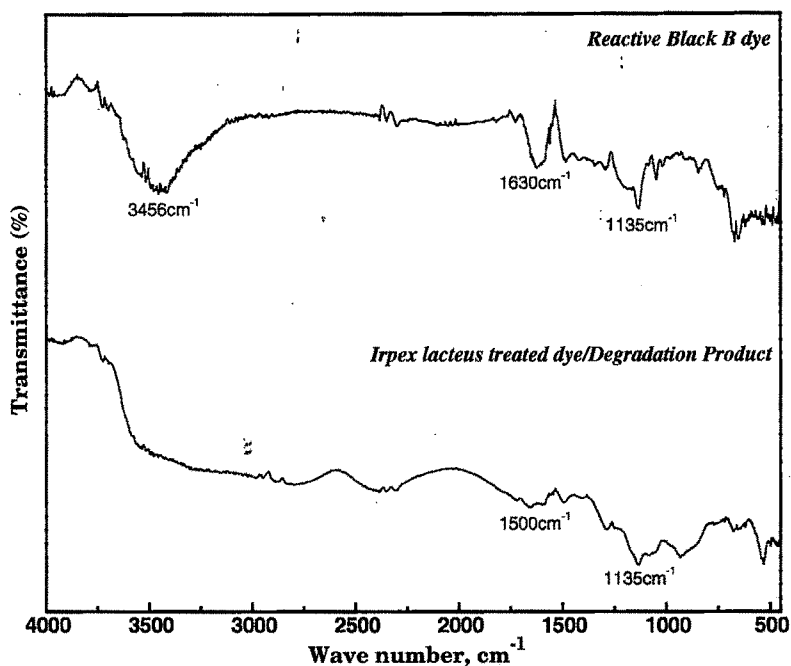


Figure 3.31: Comparison of the FTIR spectra of control dyes a) Reactive Black B; b) Reactive Golden Yellow HR, and their degradation products extracted after 48 hours of reaction with *Irpex lacteus* MnP.

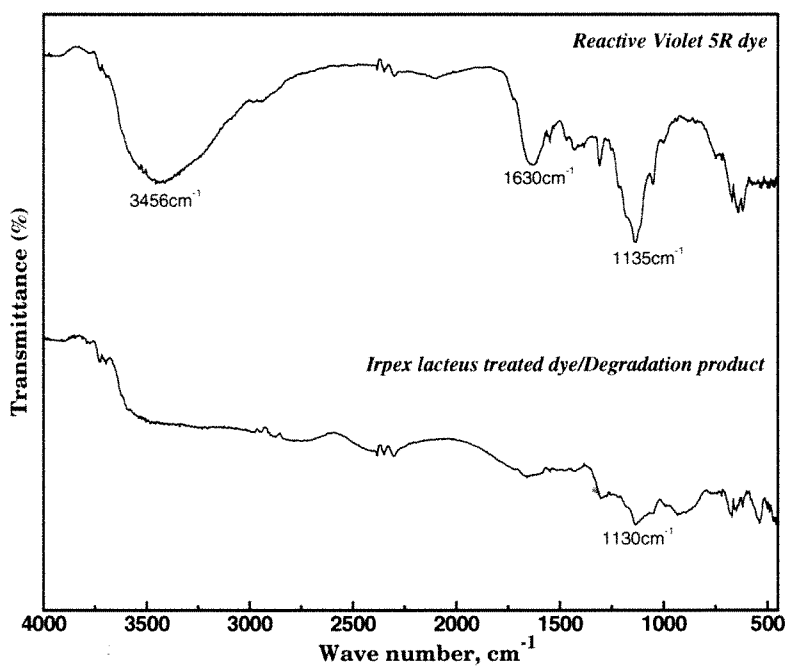
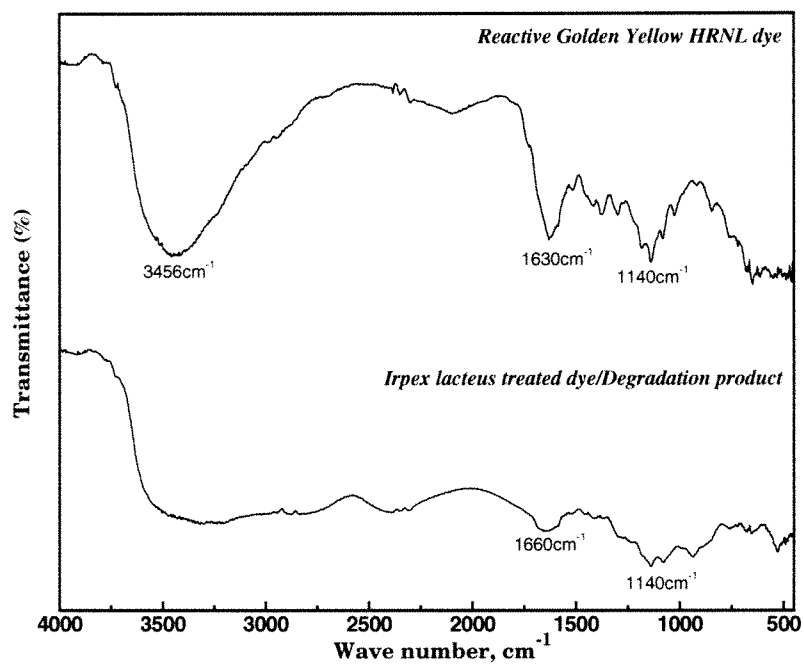


Figure 3.32: Comparison of the FTIR spectra of control dyes a) Reactive Golden Yellow HRNL; b) Reactive Violet 5R, and their degradation products extracted after 48 hours of reaction with *Irpex lacteus* MnP.

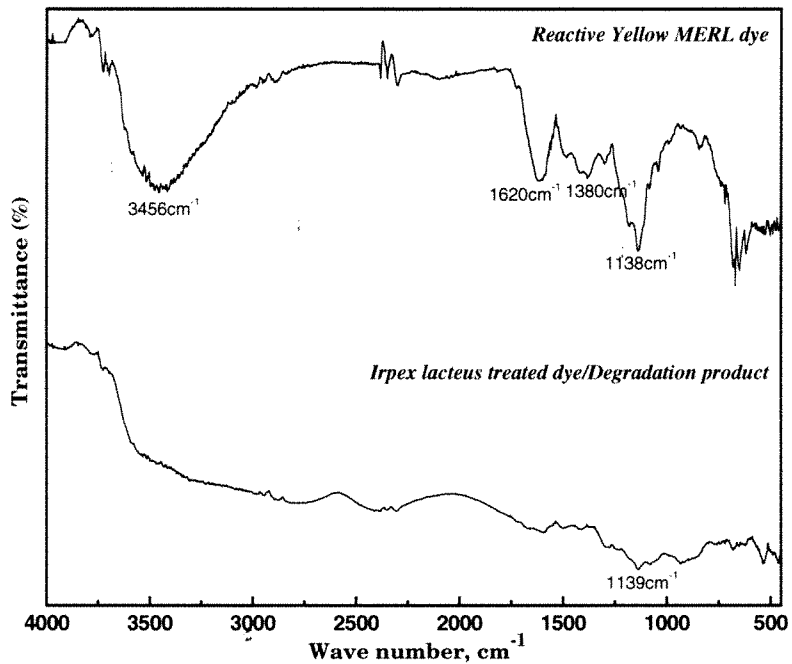
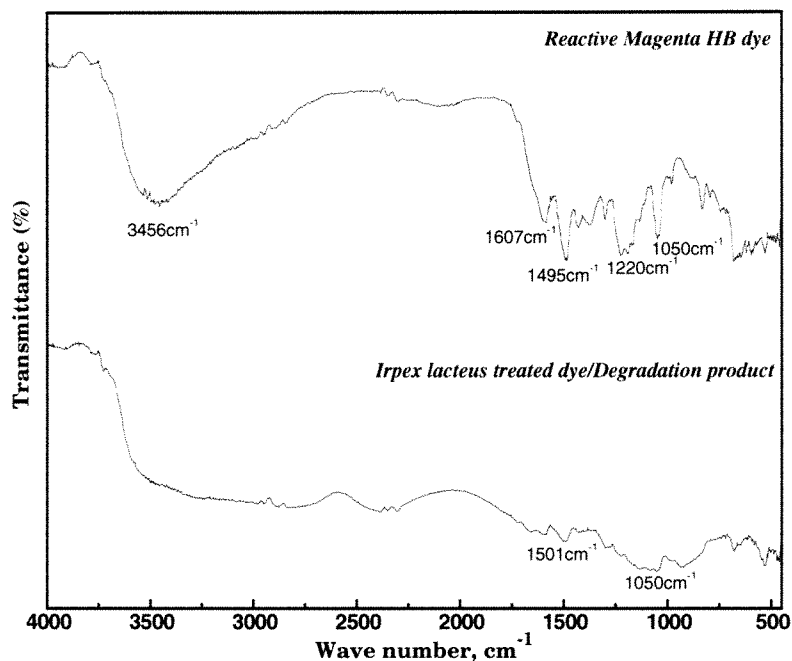


Figure 3.33: Comparison of the FTIR spectra of control dyes a) Reactive Magenta HB; b) Reactive Yellow MERL, and their degradation products extracted after 48 hours of reaction with *Irpex lacteus* MnP.

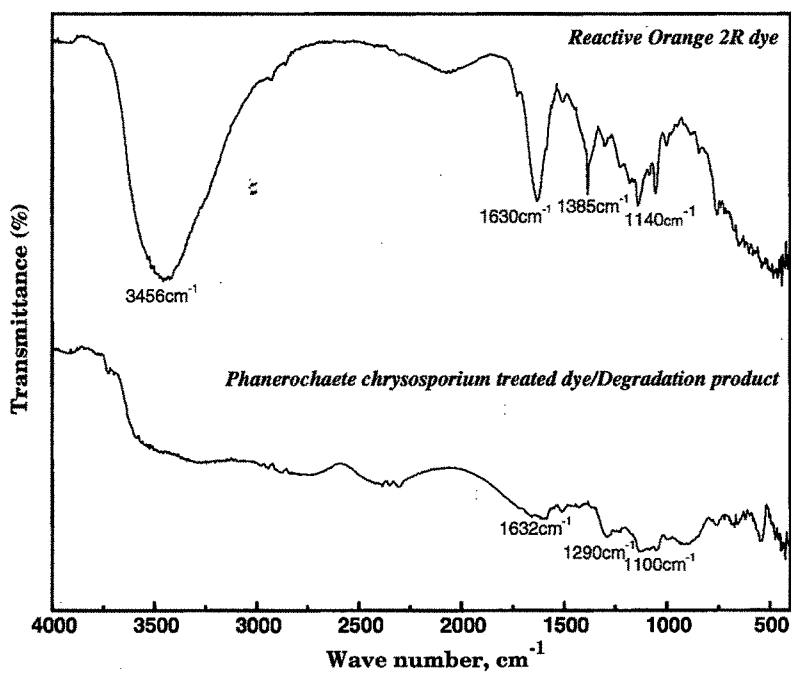
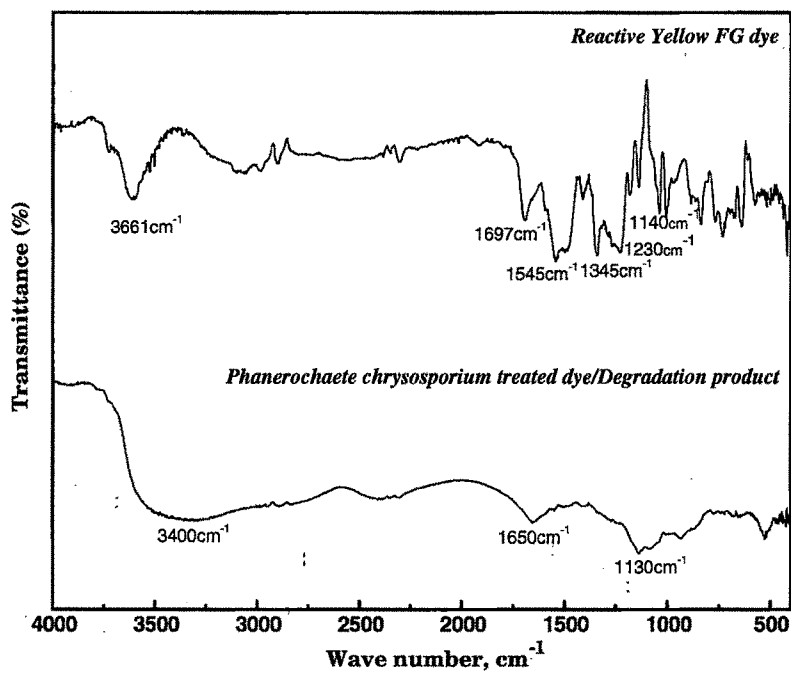


Figure 3.34: Comparison of the FTIR spectra of control dyes a) Reactive Yellow FG; b) Reactive Orange 2R, and their degradation products extracted after 48 hours of reaction with *Phanerochaete chrysosporium* MnP.

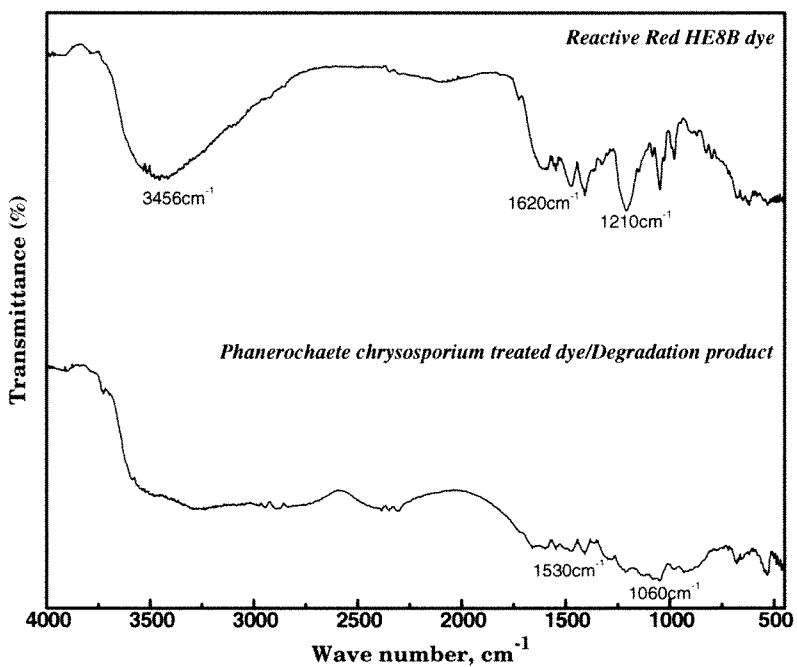
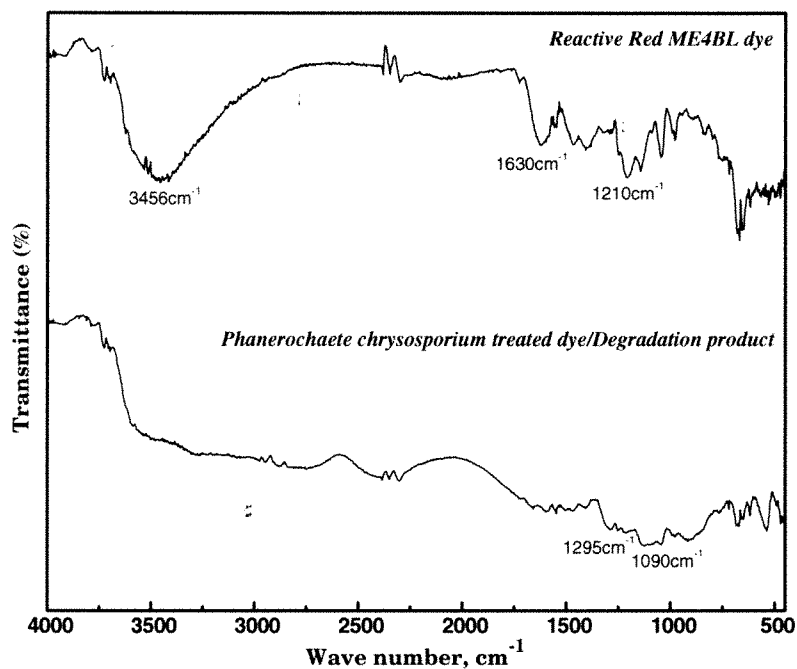


Figure 3.35: Comparison of the FTIR spectra of control dyes a) Reactive Red ME4BL; b) Reactive Red HE8B, and their degradation products extracted after 48 hours of reaction with *Phanerochaete chrysosporium* MnP.

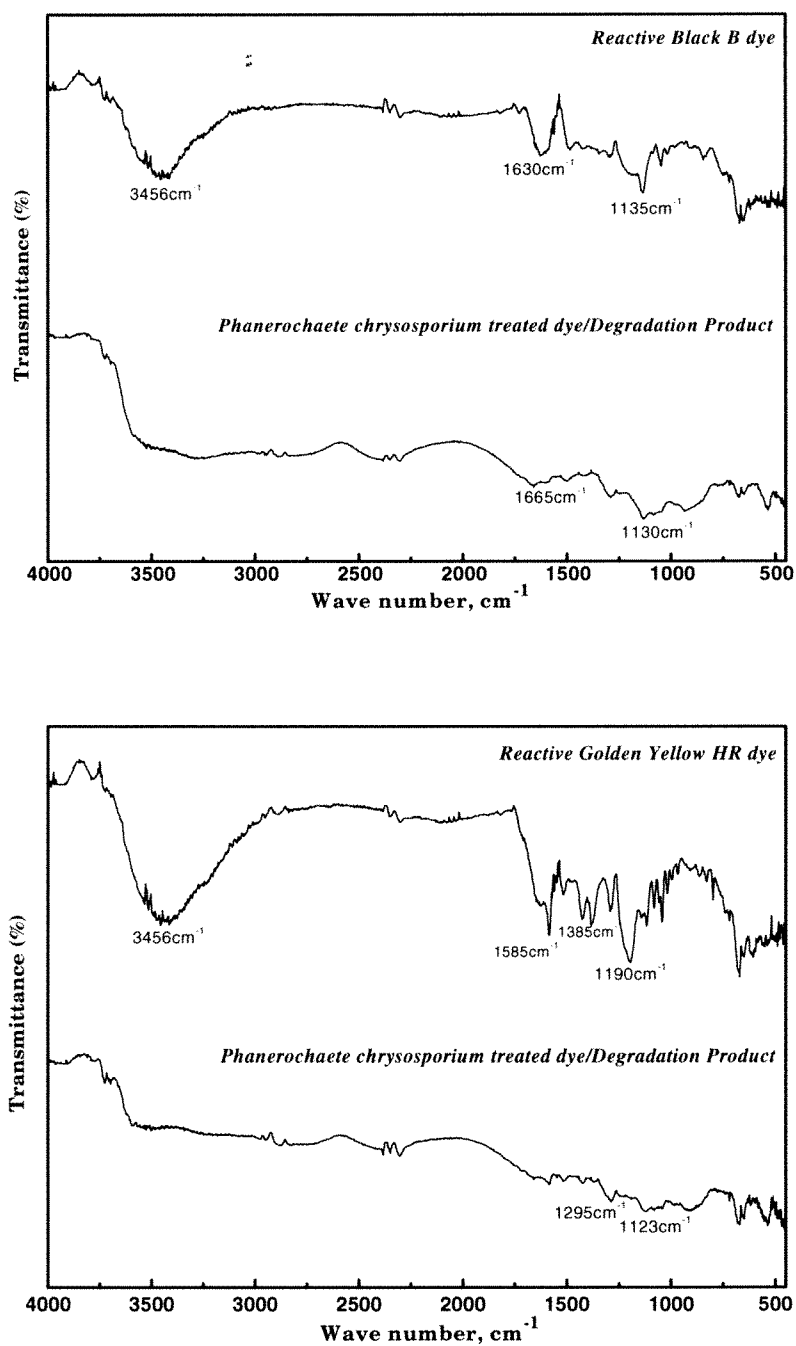


Figure 3.36: Comparison of the FTIR spectra of control dyes a) Reactive Black B; b) Reactive Golden Yellow HR, and their degradation products extracted after 48 hours of reaction with *Phanerochaete chrysosporium* MnP.

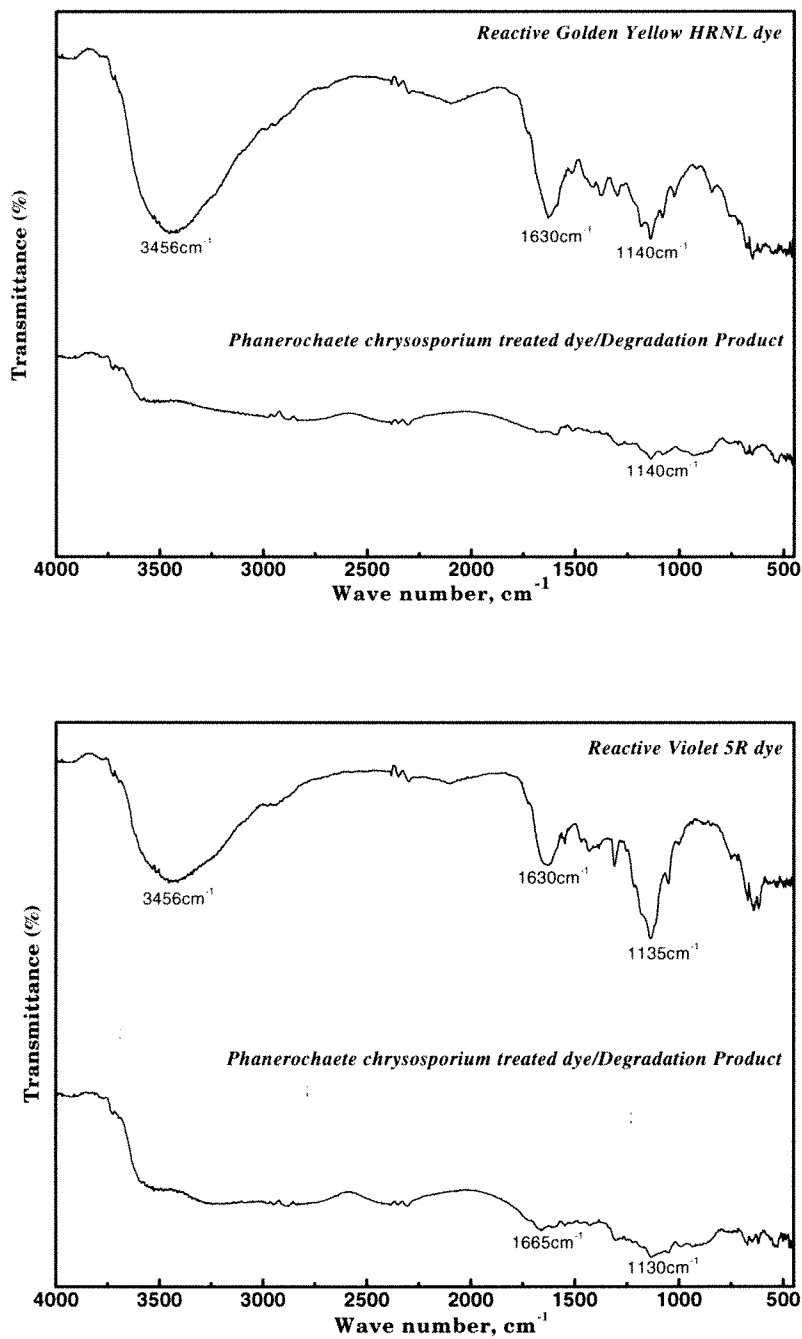


Figure 3.37: Comparison of the FTIR spectra of control dyes a) Reactive Golden Yellow HRNL; b) Reactive Violet 5R, and their degradation products extracted after 48 hours of reaction with *Phanerochaete chrysosporium* MnP.

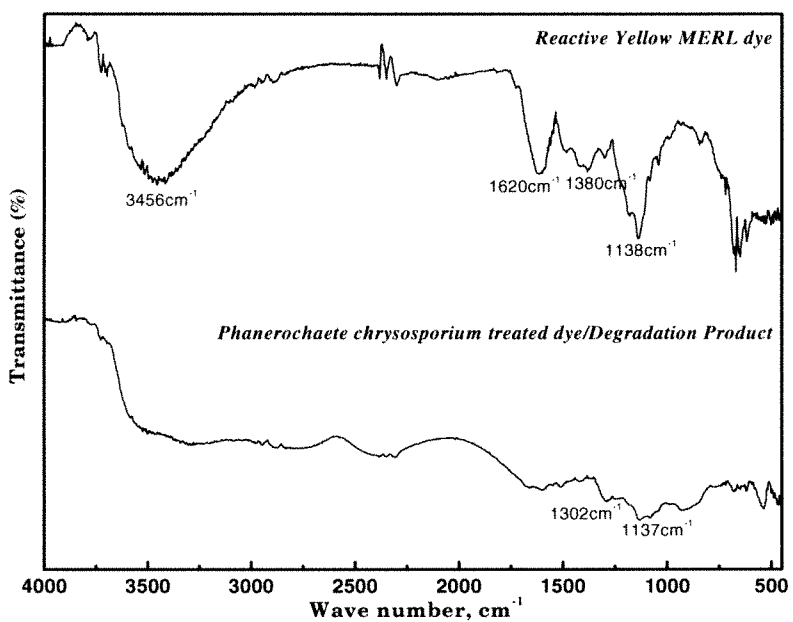
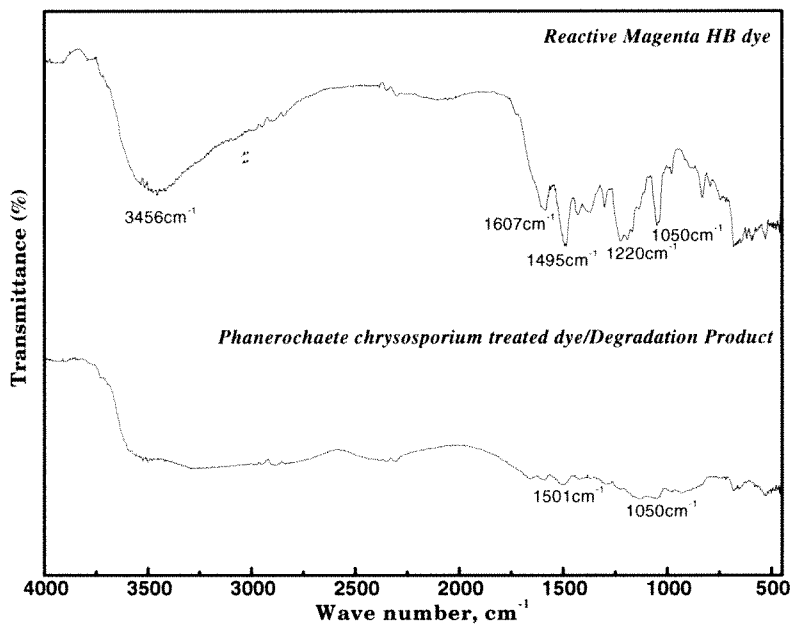


Figure 3.38: Comparison of the FTIR spectra of control dyes a) Reactive Magenta HB; b) Reactive Yellow MERL, and their degradation products extracted after 48 hours of reaction with *Phanerochaete chrysosporium* MnP.

Figure 3.39: Portion of infected wood (A, B) and transverse (C-F) view of xylem showing fungal invasion in different cell types of *Ailanthus excelsa* wood.

- A: Portion of the wood showing naturally infected (arrow) and beetle tunnels that are attacked by fungi (arrowheads).
- B: Tunnels made by beetles are infected with fungi (arrowhead), which develops brown-black colour around the tunnels.
- C: All the cell types of secondary xylem showing fungal infection. Note the fungal hyphae in vessels and rays (arrowhead).
- D: Hyphae traversing through axial elements of xylem (arrow). Arrowhead shows hyphae into vessel lumen.
- E: Vessel lumen with fungal filaments (arrows).
- F: Fungal hyphae (arrow) passing through vessel lumen, vessel associated parenchyma and ray cells. Note that vessel walls and ray cell wall is relatively unaffected as compared to xylem fibres (arrowhead).

Figure 3.39: (A, B): Scale bar = 15 cm; (C-E) = 100 μm ; (F) = 50 μm

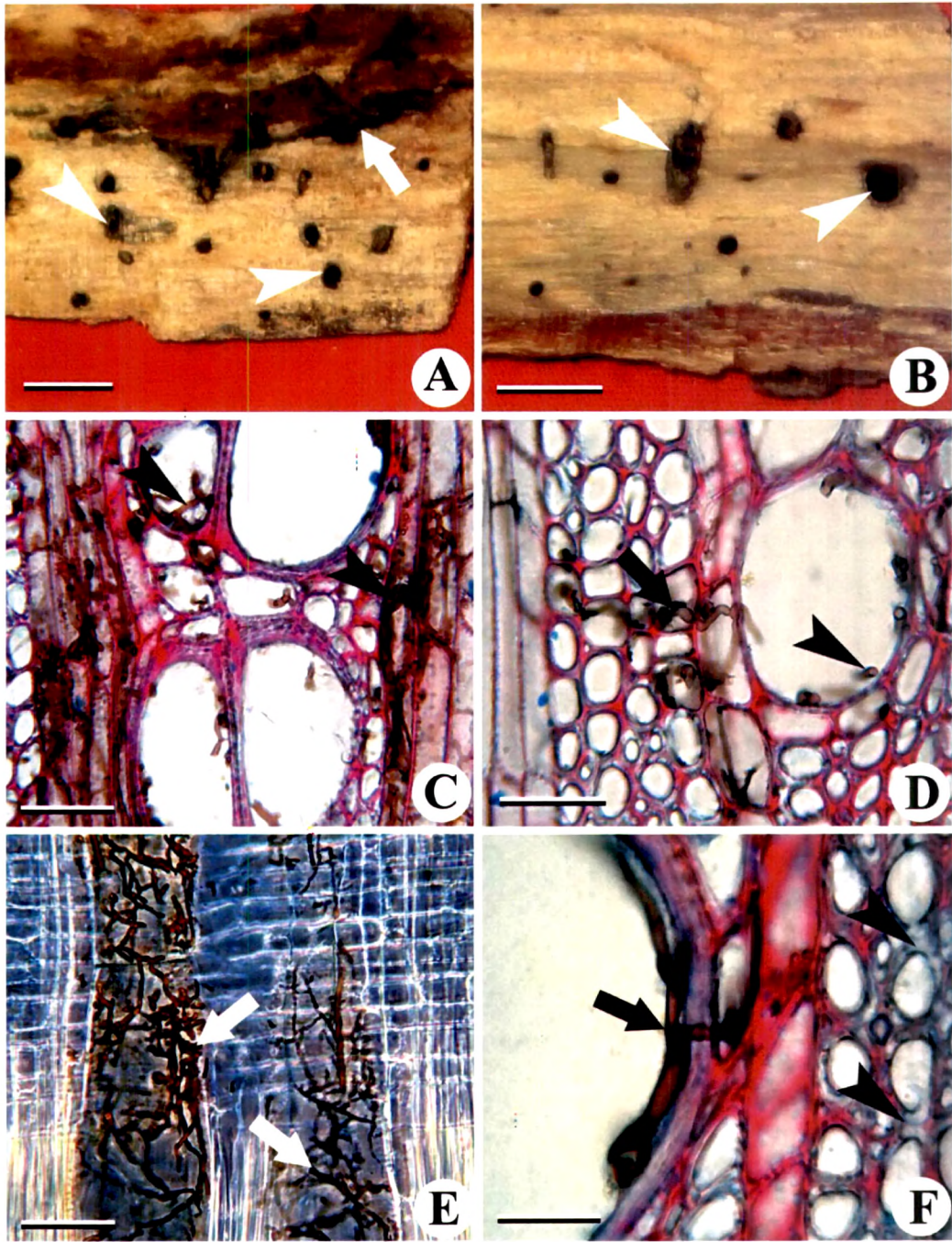


Figure 3.39

Figure 3.40: Transverse (A-C, E, F) and tangential longitudinal (D) view of infected wood of *Ailanthus excelsa* showing different stages of wood decay.

- S3 intact
- A: Severely infected wood portion showing tunnels of various shapes and size. Arrowheads indicate "C" shaped cavity in the S₂ layer of fibre. Note the intact wall layer adjacent to fibre lumen (arrow).
 - B: Path of the fungal hyphae. Arrowheads indicate fungal mycelia traversing radially through the rays.
 - C: Fungal hyphae passing through the xylem fibres (arrowheads). Arrows indicates transversely cut fungal hyphae.
 - D: Xylem fibres showing erosion holes on the tangential wall (arrowheads).
 - E: Vessel elements and adjacent xylem derivatives showing fungal invasion.
 - F: Degraded fibres showing hyphal tunneling. Note that tunneling occurs only in the S₂ layer while S₃ layer remains relatively unaffected (arrowhead). Arrow indicates cavities consistently separated from each other.

Figure 3.40: (A, F): Scale bar = 50 μm ; (B-E) = 100 μm

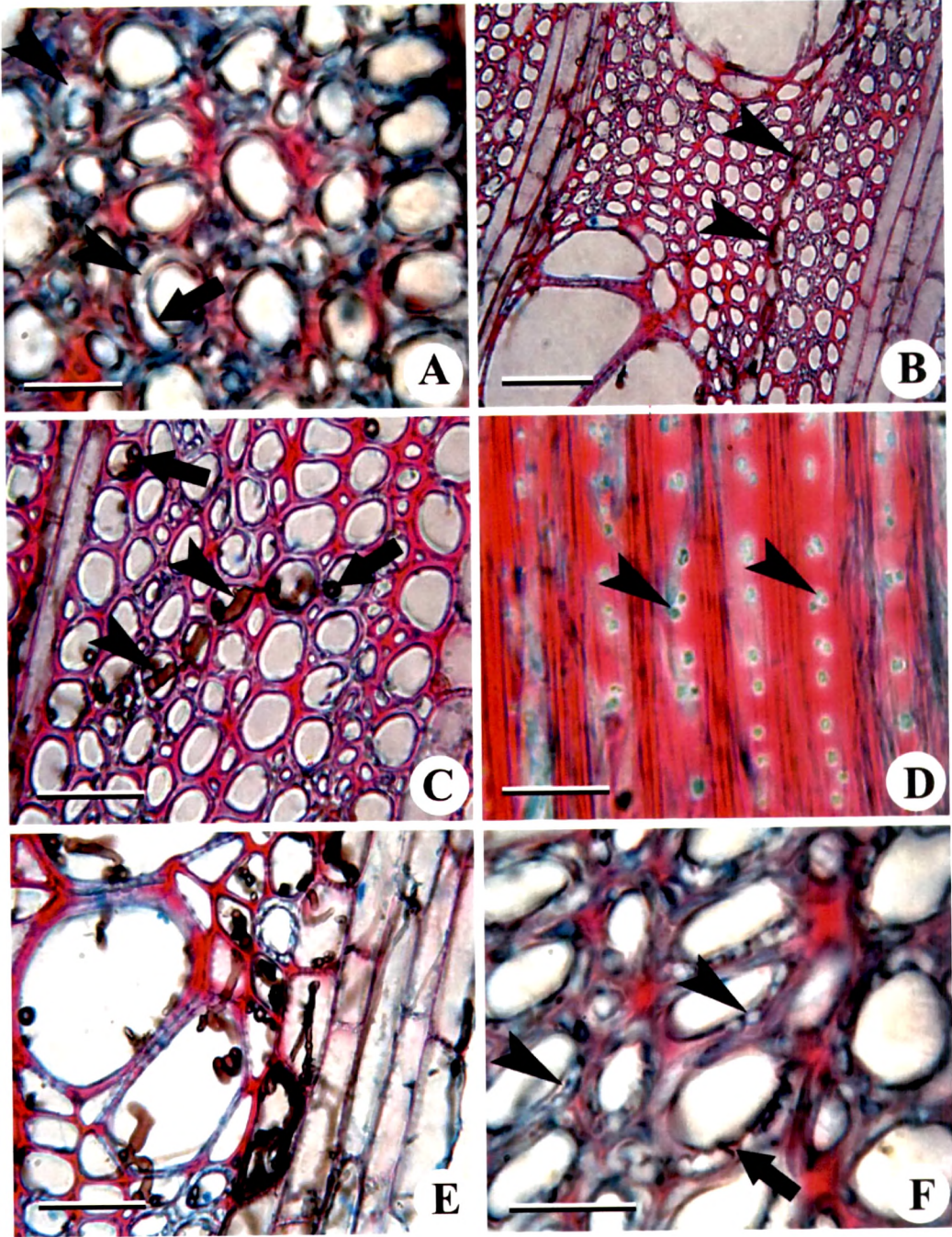


Figure 3.40

cell corner seems intact with
S₂ wall region showing
delamination

Figure 3.41: Transverse (A–F) view of infected wood of *Ailanthus excelsa* showing different stages of wood decay.

- A: Initiation of degradation at the cell corners and along the middle lamella of fibre walls (arrowheads). Note that no fungal mycelia are observed at this stage.
- B: Initiation of formation of cavity formation in the S₂ layer of the cell wall (arrowheads). Note that the cavities are very small in the beginning.
- C: Fusion of cavities and transverse hyphal growth leads to formation of large cavities (arrowheads).
- D: Fusion of adjacent cavities (arrows) and fibres walls showing “T” shaped cavities and L bending (arrowheads) of hyphae in the S₂ layer.
- E: Fibres walls showing “T” shaped cavities and L bending (arrows) of hyphae in the S₂ layer. Note the troughs in the cell wall (arrowheads).
- F: Fungal mycelia adjacent to the cell wall corners (arrowheads).

Figure 3.41: (A–F): Scale bar = 50 μm

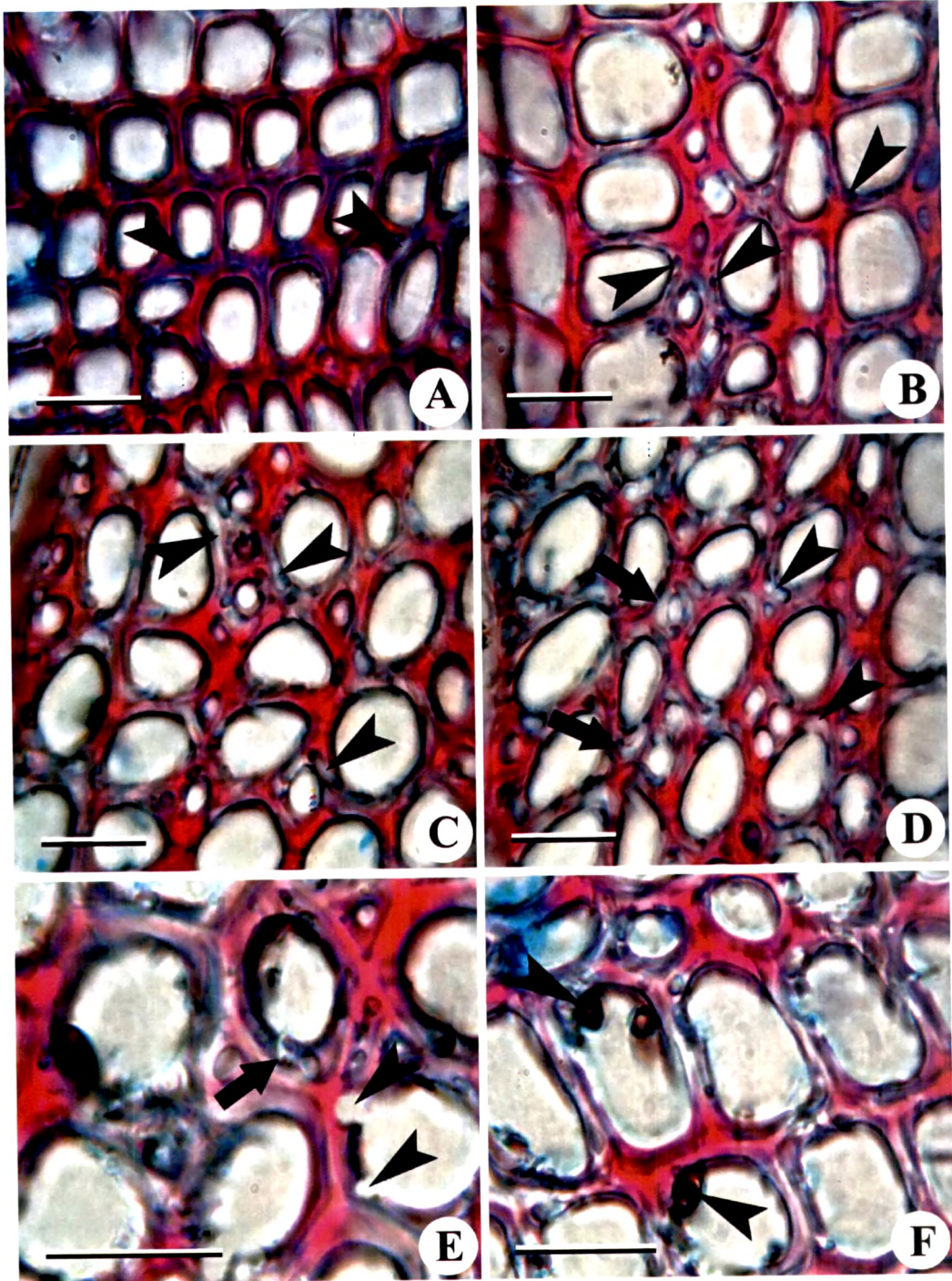


Figure 3.41

Figure 3.42: Transverse (A–F) view of infected wood of *Ailanthus excelsa* showing different stages of wood degradation.

- A: Portion of severely infected wood showing complete loss of cell wall integrity (arrows).
- B: Portion of severely infected wood showing complete loss of cell wall compounds.
- C: Vessel lumen occluded with fungal hyphae (arrowheads). Note the middle lamella of the vessel wall is stained with astra blue (arrow).
- D: Separation of vessel wall from the adjacent xylem derivatives (arrowhead).
- E: Initiation of sclerotic tissue (pseudoparenchyma) formation in one of the vessel element (arrow).
- F: In the advanced stage of decay vessel lumen is completely occluded by the pseudoparenchyma formation of fungal filaments (arrowheads).

Figure 3.42: (A–C, E, F): Scale bar = 100 μm ; (D) = 50 μm

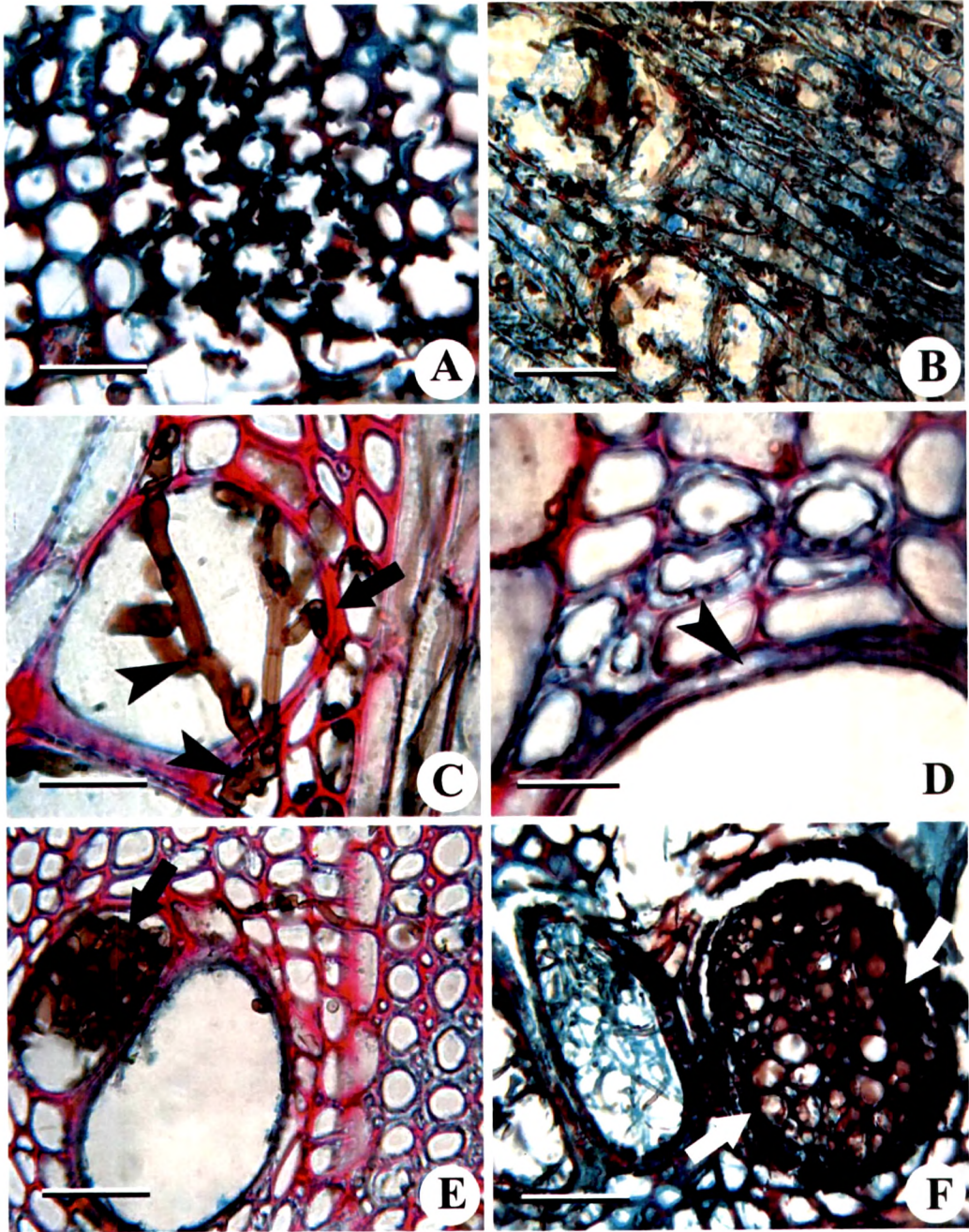


Figure 3.42

Figure 3.43: Transverse (A–E) and radial longitudinal (F) view of secondary xylem of *Azadirachta indica* showing features of decay by *Irpex lacteus*.

- A: Fungal hyphae passing through vessel lumen (arrowheads). Note that vessel lumen is filled with fungal mycelia.
- B: Narrow vessels showing fungal invasion and blockage of lumen (arrowheads).
- C: Movement of fungal mycelia through the xylem rays (arrowheads). Note that vessel associated axial parenchyma cells are also invaded with the fungi (arrow).
- D: All cell types of secondary xylem showing fungal invasion within 30 days of inoculation (arrowhead).
- E: Movement of fungal mycelia from rays (arrowheads) to adjacent tissues. Arrow indicates fungal mycelium passing through xylem fibres and axial parenchyma cells.
- F: Xylem rays serve as main path for the mycelia movement (arrowheads). Note that rays are filled with the fungal mycelia.

Figure 3.43: (A–F): Scale bar = 75 μm

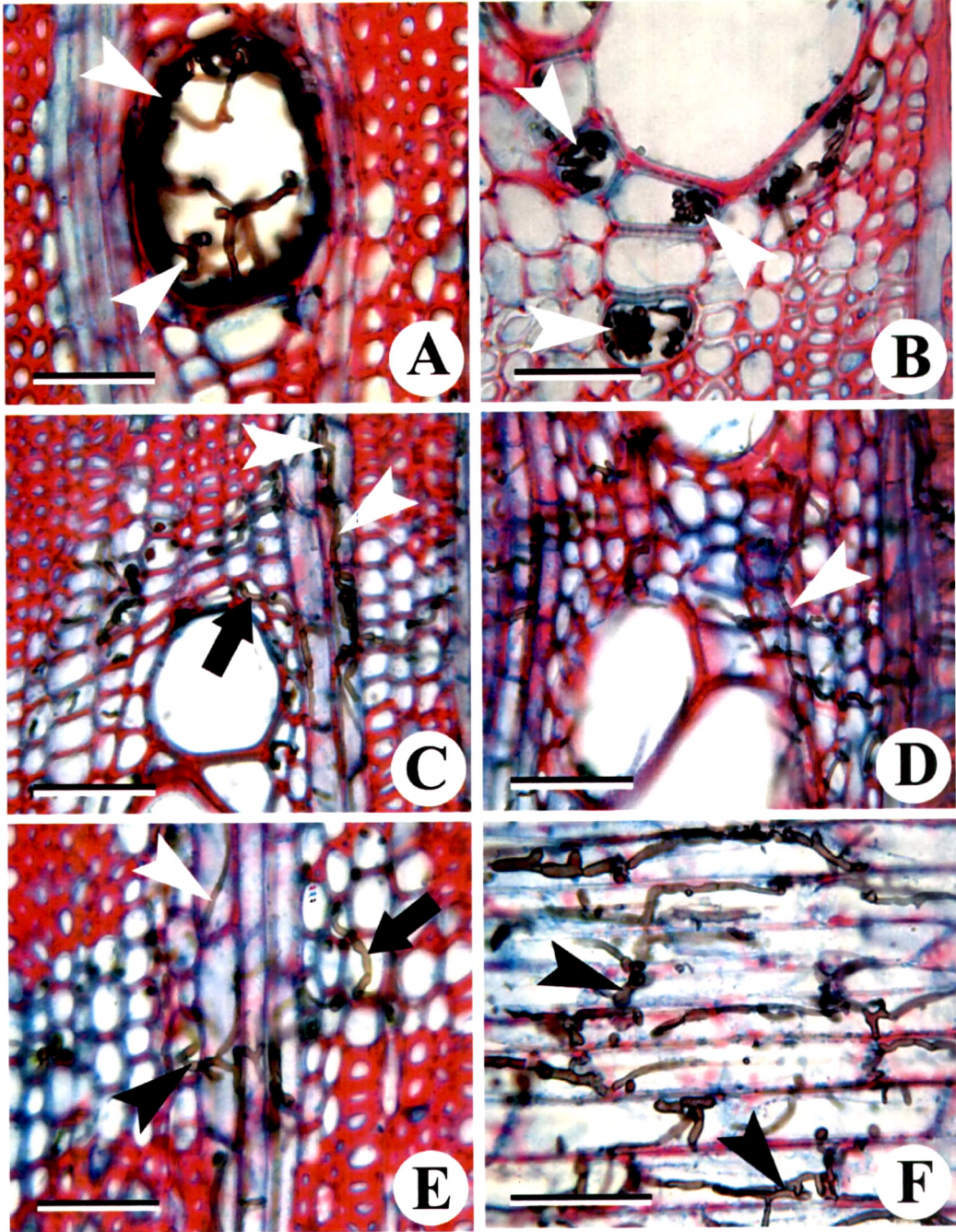


Figure 3.43

Figure 3.44: Transverse (A–F) view of secondary xylem of *Azadirachta indica* showing features of wood decay by *Irpex lacteus*.

- A: Invasion of fungal mycelia into axial parenchyma cells (arrowhead). Note the transversely cut fungal mycelia in axial parenchyma cells (arrowhead).
- B: Dissolution of middle lamella due to ligninolytic activity of enzyme resulted in the separation of xylem fibres from each other (arrowhead).
- C: Degradation of middle lamella and separation of xylem fibres from each other (arrowheads).
- D: Ray cell wall showing large erosion holes on the wall (arrowheads).
- E: Dissolution of middle lamella showing separation of ray cells (arrow).
- F: Separation of vessel walls in response to fungal activity (arrows). Note the ray cell showing separation of cell walls from middle lamella (arrowhead).

Figure 3.44: (A, B, D, E): Scale bar = 50 μm ; (C, F) = 75 μm

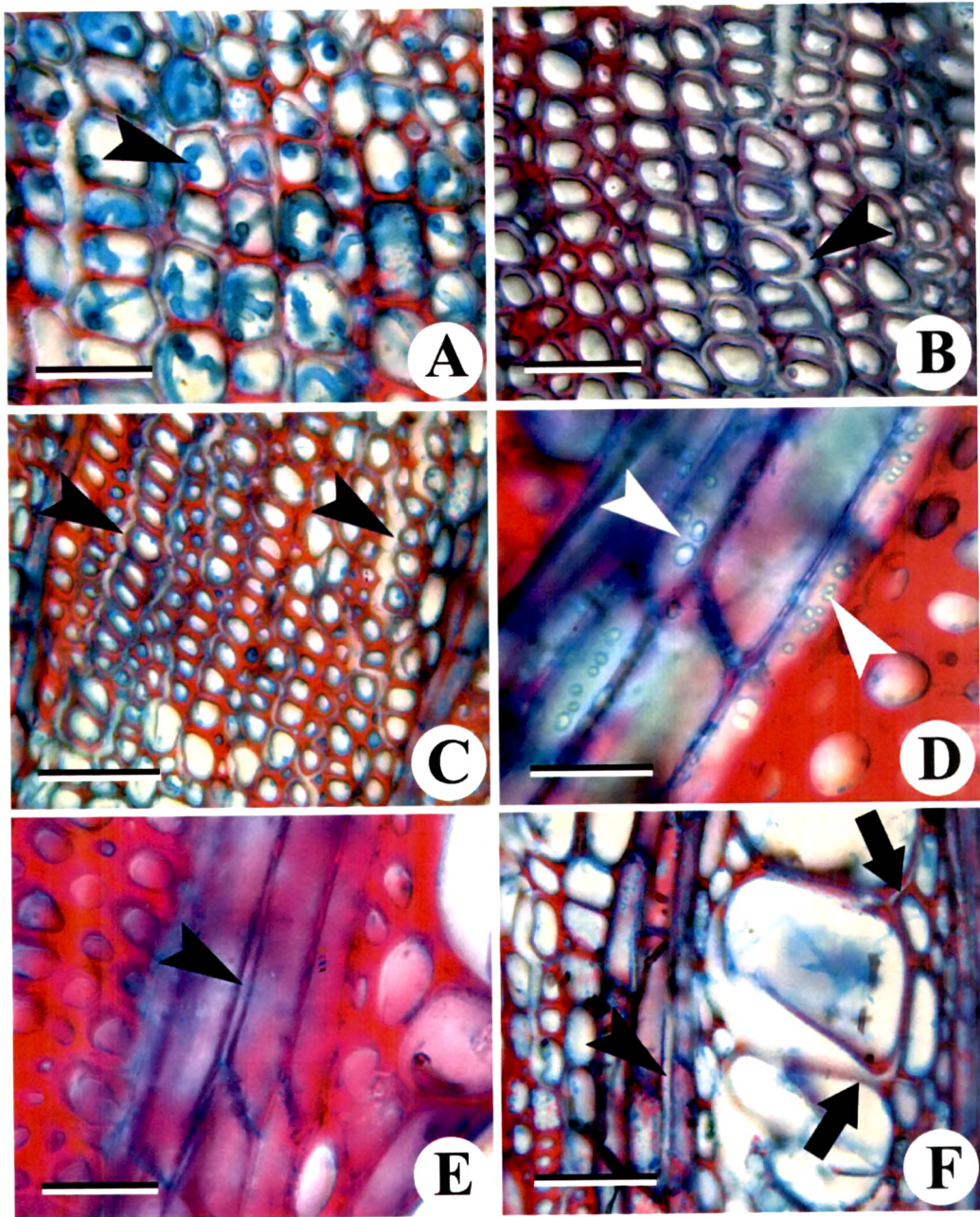


Figure 3.44

Figure 3.45: Tangential longitudinal (A–D), transverse (E) and radial longitudinal view of secondary xylem of *Azadirachta indica* showing pattern of decay by *Irpex lacteus*.

- A: Pits of the lateral walls of the fibres became larger in size and irregular in shape due to the activity of fungal enzyme (arrowheads). Note the transversely cut fungal mycelia (left arrowhead) passing through one of the pit aperture.
- B: Formation of several bore holes on the lateral walls of the xylem fibres (arrowheads). Note the irregular distribution of boreholes along with pits on the lateral wall of xylem fibres.
- C: Corners of ray cells showing blue staining with astra blue due to delignification at ray cells junctions (arrowhead).
- D: Enlarged view of ray cells corners showing delignification at ray cells junctions (arrows). Note the broken cell wall in one of the ray cell (arrowhead). Small arrowhead indicates thinning of ray cell wall.
- E: Irregularly arranged, several oval to oblong boreholes/erosion holes of various sizes formed on the lateral walls which completely damages the ray cells (arrowheads).
- F: Ray cell walls showing several boreholes at advance stage of decay (arrowheads).

Figure 3.45: (A–F): Scale bar = 50 μm

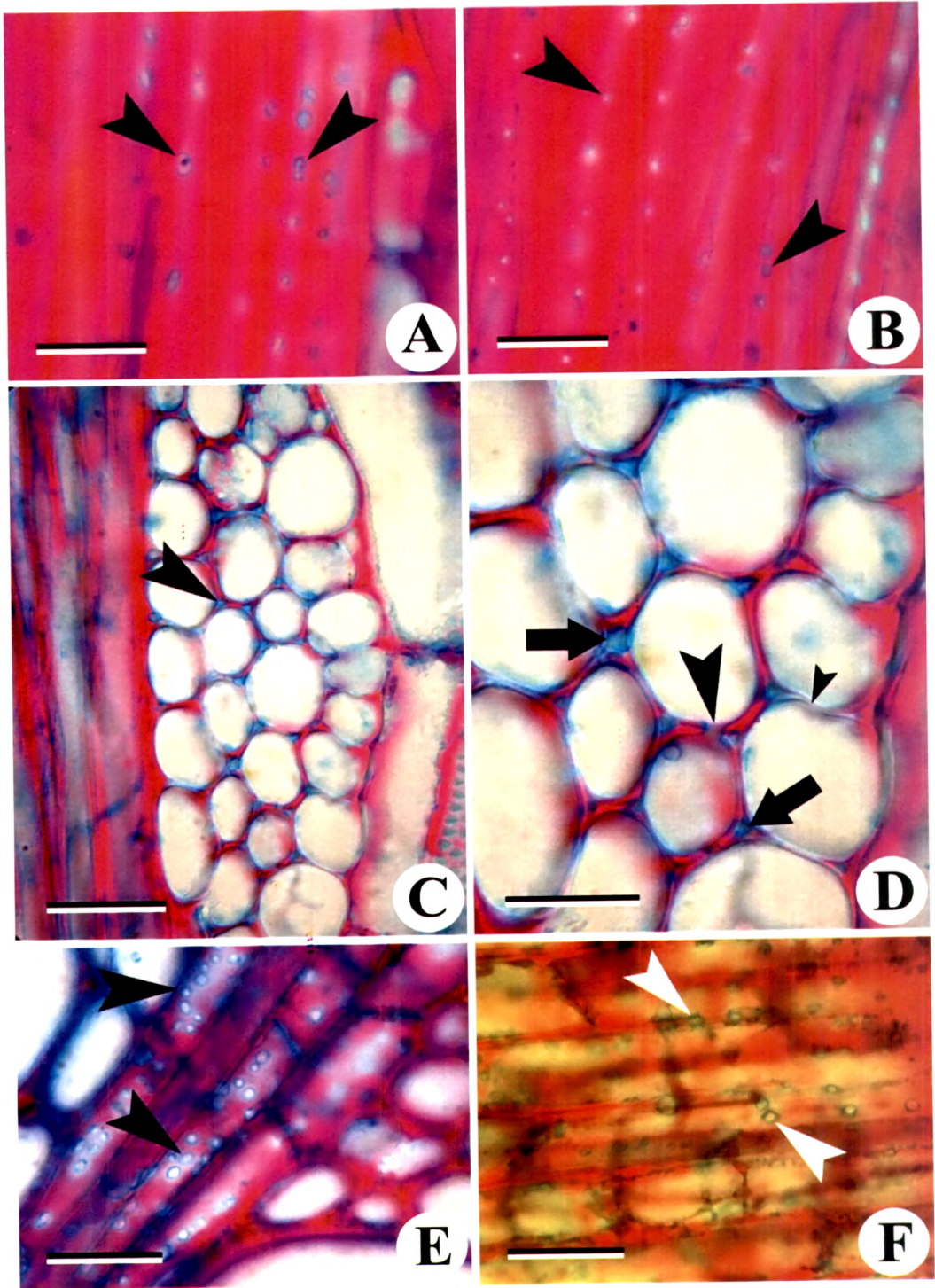


Figure 3.45

[

Figure 3.46: Radial (A, D) and tangential (B–C) longitudinal, view of secondary xylem of *Azadirachta indica* showing stages of advance decay by *Irpex lacteus*.

- A: Round erosion pits of various sizes formed in response to mycelia action (arrowheads) showing irregular distribution.
- B: Boreholes formed by the fungal mycelia showing irregular distribution of these boreholes on the lateral walls of the xylem fibres (arrowheads).
- C: Enlarged view of xylem fibres showing the boreholes of irregular size (arrowheads) after 120 days of incubation.
- D: Axial parenchyma showing the boreholes of irregular size, shape and distribution (arrowheads). Note the fungal hyphae passing through one of the borehole (small arrow).

Figure 3.46: (A–D): Scale bar = 50 μm

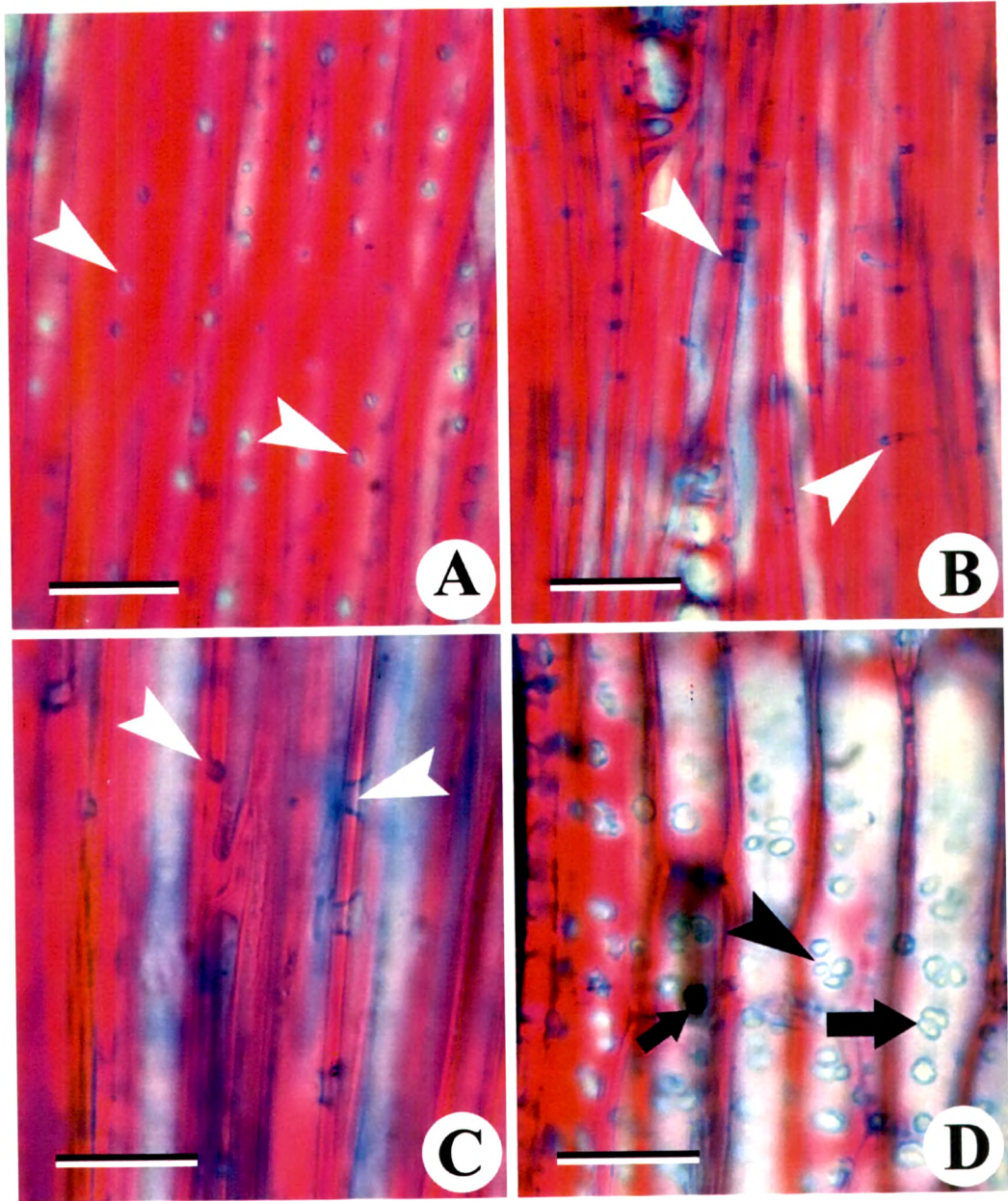


Figure 3.46

Figure 3.47: Transverse (A, B, D, E) and radial longitudinal (C, F) view of secondary xylem of *Azadirachta indica* showing features of wood decay by *Phanerochaete chrysosporium*.

- A: Dissolution of middle lamella and separation of xylem fibres from each other after 90 days fungal infection (arrowheads).
- B: Enlarged view of Fig. 9A showing dissolution of middle lamella and separation of xylem fibres (arrowheads).
- C: Ray cell walls showing several boreholes after 120 days of incubation (arrowheads). Note the fungal mycelia in the ray cells (arrow).
- D: Dissolution of middle lamella showing separation of vessel elements after 120 days of fungal inoculation (arrowhead).
- E: Irregularly arranged, oval to oblong boreholes/erosion pits of various sizes formed on the lateral walls of rays which completely damage the cell walls (arrowheads).
- F: Formation of several bore holes on the lateral walls of the xylem fibres (arrowheads). Note the irregular distribution of boreholes along with pits on the lateral wall of xylem fibres.

Figure 3.47: (A, B, D): Scale bar = 75 μm ; (C, E, F) = 50 μm

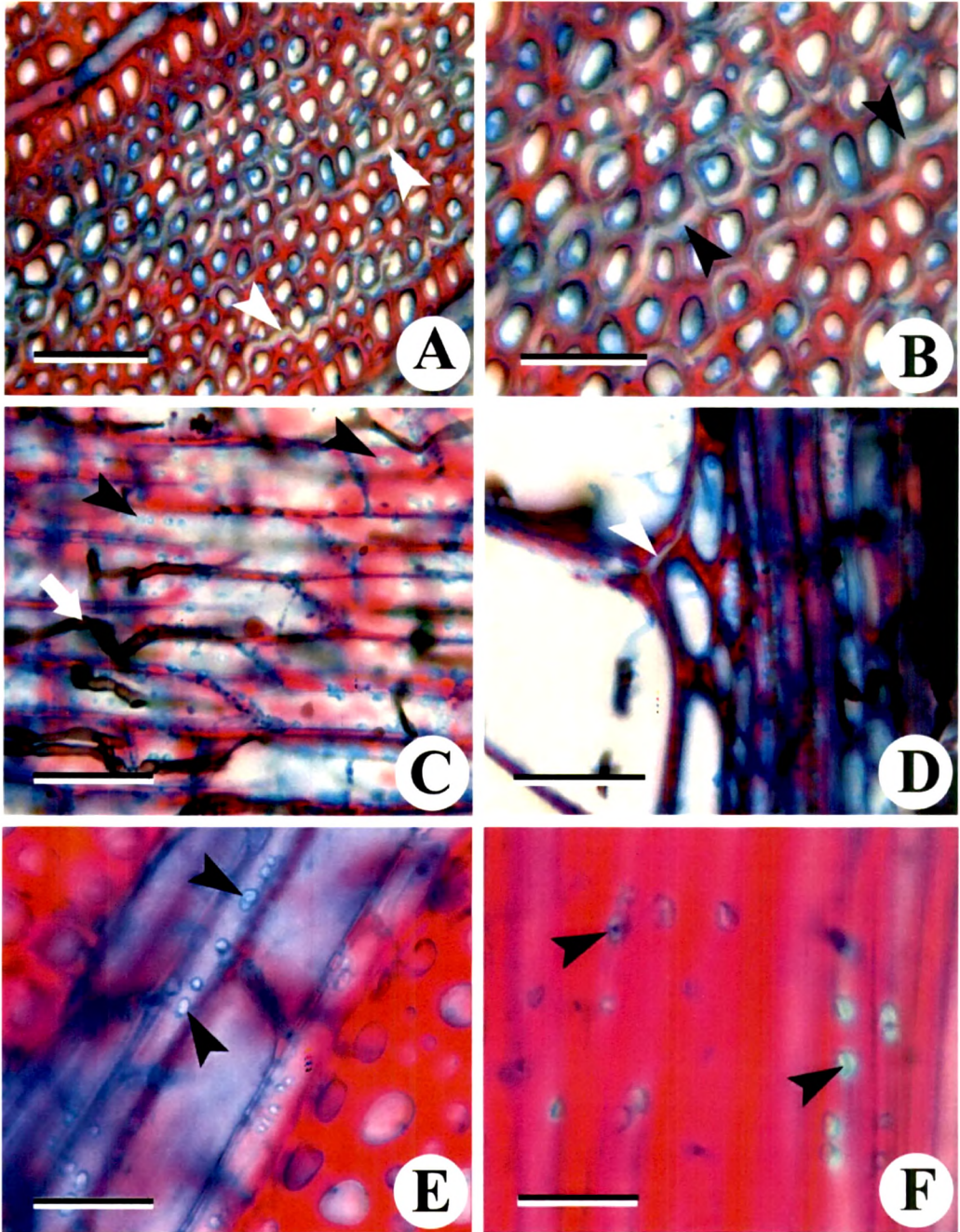


Figure 3.47

Figure 3.48: Transverse (A, E), radial (B-D) and tangential (F) longitudinal, view of secondary xylem of *Tectona grandis* invaded with *Irpex lacteus* showing stages of advance decay.

- A: Hyphae traversing through axial elements of xylem (arrow). Arrowhead shows hyphae in the vessel lumen while small arrow indicates fungal hyphae in the ray cell.
- B: Vessel lumen blocked with fungal filaments (arrows).
- C: Xylem rays showing severe invasion of *I. lacteus* forming a mycelial mat within vessel lumen (arrowheads).
- D: Fungal hyphae passing from one ray cell to next (arrow). Note the variation in the diameter of the hyphae during the early stages of invasion (arrowhead).
- E: Dissolution of middle lamella and separation of ray cells (arrowhead) and adjacent xylem fibres (arrow) indicating selective mode delignification. Note that separation fibres usually start near the cells adjacent to rays.
- F: Xylem fibres invaded with *P. chrysosporium* after 30 days of inoculation (arrowheads).

Figure 3.48: (A, C, F): Scale bar = 75 μm ; (B, D, E) = 50 μm

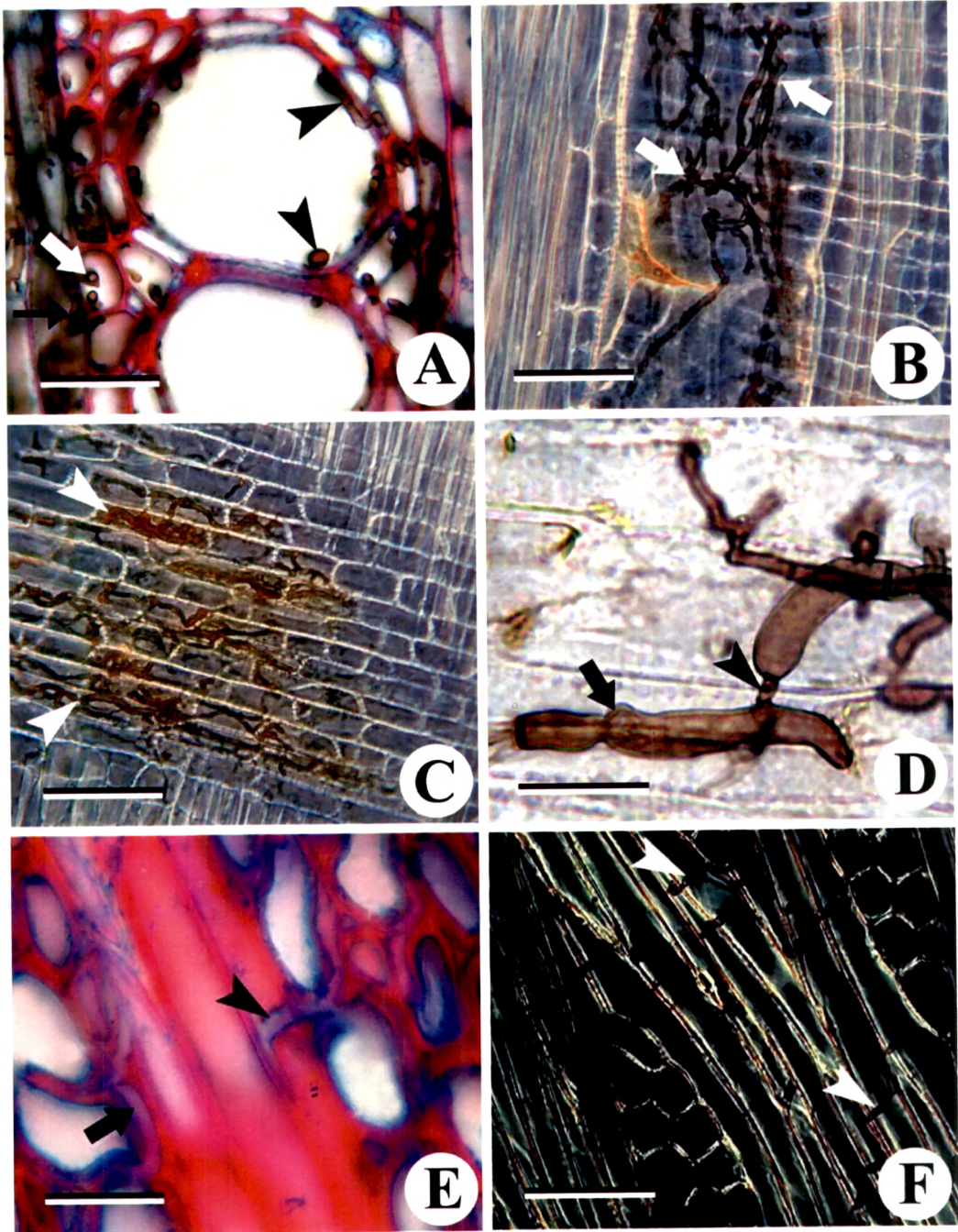


Figure 3.48

Figure 3.49: Tangential longitudinal (A) and transverse (B–F) view of secondary xylem of *Tectona grandis* showing pattern of decay by *Irpex lacteus*.

- A: Separation ray cells due to disintegration of middle lamella (arrowheads). Note the corners of ray cells showing blue staining with astra blue due to delignification (arrow).
- normal?* B: Degeneration of middle lamella resulted into separation of narrow vessel element (arrowheads).
- C: Separation of fibre walls (arrowheads) and formation of erosion trough in xylem after 90 days of exposure. Note the broken cell walls of the xylem fibres (arrows).
- D: Enlarged view of secondary xylem showing erosion troughs (arrowheads) and broken cell walls of the xylem fibres (arrow).
- E: In severely affected xylem, rays showing several boreholes on the lateral walls (arrowheads).
- F: Completely eroded xylem showing bleaching of cell wall. Compared to figure 11D, cell walls are completely bleached and stained blue coloured with astra blue due to loss of lignin. Presence of red stain indicates remnants of lignin in the cell wall.

Figure 3.49: (A–F): Scale bar = 50 μm

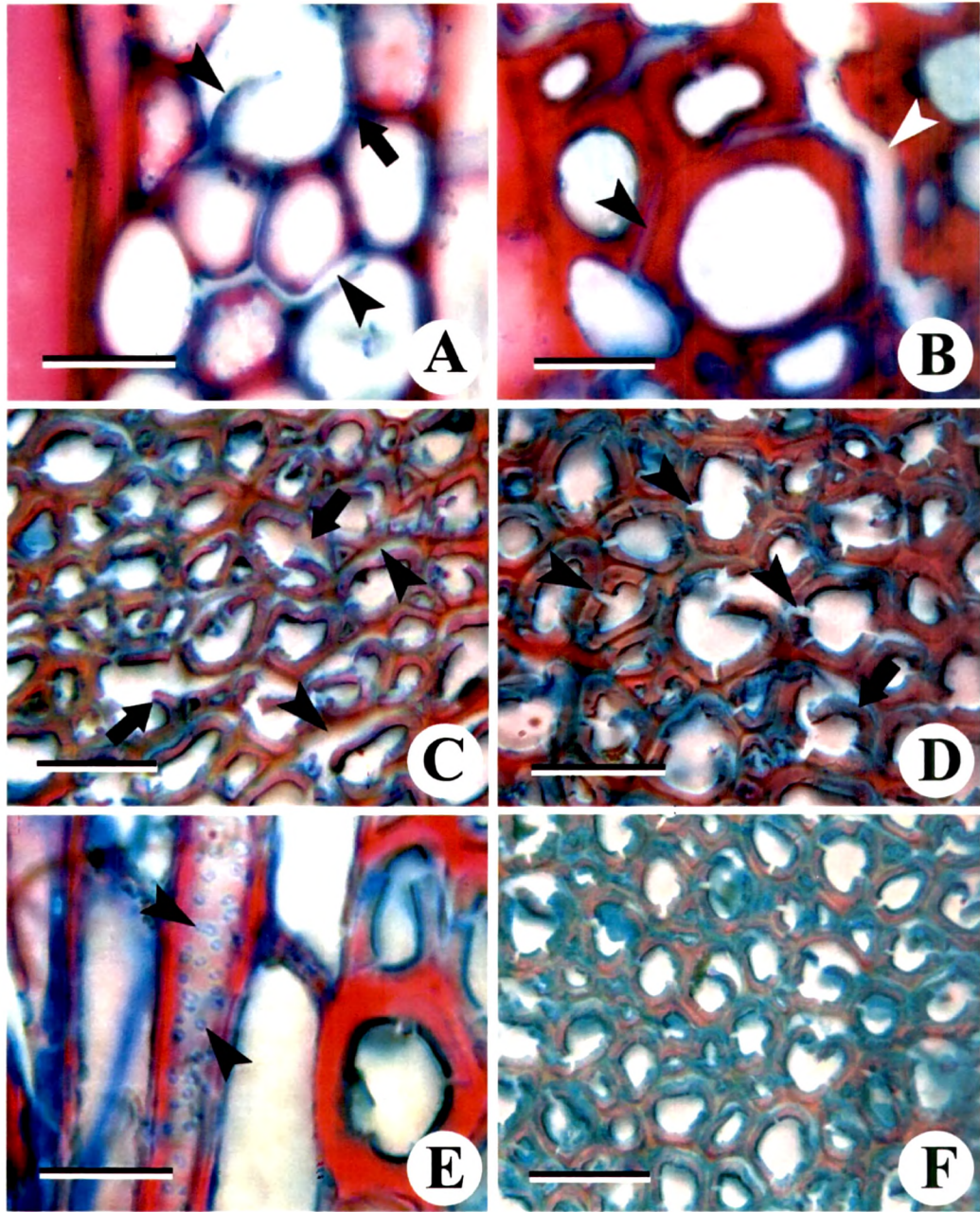


Figure 3.49

Figure 3.50: Transverse (A, C–F) and tangential longitudinal (B) view of secondary xylem of *Azadirachta indica* (A) and *Tectona grandis* (B–F) showing pattern of decay by *Irpex lacteus* (A) and *P. chrysosporium* (B–F).

- A: Completely bleached cell walls of *Azadirachta* xylem stained blue coloured with astra blue due to loss of lignin after 120 days incubation with *I. lacteus*.
- B: Initiation of cell wall separation in the rays of *Tectona*. Note that ray cells corners showing blue staining with astra blue due to delignification at cell junctions (arrowheads).
- C: Separation of fibre wall in teak begins after 60 days of incubation with *P. chrysosporium* (arrowheads).
- D: Separation of xylem fibres becomes more pronounced due to dissolution of middle lamella in wood blocks exposed to 90 days of incubation (arrowheads).
- E: Enlarged view of figure 12D showing several boreholes on ray cell walls (arrowheads) and distinctly separated xylem fibres (arrows).
- F: Irregularly arranged, oval to oblong boreholes of various sizes formed on the lateral walls of ray cells which completely damage the ray cell wall (arrows).

Figure 3.50: (A, C, F): Scale bar = 50 μm ; (D, E) = 75 μm

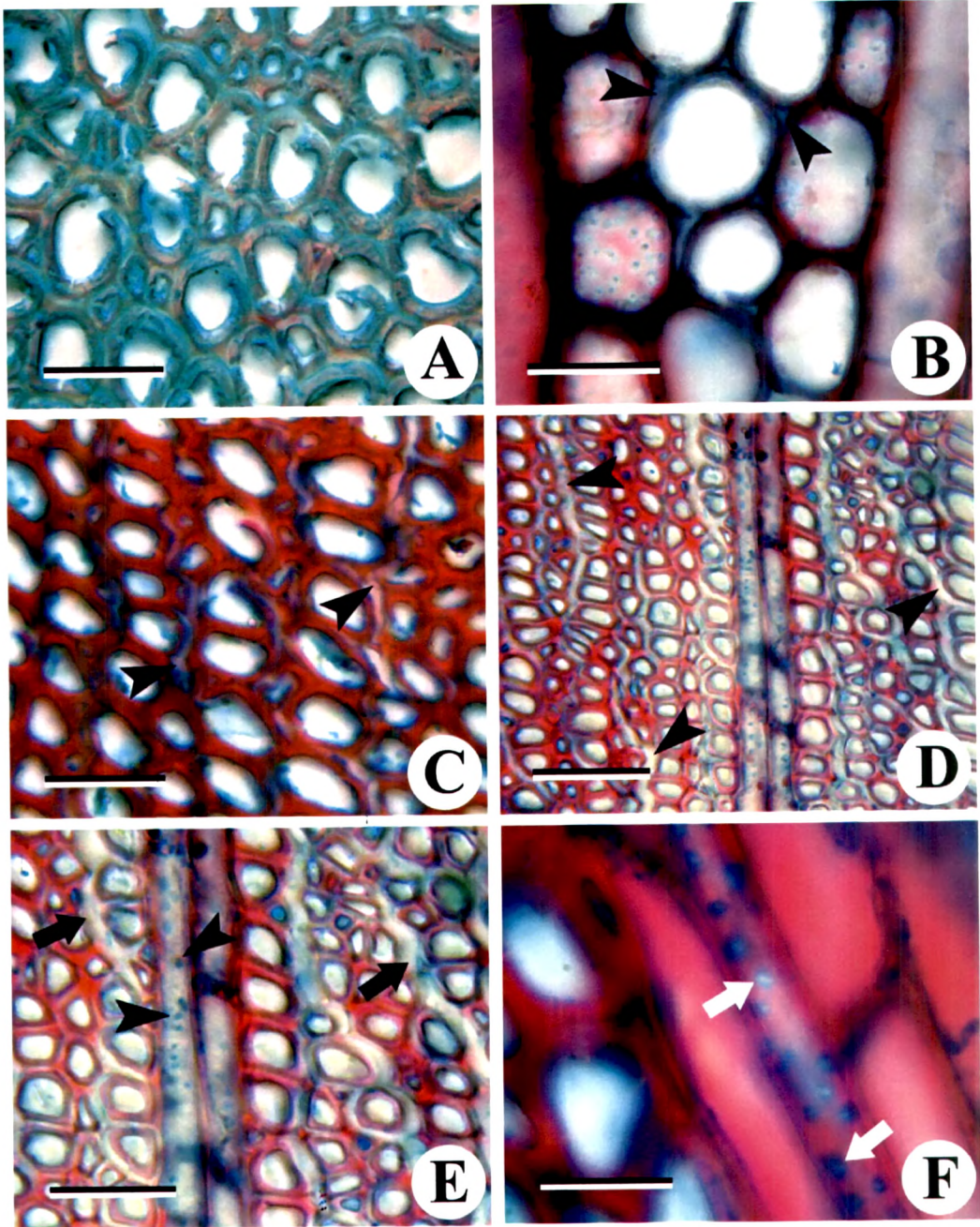


Figure 3.50



Figure 3.51: Transverse (A, B, D) and tangential longitudinal (C) view of secondary xylem of *Tectona grandis* showing pattern of decay caused by *P. chrysosporium*.

- A: Separation of secondary xylem (arrowheads) and completely bleached cell walls stained blue coloured with astra blue due to loss of lignin after 120 days incubation.
- B: Irregularly arranged, boreholes of various sizes formed due ligninolytic activity of fungal mycelia which completely damages the ray cells (arrowheads).
- C: Completely damaged ray showing degraded and broken ray cell walls (arrowheads).
- D: Severely affected wood showing delignification of secondary xylem and loss rigidity due to disintegration of lignin results into complete collapse of wood cell walls in advance stage of decay.

Figure 3.51 (A–D): Scale bar = 50 μm

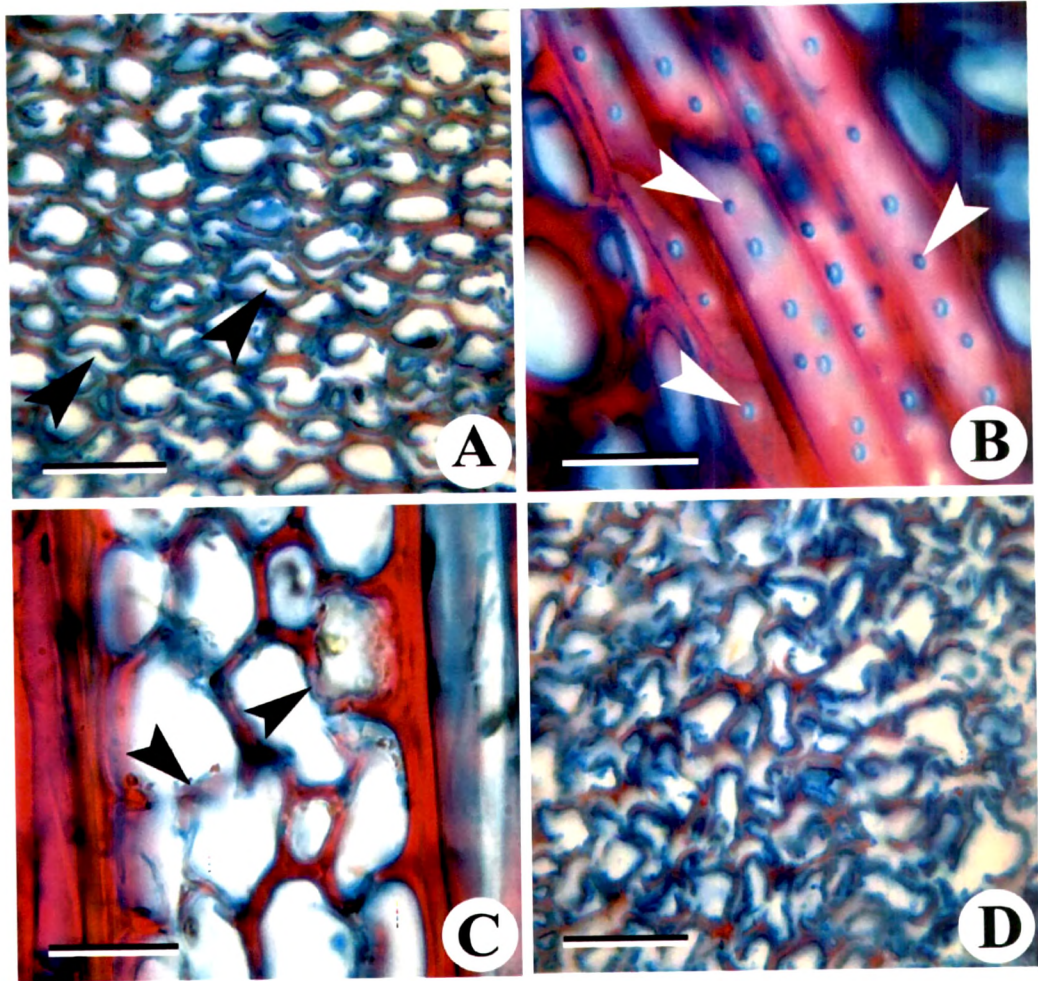


Figure 3.51

Inoculum Size	Dyes									
	KR1	KR2	KR3	KR4	KR5	KR6	KR7	KR8	KR9	KR10
	After 6 days									
1	1.1	2	1	0.2	1	1.5	1.3	1.2	1	1.1
2	2	3	2.5	0.5	2	2.5	2.8	3	2.1	1.9
3	2.3	3.5	2.8	0.8	3.2	3	3.3	3.5	2.6	2.9
4	2.5	3.7	3.5	1	3.6	3.2	3.5	3.6	2.9	3
	After 9 days									
1	7.9	8.6	7.7	6.5	8.7	8.5	8.6	8.6	8.5	8.8
2	8	8.7	7.8	6.7	8.8	8.6	8.6	8.8	8.7	8.8
3	8.4	8.7	7.8	6.9	8.8	8.8	8.7	8.9	8.7	9
4	8.7	9	7.9	7	9	9	8.9	9	9	9

Table 3.1: Influence of inoculum size on solid plate dye decolourisation by *Irpex lacteus*

Inoculum Size	Dyes									
	KR1	KR2	KR3	KR4	KR5	KR6	KR7	KR8	KR9	KR10
	After 3 days									
1	3.1	3.8	3.4	2.2	3.2	3.5	3.3	3.2	3.2	3
2	3.3	4	3.6	2.2	3.3	3.6	3.5	3.5	3.5	3.3
3	3.5	4	3.7	2.4	3.5	3.8	3.6	3.6	3.6	3.5
4	3.5	4.3	3.8	2.6	3.7	3.8	3.8	4	3.9	3.6
	After 9 days									
1	8.5	9	8.3	7	8.7	8.5	8.6	8.6	8.5	8.8
2	8.6	9	8.4	7.2	8.8	8.7	8.8	8.7	8.6	8.8
3	8.8	9	8.5	7.3	8.9	8.8	8.8	8.9	8.7	9
4	9	9	8.7	7.6	9	8.9	9	9	8.8	9

Table 3.2: Influence of inoculum size on solid plate dye decolourisation by *Phanerochaete chrysosporium*

Dyes	Inoculum Size				
	3	6	9	12	15
	After 6 days				
KR1	53.13	65.69	70.04	65.67	72.42
KR2	45.04	75.00	76.82	79.23	81.47
KR3	43.53	54.14	57.03	63.88	78.19
KR4	27.90	45.40	70.57	75.45	87.62
KR5	45.55	31.27	55.55	60.67	70.5
KR6	64.49	63.99	82.07	87.76	92.65
KR7	43.05	63.88	64.39	70.82	86.66
KR8	50.07	53.06	70.27	81.20	71.21
KR9	52.46	53.76	64.52	68.43	74.74
KR10	46.71	44.63	53.61	81.35	84.49

Table 3.3: Influence of inoculum size on % dye decolourisation by *Irpex lacteus*

Dyes	Inoculum Size				
	3	6	9	12	15
	After 6 days				
KR1	36.65	76.20	80.97	91.39	93.31
KR2	28.53	56.68	72.35	88.87	91.76
KR3	59.93	92.39	87.75	90.75	93.54
KR4	44.4	56.26	68.32	70.54	73.77
KR5	50.42	93.08	95.00	97.70	98.65
KR6	46.04	62.92	77.51	84.84	85.02
KR7	34.15	61.74	78.72	69.14	87.36
KR8	48.16	73.42	89.96	87.32	89.76
KR9	33.08	88.78	85.12	88.29	90.18
KR10	21.49	78.70	88.94	95.41	96.52

Table 3.4: Influence of inoculum size on % dye decolourisation by *Phanerochaete chrysosporium*

Particle Size	Enzyme Activity (IU/ml)		
	MnP	MIP	Laccase
<1	420.06	316.17	163.03
1	480.36	440.12	195.19
1.5	447.05	324.49	181.15
2	397.56	249.48	52.94
2.5	344.86	234.34	12.40
3	330.94	138.78	13.98
3.5	249.72	137.26	10.57
4	450.45	359.33	76.17
>4	432.94	257.20	60.30

Table 3.5: Optimisation of particle size for ligninolytic enzyme production by *Irpex lacteus*

Particle Size	Enzyme Activity IU/ml		
	MnP	MIP	Laccase
<1	385.89	363.10	67.17
1	487.90	475.92	177.32
1.5	316.1	242.55	50.21
2	478.84	187.96	56.71
2.5	336.96	146.13	53.00
3	262.61	66.26	21.27
3.5	155.56	104.98	28.32
4	280.60	67.35	28.86
>4	326.99	199.87	72.88

Table 3.6: Optimisation of particle size for ligninolytic enzyme production by *Phanerochaete chrysosporium*

Incubation Time (Days)	Enzyme Activity (IU/ml)		
	MnP	MIP	Laccase
3	356.53	272.27	68.2
6	381.76	329.05	69.6
9	480.36	440.12	195.19
12	379.57	335.31	135.31
15	365.16	263.7	75.92
18	265.47	203.34	51.55

Table 3.7: Optimisation of incubation time for ligninolytic enzyme production by *Irpex lacteus*

Incubation Time (Days)	Enzyme Activity (IU/ml)		
	MnP	MIP	Laccase
3	378.11	339.39	60.18
6	487.9	475.92	177.32
9	472.64	334.77	83.34
12	481.82	419.08	60.5
15	323.7	185.22	41.27
18	158.84	104.01	18.6

Table 3.8: Optimisation of incubation time for ligninolytic enzyme production by *Phanerochaete chrysosporium*

Reaction Time	Enzyme Activity (IU/ml)		
	MnP	MIP	Laccase
5	495.21	342.19	127.45
10	560.6	534.4	263.22
15	519.40	464.64	194.36
20	511.30	451.29	190.23
25	490.88	442.23	190.32
30	425.88	442.10	184.20
35	410.39	398.95	172.23
40	390.24	384.56	160.10
45	337.65	312.11	123.00

Table 3.9: Influence of reaction time on ligninolytic enzyme activity produced by *Irpex lacteus*

Reaction Time	Enzyme Activity (IU/ml)		
	MnP	MIP	Laccase
5	580.99	491.36	201.76
10	607.35	539.27	263.03
15	523.34	508.70	222.14
20	504.03	476.44	198.67
25	496.73	438.75	181.35
30	487.34	429.71	176.93
35	477.20	388.50	175.33
40	461.29	372.44	169.39
45	401.33	362.16	161.25

Table 3.10: Influence of reaction time on ligninolytic enzyme activity produced by *Phanerochaete chrysosporium*